PB88-238191

Comparison of the RADM (Regional Acid Deposition Model) Dry Deposition Module with Site-Specific Routines for Inferring Dry Deposition

(U.S.) Argonne National Lab., IL

Prepared for

Environmental Monitoring Systems Lab.
Research Triangle Park, NC

Aug 88

U.S. Department of Commerce
National Technical Information Service
NTIS

TECHNICAL REPORT DATA
(Please read Instructions on the reverse before completing)

1. REPORT NO. EPA/600/4-88/027	2.
3. RECIPIENT'S ACCESSION NO. PB88-238191/AS	
4. TITLE AND SUBTITLE Comparison of the RADM Dry Deposition Module with Site-Specific Routines for Inferring Dry Deposition	5. REPORT DATE August 1988
	6. PERFORMING ORGANIZATION CODE
7. AUTHOR(S) M. L. Wesely and B. M. Lesht	8. PERFORMING ORGANIZATION REPORT NO.
9. PERFORMING ORGANIZATION NAME AND ADDRESS Center for Environmental Research Argonne National Laboratory Argonne, Illinois 60439	10. PROGRAM ELEMENT NO.
	11. CONTRACT/GRANT NO. IAG DW89932525-01
12. SPONSORING AGENCY NAME AND ADDRESS Environmental Monitoring Systems Laboratory U. S. Environmental Protection Agency Research Triangle Park, North Carolina 27711	13. TYPE OF REPORT AND PERIOD COVERED
	14. SPONSORING AGENCY CODE EPA-600/08

15. SUPPLEMENTARY NOTES

16. ABSTRACT

The dry deposition module of the Regional Acid Deposition Model (RADM) is used to compute the dry deposition velocities (downward flux divided by concentration at a specified height) for SO_2, SO_4^{2-}, O_3, and HNO_3, among others. With its computerized landuse map, the module can provide estimates of the deposition velocities for a given set of meteorological and surface conditions that are representative of an area located anywhere in the contiguous United States and nearby locations. As part of this project, the module has been modified to accept data on meteorological and surface conditions observed at measurement stations rather than use inputs computed with RADM. The purpose of these modifications was to make site-specific estimates of dry deposition velocities, and compare these with results from the site-specific inferential technique that has been developed at the Atmospheric Turbulence and Diffusion Division (ATDD) of NOAA's Air Resources Laboratory. Goals of the comparisons include estimating the relative uncertainties of the two techniques, suggesting improvements, and examining the ability of the modified module to provide estimates of dry deposition for expanded areas around the measurement sites.

17. KEY WORDS AND DOCUMENT ANALYSIS

a. DESCRIPTORS	b. IDENTIFIERS/OPEN ENDED TERMS	c. COSATI Field/Group

18. DISTRIBUTION STATEMENT Release to Public	19. SECURITY CLASS *(This Report)* Unclassified	21. NO. OF PAGES 105
	20. SECURITY CLASS *(This page)* Unclassified	22. PRICE A06 $19.95

EPA Form 2220-1 (Rev. 4-77) PREVIOUS EDITION IS OBSOLETE

PB88-238191

EPA/600/4-88/027
August 1988

COMPARISON OF THE RADM DRY DEPOSITION MODULE WITH SITE-SPECIFIC ROUTINES FOR INFERRING DRY DEPOSITION

by

M. L. Wesely and B. M. Lesht
Center for Environmental Research
Biological, Environmental, and Medical Research Division
Argonne National Laboratory, Argonne, IL 60439

Interagency Agreement DW89932525-01
with the U.S. Department of Energy

Project Officer

Steven M. Bromberg
Environmental Monitoring Systems Laboratory
Research Triangle Park, North Carolina 27711

ENVIRONMENTAL MONITORING SYSTEMS LABORATORY
OFFICE OF RESEARCH AND DEVELOPMENT
U.S. ENVIRONMENTAL PROTECTION AGENCY
RESEARCH TRIANGLE PARK, NORTH CAROLINA 27711

NOTICE

The information in this document has been funded partly by the United States Environmental Protection Agency through Interagency Agreement DW89932525-01 to the U.S. Department of Energy. It has been subject to the Agency's peer and administrative review, and it has been approved for publication as an EPA document.

ABSTRACT

The computer module for calculating dry deposition velocities in the Regional Acid Deposition Model (RADM) has been modified to use site-specific data provided by measurement stations such as CORE (COre Research Establishment, for dry deposition) satellite sites. Data collected during 1986 at seven widely separated sites in the eastern United States were used to estimate weekly averages of deposition velocities for SO_2, O_3, HNO_3, and SO_4^{2-} with both the modified RADM module and the inferential technique. The data and the computer coding for the inferential technique were provided by the Atmospheric Turbulence and Diffusion Division of the National Oceanic and Atmospheric Administration's Air Resources Laboratory. Comparison of results obtained with the two techniques indicates that some systematic differences exist, even when the module uses distributions of landuse types that match as closely as possible the observed vegetation coverages used in the inferential technique. When one ignores the systematic differences that could easily be removed by minor changes in the algorithms for computing resistances to deposition, the relative uncertainties for SO_2 and O_3 deposition velocities are approximately ±30%. Overall, the relative uncertainties in the deposition velocities for HNO_3 and SO_4^{2-} are about ±30% and ±50%, respectively. Use of the landuse map to extrapolate to areas as large as RADM grid cells (approximately 80 km square) around the measurement stations produces weekly averages within ±20% of those for SO_2, O_3, and SO_4^{2-} and approximately ±30% for HNO_3, if one avoids landuse types such as urban and water areas that are both nonrepresentative and have very different characteristics from the measurement sites. These estimates do not represent true uncertainty or accuracy because additional uncertainty is caused by other factors such as siting of instrumentation for collecting input data and the inability of the algorithms used in the computational schemes to address the effects of the many surface nonuniformities that typically exist in the areas surrounding measurement sites.

CONTENTS

Abstract..... iii

Tables..... vi

Figures..... vii

Acknowledgements..... viii

Section

1. Introduction..... 1

2. Modifications of the RADM Module to Use Site-Specific Data.... 3

3. Use of Observations and Descriptions of Surface Conditions.... 8

4. Comparisons of Results..... 14

5. Other Considerations..... 23

6. Conclusions..... 26

References..... 31

Appendix I. Coding for the modified module..... 33

Appendix II. Graphs of v_d estimates for various landuse types, at PSU.. 45

Appendix III. Plots of v_d estimates for 1986, by site and technique.... 57

Appendix IV. Plots of v_d estimates for additional substances..... 87

TABLES

Number		Page
I	Landuse types, seasonal categories, and surface aerodynamic roughness lengths used to describe surface conditions in the module	7
II	Site names, locations, and surface vegetation (within one kilometer in all directions)	9
III	Landuse distributions and computed HNO_3 deposition velocities at each location	10
IV	Differences between weekly averaged deposition velocities computed with the module applied with the local site landuse types and those found with the inferential method	18
V	Differences between weekly averaged deposition velocities computed with the module using the landuse types for RADM grid cells and those found with the module using local site landuse types	22

FIGURES

Number		Page
1	Weekly averaged wind speeds observed at four measurement stations	12
2	Scatter diagrams of deposition velocities computed with the modified module using local site landuse distributions, versus estimates made with the inferential technique	15
3	Estimates of SO_2, HNO_3, and SO_4^{2-} deposition at ARG, computed as the product of weekly averages of deposition velocities and concentrations	24

ACKNOWLEDGEMENTS

This research was funded as part of the National Acid Precipitation Assessment Program by the U.S. Environmental Protection Agency (EPA) through IAG DW89932525-01 to the U.S. Department of Energy. The meteorological data and surface observations used in this report were supplied by Dr. T. P. Meyers and colleagues at the NOAA Atmospheric Turbulence and Diffusion Division (ATDD) in Oak Ridge, TN. This work was carried out with advice and guidance from Mr. Steven M. Bromberg of the Environmental Monitoring Systems Laboratory of the U.S. Environmental Protection Agency and Mr. Bruce B. Hicks of NOAA/ATDD.

SECTION 1

INTRODUCTION

The dry deposition module of the Regional Acid Deposition Model (RADM) has been developed to compute the dry deposition velocities (downward flux divided by concentration at a specified height) for SO_2, SO_4^{2-}, O_3, HNO_3, and several other substances important in deposition of acidifying substances or their precursors (Walcek *et al.*, 1986; Wesely, 1988). The module is capable of providing estimates of the dry deposition velocities for a given set of meteorological and surface conditions representative of a specified area in the contiguous United States and nearby locations. To compute dry deposition rates, the deposition velocities are multiplied by grid-averaged concentrations as computed by RADM. Although the computational procedures are based on considerable experimental information, uncertainties are substantial because the deposition velocities have not been measured over all the varied types of surfaces found in the field. Furthermore, data on meteorological conditions are computed by RADM for rather large grid squares, approximately 80 km on a side, and the surface conditions are specified by quite general categories of season and landuse. Thus, dry deposition velocities derived for a small, subgrid area and a short period of time might be seriously in error.

In contrast to the approach taken with the RADM dry deposition module, methods have been developed to infer deposition velocities for specific sites with observations made locally, so that monitored air concentrations can be used to infer dry deposition rates (Hicks *et al.*, 1985; Hicks *et al.*, 1988). Many aspects of the site-specific inferential technique are quite similar to those used in the RADM module. For example, the formulas employed to describe the gas-phase resistances to vertical transfer above the surface are based on the same micrometeorological principles. Also, the algorithms used to estimate surface resistances to uptake were to a large extent derived with the same body of experimental information in mind, at least for surfaces with healthy vegetation. A notable difference, however, is that the parameterizations for the site-specific approach are tailored to describe surface uptake resistances of dominant plant species and do not rely on

general landuse categories. This enables the site-specific routines for calculating deposition velocities to include more precise descriptions of amounts and types of surface cover from site to site and to better estimate responses to changes in environmental parameters such as temperature and solar radiation. Differences also may occur because of differences in interpretation of the few experimental data currently available for surfaces without actively growing vegetation.

The purpose of this report is to compare deposition velocities computed with the RADM module with those computed by use of the site-specific inferential approach. To this end, a version of the coding for the site-specific approach provided in January 1988 by Dr. T. P. Meyers of the Atmospheric Turbulence and Diffusion Division (ATDD) of National Oceanic and Atmospheric Administration's (NOAA) Air Resources Laboratory is used. Dr. Meyers and his colleagues at ATDD also provided the test data, which consist of observations for 1986 at seven sites including three CORE (COre Research Establishment, for dry deposition) sites and four CORE satellite locations (Hales *et al.*, 1987). Differences in the results of the two computational schemes should indicate some of the uncertainties and difficulties involved when dry deposition is computed with RADM and when locally monitored air concentrations are used to infer dry deposition rates. In addition, we anticipate that some improvements in these approaches might be suggested.

SECTION 2

MODIFICATIONS OF THE RADM MODULE TO USE SITE-SPECIFIC DATA

The dry deposition module as described by Wesely (1988) has been modified to operate with inputs of hourly observations made at specific sites rather than with inputs generated by RADM. A copy of the code is given in Appendix I. Major changes were of course made with regard to input-output statements, which now conform in part with those in the site-specific, inferential approach. While no modifications were needed for the variables such as average wind speed (u, at a height of 10 m), solar irradiation, air temperature, and relative humidity, other parameters provided by RADM are not available from the site-specific data and thus must be derived or replaced in the module. These parameters include friction velocity (u_*), surface sensible heat flux, and height of the planetary boundary layer (z_i).

The aerodynamic (r_a) and sublayer (r_b) resistances in the unmodified RADM module are computed with knowledge of friction velocity and sensible heat flux. In the modified module, algorithms from the inferential method have been used to estimate these gas-phase resistances from the mean wind speed and the standard deviation of the horizontal wind direction (σ_θ) as described by Hicks *et al.* (1988). Some refinements have been made, however, to make the modified module imitate the RADM module. One refinement is that the aerodynamic resistances over landuse types other than the resistance (r_{ad}) of the dominant type at the local site are found as

$$r_{ai} = r_{ad}[\ln(10/z_o)/\ln(10/z_{od})]^{1.5}, \qquad (1)$$

where z_{od} is the aerodynamic surface roughness length for the dominant type, z_{oi} is for another type, and the reference height is 10 m. This procedure corresponds to the RADM practice of assuming that the product uu_* is constant over different surfaces in a 80-km grid square (Walcek *et al.*; 1986, Sheih *et al.*, 1986). Such adjustments allow a more realistic variation of r_a with surface roughness in an area several kilometers on a side. In addition, more

realistic estimates of r_b can be expected because they depend on friction velocity (Hicks *et al.*, 1988), which for the dominant landuse type is

$$u_{*d} = (u/r_{ad})^{0.5}, \tag{2a}$$

and for surfaces with different landuse types is

$$u_{*i} = u_{*d}[\ln(10/z_{od})/\ln(10/z_{oi})]^{0.5}. \tag{2b}$$

These changes account for different surface roughnesses but assume near-neutral atmospheric stability and, as a result, tend to overestimate the differences in r_a and r_b in unstable conditions and to underestimate the differences in stable conditions.

No adjustments such as given by Equations (1) and (2) are in the current version of the computer routines for the site-specific inferential approach, although use of such procedures may be desirable because the sites often have vegetation nearby with surface roughness lengths that are different by a factor of ten from that in the immediate vicinity of the meteorological measurement tower. For example, if the immediate surface is grass with a z_o of 5 cm and trees nearby have a z_o of 50 cm, r_a+r_b would change by approximately 50%. This would cause a variation of 50% in the deposition velocity for the extreme case of a substance such as HNO_3 that has a very small surface resistance. One must keep in mind, however, that the values of σ_θ found in the field might not be extremely accurate or might be taken at a site where the horizontal wind fluctuations are affected by a mixture of surface types upwind; such ambiguities lessen the importance of the adjustments made with Equations (1) and (2).

Another refinement with regard to estimating gas-phase resistances is in the method of estimating the surface deposition velocity v_{ds} for SO_4^{2-} in particles. In the calculation scheme for SO_4^{2-}, the inverse of v_{ds} replaces r_b plus any surface resistances, such as that due to bounce-off of particles. In the RADM module, computation of v_{ds} during moderately to strongly unstable atmospheric conditions requires knowledge of the mixed layer inversion height divided by the Obukhov stability length (z_i/L), as derived by Wesely *et al.*

(1985). For such conditions, the value of z_i/L can be estimated from the following formulation given by Panofsky and Dutton (1984):

$$\sigma_v/u_* = (12 - 0.5z_i/L)^{1/3}, \quad (3)$$

where the standard deviation σ_v of the lateral horizontal wind velocity can be estimated as $\sigma_\theta u$. This is an appropriate method for calculating v_{ds} because it conforms with the original reason suggested by Wesely et al. (1985) for employing z_i/L, which is that it provides a measure of the gustiness of horizontal wind fluctuations during unstable atmospheric conditions. The formulation used for v_{ds} in the site-specific inferential approach is currently $0.01u_*$, which is probably inferior but could easily be upgraded to follow the procedures used in the modified module.

The module is modified also with regard to identification of times when the surface is wetted by dew or rain. Wetting of the surface can cause a substantial increase in deposition velocity for substances with a moderately high solubility in water; dew is particularly effective in increasing SO_2 deposition for short periods of time. In the RADM module, identification of surface wetting is made entirely external to the module, but in the modified module a surface wetness sensor and a rain gauge at the monitoring stations provide the information directly. The modified module uses the same procedures as the site-specific inferential approach except that dew is identified with an algorithm derived from information provided by Monteith (1973), in an attempt to obtain information more reliable than that provided by the wetness sensor. Specifically, surface wetness caused by dew is assumed to occur when no rain occurs and the product (100-RH)(u+0.6) is less than 19% m s^{-1}.

These modifications to the RADM module clearly change its character somewhat. However, the most critical component for calculation of deposition velocities for most substances (excluding HNO_3) is the surface resistance (r_c), which is computed by procedures that for all practical purposes are identical in the RADM module and the modified module. Indeed, the reference set of resistance values given in data file MODINP.DAT on the last page of Appendix I and the coding to manipulate these values to obtain the bulk

surface resistances for the various substances are the same as those given for the RADM module (Wesely, 1988). Furthermore, the landuse map, assigned values of z_o, and seasonal categories are the same, as summarized in Table I.

Identification of seasonal categories is problematic for both versions of the module. In the modified module, they are identified by time of year and the percentage of full leaf coverage in the local vegetation, which is part of the site-specific data available. Seasonal category 1 (midsummer with lush vegetation) is assumed to be appropriate when leaf cover exceeds 90% of the maximum; category 2 (autumn with unharvested cropland) is assumed during the second half of the calendar year when leaf coverage is between 25 and 90%; category 5 (transitional spring with partial green coverage) has the same criteria as category 2 except that the date is for the first half of the calendar year. Seasonal category 3 (late autumn after frost, no snow) is assumed when leaf coverage is less than 25% and no snow is present. Seasonal category 4 (winter with snow on the ground) is assumed when leaf coverage is less than 25% and the wetness sensor indicates precipitation while the temperature is less than 0.5 °C; snow is assumed to remain as long as the temperature remains less than 5 °C. This procedure for determining when snow cover is present is untested, but such an expedient is necessary because snow cover is not recorded at the measurement station.

With these changes, the modified module appears to be as easy to implement as the site-specific inferential technique described by Hicks *et al.* (1988). Although the mechanics of implementation may be simple, our main concern is still whether the estimates of deposition velocities found with the modified module have a low level of uncertainty compared to the inferential method.

TABLE I

Landuse types, seasonal categories, and surface aerodynamic roughness lengths used to describe surface conditions in the module.

Landuse type	z_o (m) Seasonal category[a] 1	2	3	4	5
1. Urban land	1.00	1.00	1.00	1.00	1.00
2. Agricultural land	0.25	0.10	0.005	0.001	0.03
3. Range land	0.05	0.05	0.05	0.001	0.02
4. Deciduous forest	1.00	1.00	1.00	1.00	1.00
5. Coniferous forest	1.00	1.00	1.00	1.00	1.00
6. Mixed forest including wetland	1.00	1.00	1.00	1.00	1.00
7. Water, both salt and fresh water	*	*	*	*	*
8. Barren land, mostly desert	0.002	0.002	0.002	0.002	0.002
9. Non-forested wetland	0.15	0.10	0.10	0.001	0.10
10. Mixed agricultural and range land	0.10	0.08	0.02	0.001	0.03
11. Rocky open areas, low-growing shrubs	0.10	0.08	0.06	0.04	0.06

[a]Seasonal categories are (1) midsummer with lush vegetation, (2) autumn with unharvested cropland, (3) late autumn after frost and no snow, (4) winter with snow on the ground, and (5) transitional spring with partial green coverage.
*Computed.

SECTION 3

USE OF OBSERVATIONS AND DESCRIPTIONS OF SURFACE CONDITIONS

INPUT DATA

The observational data used in these analyses were collected during 1986 from the seven sites listed in Table II. The sites specified as ARG, OAK, and PSU are CORE stations, and the remainder are CORE satellite stations (Hales *et al.*, 1987). The data consist of hourly averages of mean wind speed (u) at a height of 10 m; the standard deviation of the horizontal wind direction (σ_θ) at a height of 10 m; solar irradiation; air temperature and relative humidity at a height of 10 m; rainfall amount; and surface wetness from a sensor that indicates the presence of moisture from dewfall and rainfall. Other data include one observation per week of the fraction of full leaf cover and the information given in Table II on surface vegetation characteristics. Although the deposition velocities (v_d) are computed for every hour, discussion in this report will address averages over periods of at least one week.

The distributions of landuse types at each of the seven sites are given in Table III. The local site distributions are derived from the descriptions of local surface vegetation (Table II); the landuse type of agricultural land rather than range land is indicated for the grass surface at ARG because the typical soil moisture and depth of the vegetative canopy are more suitable for the conditions assumed for agricultural land. For the landuse map cells in Table III, the areas correspond to the smallest cells (1/4 deg longitude by 1/6 deg latitude, roughly 20 km square) that include the locations of each measurement station. The uncertainties in the distributions within the landuse map cells are probably larger than for the other areas addressed in Table III, in part because these cells are at the limit of resolution of the landuse map. For example, the cell for ARG is designated as 65% urban, but the area within 10 km of the ARG site is actually mostly suburban with the abundance of lawns and trees usual for this region. For the RADM cells, the landuse distributions are the averages for the landuse map cells in the RADM-defined grid squares (approximately 80 km on a side) that encompass each site. Landuse types 8 through 11 are not listed in Table III because they do

TABLE II

Site names, locations, and surface vegetation (within one kilometer in all directions).

General location	Site ID	Location		Local surface vegetation (coverage)	
		N lat. (deg)	W long. (deg)	Primary	Secondary
Argonne National Laboratory, IL	ARG	41.70	87.98	grass (50%)	white oak (50%)
Bondville (Champaign), IL	BON	40.05	88.37	maize (50%)	soybeans (50%)
Oak Ridge, TN	OAK	35.96	84.28	white oak (70%)	loblolly pine (30%)
Panola State Park, GA	PAN	33.63	84.18	loblolly pine (50%)	chestnut, red oak (50%)
Pennsylvania State Univ., PA	PSU	40.72	77.92	maize (30%)	white oak (30%)
West Point, NY	WST	41.35	74.05	maple (60%)	white oak (30%)
Whiteface Mountain, NY	WHT	44.39	73.86	white birch (70%)	maple (10%)

not occur for any of these areas. Clearly, the distributions for the landuse map cells and the RADM cells are independent of local surface observations and rely only on the geographic locations specified.

A linear weighting of deposition velocities with landuse coverages is used in the module. The averaged deposition velocities for any area with the same representative meteorological and surface observations therefore differ only because of the use of different landuse distributions, which are described with one line of input data code for the modified module. Hence, it is very simple to exercise the module for various areas surrounding the measurement stations when the landuse distributions are known. In the inferential technique, the the overall surface resistance for a local site is

TABLE III.

Landuse distributions and computed HNO_3 deposition velocities at each location. The inferential method uses the information on plant species given in Table II rather than landuse data.

Site	Defined area	Year average v_d for HNO_3 ($cm\ s^{-1}$)	Percent cover by landuse type						
			1	2	3	4	5	6	7
ARG	Inferential method	2.06							
	Local site	2.38	0	50	0	50	0	0	0
	Landuse map cell	2.57	65	35	0	0	0	0	0
	RADM cell	1.95	23	62	0	2	0	0	13
BON	Inferential method	1.84							
	Local site	1.53	0	100	0	0	0	0	0
	Landuse map cell	1.60	5	95	0	0	0	0	0
	RADM cell	1.56	2	98	0	0	0	0	0
OAK	Inferential method	1.02							
	Local site	1.36	0	0	0	70	30	0	0
	Landuse map cell	1.02	0	40	0	55	0	0	5
	RADM cell	1.11	3	30	0	64	0	0	3
PAN	Inferential method	1.25							
	Local site	1.39	0	0	0	50	50	0	0
	Landuse map cell	1.18	0	30	0	15	20	35	0
	RADM cell	1.22	13	22	0	28	6	29	2
PSU	Inferential method	1.97							
	Local site	2.22	0	50	0	50	0	0	0
	Landuse map cell	2.61	15	20	0	65	0	0	0
	RADM cell	2.61	4	20	0	73	3	0	0
WST	Inferential method	1.87							
	Local site	2.20	0	0	0	100	0	0	0
	Landuse map cell	1.57	10	40	0	40	0	0	10
	RADM cell	1.72	41	3	0	28	0	2	26
WHT	Inferential method	1.88							
	Local site	2.25	0	0	0	100	0	0	0
	Landuse map cell	2.08	0	0	0	70	15	5	10
	RADM cell	1.97	1	6	0	28	10	43	12

computed as the summation of surface resistances in parallel, which include the resistances for the two dominant plant species (Table II) scaled according to their relative coverage amounts and an observed average leaf area index for the site.

Variations in the values of r_a+r_b depict changes in the above-canopy, gas-phase resistances as affected by changes primarily in wind speed, surface roughness, and atmospheric stability. To illustrate such effects, the yearly averages of v_d for HNO_3 are listed in Table III. These values are equal to $(r_a+r_b)^{-1}$, where r_b is specifically for HNO_3 but has values within ±50% of those for the other substances considered. The differences in the values of v_d at each site appear to be rather random and not biased systematically. The values for OAK and PAN, however, are notably smaller than those for the other sites. Since the surface roughnesses (z_o in Table I) for the prevalent landuse types (Table III) at these two locations are not greatly different from roughnesses for the prevalent landuse types at the other sites, the interrelated factors of wind speed and atmospheric stability apparently are atypical at OAK and PAN. A comparison of weekly averages of wind speed is shown in Figure 1 for these two sites and two others. The wind speeds at OAK and PAN are indeed unusually small, possibly because of measurements at relatively sheltered locations, instrument malfunctions, more frequent synoptic stagnation events at these southerly locations, or a combination of these factors. Further study is needed to determine the causes. Another interesting feature of Figure 1 is that the weekly averaged wind speeds at ARG and PSU relative to each other contain the same general trends and have similar major week-to-week variations, presumably because of similar synoptic changes. These trends and weekly variations are much less evident at OAK and PAN.

DEPOSITION VELOCITIES FOR VARIOUS LANDUSE TYPES

The above discussion is not intended to imply that meteorological conditions are more important than surface and substance characteristics. Usually these characteristics have a dominant effect on deposition velocities. To illustrate this effect, the figures in Appendix II show deposition velocities computed with the modified module for four substances and eight different landuse types, for the observations made at PSU during 1986. While

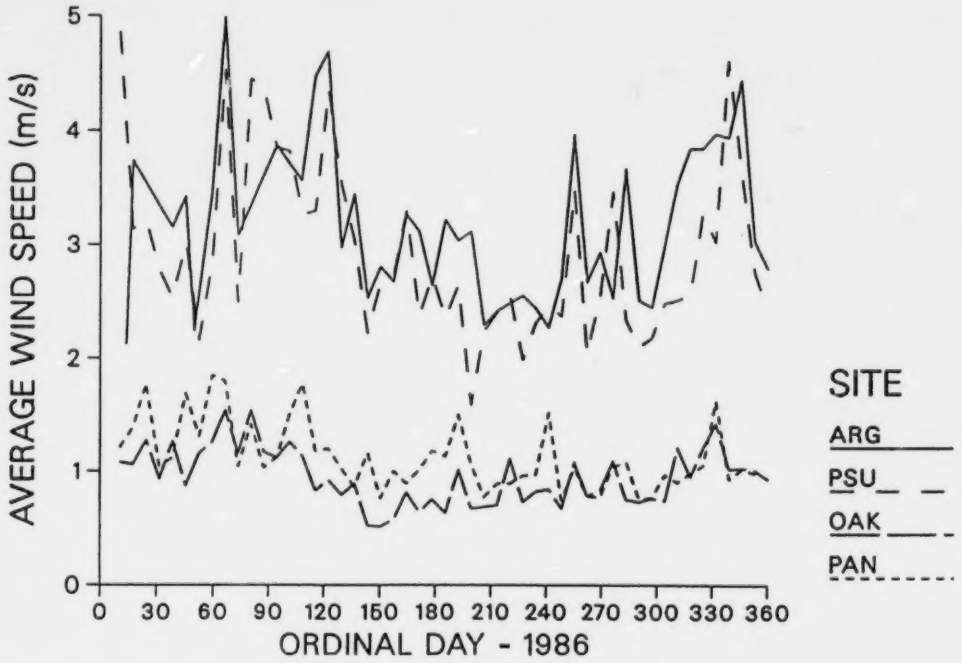

Fig. 1. Weekly averaged wind speeds observed at four measurement locations.

variations in v_d for HNO_3 show the strong effects of changes of mean wind speed and surface roughness associated with each landuse type (Figures II.5 and II.6), variations in in v_d for SO_2, O_3, SO_4^{2-}, and H_2O_2 are apparently caused by several other factors considered in the module. For example, the wetness of the surface and the presence of green, healthy vegetation accounts for most of the variations in v_d for SO_2 (Figures II.1 and II.2). The spikes for urban areas are caused by the assumption of very low resistances of surfaces wetted by rainfall and dew. Barren land (mostly desert) and water, though not present in the PSU area, represent extremes in moisture and thus extremes in deposition velocities. Extrapolation to water surfaces from land-based measurements is quite difficult and perhaps unrealistic in this case; the unusual, sustained peaks in v_d for SO_2 (Figure II.2) are probably due to small values of gas-phase resistance (surface resistance is zero) when u and σ_θ are large.

The deposition velocities shown in Appendix II for O_3 are relatively large above healthy green vegetation, are small for water and wetted surfaces, and are significant above senescent vegetation and nonvegetated land surfaces

(Figures II.3 and II.4). These differences reflect the assumptions made about surface resistances in the module. During the winter (seasonal categories 3 and 4), O_3 deposition velocities are usually smaller than SO_2 deposition velocities because of the frequent wetting of the surface by rain, fog, dew, frost, and snow, as detected by the wetness sensor at PSU. Hydrogen peroxide (Figures II.9 and II.10) tends to have higher deposition velocities than SO_2 and O_3 because H_2O_2 has both a rather high aqueous solubility, like SO_2, and a rapid chemical reactivity, like O_3 (Wesely, 1988). The deposition velocities computed for H_2O_2, however, are predictions without supporting field data, as is true for ten other substances that will be discussed later.

The computed deposition velocities for SO_4^{2-} (Figures II.7 and II.8) show variations unlike those for the other substances because the factors that have been found to control the deposition velocity for SO_4^{2-} are mainly wind speed, atmospheric stability, and type of surface and do not include surface wetness or the physiological status of vegetation. A special situation is assumed to exist in urban areas and above water, where the deposition velocities are limited by the small-scale smoothness of the surfaces involved. An unusual feature of the data is the series of peaks in deposition velocity between ordinal days of approximately 70 and 150 (Figures II.8). This springtime period is characterized by gusty winds that cause large σ_θ values that are interpreted as windy, unstable conditions resulting in relatively large deposition velocities for SO_4^{2-}.

SECTION 4

COMPARISONS OF RESULTS

WEEKLY AVERAGES

Weekly averages of deposition velocities for SO_2, O_3, HNO_3, and SO_4^{2-} at the seven sites during 1986 are shown graphically in Appendix III. The four graphs for each site display the results of the inferential technique and of the modified module applied with the three assumed areas and landuse distributions listed in Table III. To estimate the relative uncertainties of the algorithms used in the inferential and module computations of deposition velocity, the module executed with the landuse distributions for the local site should be used because they were chosen to conform as closely as possible to the surface vegetation descriptions employed in the inferential technique (Table II). For example, the ARG landuse distributions include 65% urban for the landuse map cell and 13% water for the RADM cell, which are not representative of the coverage of 50% agricultural land and 50% deciduous forest at the local site.

Scatter plots of the data produced with the inferential technique and with the module using the landuse distributions for the local sites are shown in Figure 2. Explanations for the structure and patterns that exist in these scatter plots and the associated figures of Appendix III are usually quite complicated, requiring discussion of the details of algorithms and computational procedures. Because such discussion can be carried out only to a limited extent in this report, the reader is referred to the descriptions by Hicks *et al.* (1985) and Wesely (1988) for further information to help in interpreting the results.

The unusual feature of a nearly vertical line of points for SO_2 and O_3 (Figures 2a and 2b) indicates that a minimum deposition velocity is computed with the inferential technique at the same time that strong variations are calculated with the module. The minimum deposition velocity corresponds to the inverse of the resistance of 1500 s m^{-1} assumed in the inferential technique for the sum of soil surface resistance to uptake and the gas-phase

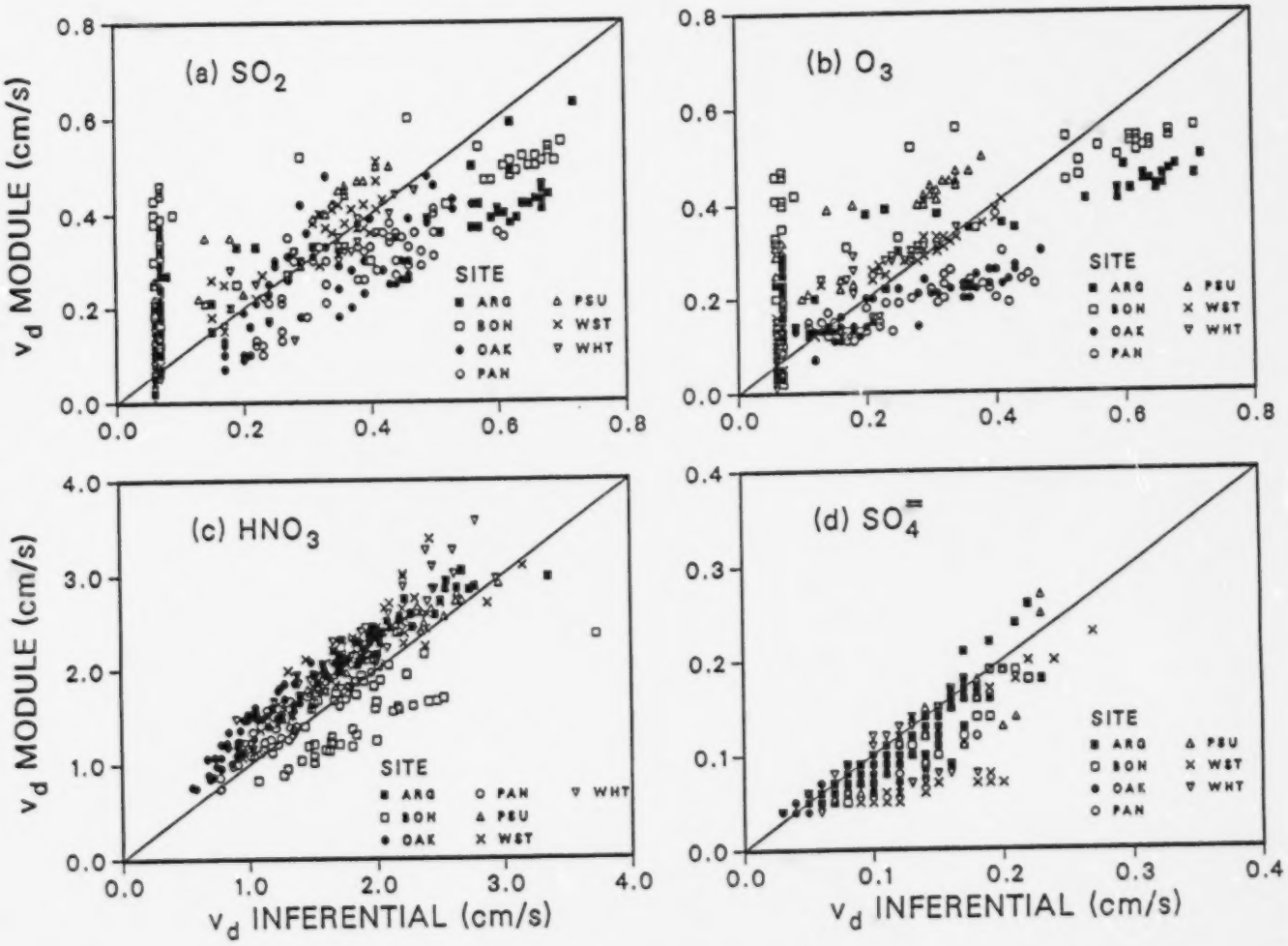

Fig. 2. Scatter diagrams of deposition velocities computed with the modified module using local site landuse distributions, versus estimates made with the inferential technique.

resistance for transport through a vegetative canopy. This sum unfortunately represents the only pathway of small resistance in the inferential technique (with the present model) when the leaves of vegetation are inactive or absent or when vegetative cover is removed as a result of agricultural practices. A more realistic and complex situation is assumed with the module, in which soil resistances are assigned smaller, more representative numbers, and gas-phase resistances in canopies are varied according to landuse type, season, and time of day. (In addition, a significant sink of O_3 is assumed to exist at times in the lower portions of vegetative canopies, but this sink has a relatively minor effect.) Hence, we expect the largest discrepancies between the inferential and module approaches to occur when a large amount of bare soil is exposed without a complete canopy cover. Such is the case during the nonsummer seasons at sites that have a preponderance of agricultural land, as is evident in Appendix III for ARG (Figures III.1 and III.2), BON (Figures III.5 and III.6), and PSU (Figures III.17 and III.18).

It is instructive to consider next the deposition velocities for HNO_3 and thus examine the gas-phase resistances represented by the inverse of v_d for HNO_3, because these gas-phase resistances enter at least partially in the computations of deposition velocities for all substances. The feature of a nearly vertical line of points is not seen in the plot for HNO_3 in Figure 2c, because its deposition is not unduly restricted by soil surface resistance in the inferential computational procedures. In fact, the bulk surface resistance for HNO_3 is always assumed to be very small. The module estimates of v_d for HNO_3 tend to be larger than those obtained with the inferential technique in part because of the effects of applying Equations (1) and (2) when the dominant landuse type assumed has a smaller value of z_o than the other types for the site. Another factor is that the changeover from stable to unstable conditions is assumed to occur in the procedures used with the module when σ_θ exceeds $1.1[\ln(10/z_{od})]^{-1}$, which is when larger values of r_a and r_b are imposed (decreasing v_d). This changeover point is usually larger than the value of 0.2 rad presently used with the inferential technique [for which Hicks *et al.* (1985) specified 0.175]. Conversely, this factor and the action of Equations (1) and (2) tend to increase r_a+r_b and thus decrease v_d when one landuse type is assigned all of the coverage and has a very small designated value of z_o, such as agricultural land after harvest and in the

winter. Such a case occurs for BON, as is evident in Figure 2c and in Appendix III (Figures III.5 and III.6) for ordinal days less than 150 and greater than 280.

The deposition velocities for SO_4^{2-} are quite small, particularly for the module estimates. The values produced by the module are extremely sensitive via Equation (3) to the values of measured σ_θ, which might be underestimated if the wind vanes in the field are not properly maintained. On the other hand, the assumption used by the inferential technique that $v_{ds} = 0.01u_*$ will lead to overestimates of SO_4^{2-} deposition velocities in moderately unstable atmospheric conditions.

SEASONAL AVERAGES

A rather large amount of scatter exists in the weekly averaged estimates of deposition velocities plotted in Figure 2. Aside from the nearly vertical lines of points on the left-hand sides of Figures 2a and 2b, the inferential technique on the average produces larger estimates of deposition velocities than does the modified module for SO_2, O_3, and SO_4^{2-} and slightly smaller estimates for HNO_3. Much of the discussion above suggested that systematic differences between the two approaches may be different from season to season, which would increase the overall scatter of the data in Figure 2. If such systematic differences can be understood, then judgements might be possible on how to improve various aspects of the approaches, or appropriate research might be suggested to reduce the uncertainties of deposition velocity estimates.

Deposition velocities averaged over seasonal categories at each of the seven sites are compared in Table IV. Seasonal categories 3 and 4 are combined for this comparison because switching between these categories is accomplished on an hour-to-hour basis rather than weekly; inspection of the results has shown that the effects of snow in these data sets are minor. As was already discussed, the deposition velocities for SO_2 and O_3 computed with the inferential technique are relatively small for a significant portion of the time at ARG, BON, and PSU. That is, the surface resistances for sparse vegetation and bare soil are computed to be much larger with the inferential technique, as presently configured, than with the dry deposition module. As

TABLE IV

Differences between weekly averaged deposition velocities computed with the module (subscript m) applied with the local site landuse types and those found with the inferential method (subscript i).

			SO_2				O_3				HNO_3				SO_4^{2-}			
	C	n	Δv_d	ΔV_d	σ_i	σ_m	Δv_d	ΔV_d	σ_i	σ_m	Δv_d	ΔV_d	σ_i	σ_m	Δv_d	ΔV_d	σ_i	σ_m
ARG:	1	23	0.19	37	10	18	0.16	32	22	15	-0.38	-18	14	11	0.01	6	17	20
	2	4	-0.05	-19	93	54	-0.08	-46	56	23	-0.42	-20	15	11	0.01	11	24	16
	3,4	15	-0.14	-92	50	49	-0.13	-88	53	48	-0.24	-11	23	14	0.02	19	34	43
	5	4	0.03	9	45	12	0.00	-1	46	11	-0.25	-9	4	5	-0.02	-7	13	16
BON:	1	16	0.13	24	12	12	0.09	16	14	10	0.00	0	16	10	0.04	30	17	22
	2	3	-0.12	-50	49	27	-0.18	-70	47	17	0.18	12	16	19	0.01	12	28	20
	3,4	25	-0.24	-99	61	41	-0.18	-99	56	68	0.51	33	22	20	0.01	11	41	48
	5	3	0.00	2	18	8	-0.06	-10	29	2	0.57	25	40	18	0.03	18	11	22
OAK:	1	24	0.11	29	15	24	0.11	40	24	15	-0.25	-26	22	20	0.00	1	26	26
	2	3	-0.02	-5	15	8	0.04	27	19	5	-0.41	-36	28	28	0.00	6	11	20
	3,4	20	0.03	12	20	57	0.02	16	28	19	-0.45	-32	19	13	0.01	13	35	21
	5	3	0.17	58	5	12	0.14	47	8	14	-0.22	-16	20	19	0.00	4	6	11
PAN:	1	25	0.12	32	16	15	0.13	45	26	16	-0.09	-8	24	24	0.01	10	32	28
	2	4	-0.03	-8	8	8	0.01	11	26	10	-0.35	-25	28	28	0.01	8	15	17
	3,4	16	0.06	24	12	36	0.04	23	23	16	-0.20	-14	24	21	0.03	27	36	30
	5	5	0.15	41	8	12	0.15	50	8	7	0.01	1	21	22	0.01	8	15	16
PSU:	1	17	-0.08	-20	10	11	-0.11	-30	12	12	-0.32	-16	9	9	0.01	4	14	15
	2	6	-0.06	-33	37	8	-0.10	-54	33	10	-0.30	-16	21	16	0.03	27	20	16
	3,4	25	-0.14	-99	24	33	-0.10	-85	22	59	-0.21	-10	20	16	0.02	24	47	50
	5	3	-0.11	-33	30	7	-0.16	-48	26	4	-0.15	-6	5	3	-0.03	-12	13	21
WST:	1	18	-0.03	-8	11	12	0.00	-1	21	19	-0.20	-12	32	25	0.01	9	41	38
	2	5	-0.06	-30	36	23	0.00	-3	29	7	-0.31	-18	27	22	0.06	68	43	16
	3,4	25	-0.04	-48	28	50	-0.04	-46	22	44	-0.45	-20	20	15	0.05	50	40	30
	5	3	0.00	0	28	33	-0.01	-5	20	9	-0.01	-1	29	27	0.03	14	30	28
WHT:	1	15	0.03	8	21	26	-0.03	-11	17	14	-0.31	-16	21	20	0.00	-3	19	20
	2	5	0.01	7	52	43	0.00	-2	31	4	-0.38	-21	28	26	0.02	28	26	24
	3,4	27	-0.01	-19	34	70	-0.01	-18	21	72	-0.44	-19	27	25	0.03	35	37	24
	5	3	0.00	0	15	4	-0.04	-17	31	20	-0.14	-8	24	22	0.00	0	36	31

C is the seasonal category, n is the number of weeks, Δv_d is the difference (cm s^{-1}), ΔV_d is the percentage difference (relative to the mean), and σ is standard deviation expressed as a percentage (relative to the mean deposition velocity).

is shown in Table IV, this discrepancy occurs mostly for seasonal categories 3 and 4, which is consistent with the results shown in in Appendix III (Figures III.1, III.2, III.5, III.6, III.17, and III.8, typically for ordinal days less than 120 and greater than 270). Some of this discrepancy also occurs for seasonal category 5 (usually for less than a month between days 80 and 130), when the vegetative cover is sparse in agricultural areas. For seasonal category 2 (autumn leaf areas between 25% and 90% of the maximum, assumed to correspond to unharvested cropland), the inferential estimates are also slightly smaller, but comparison to the standard deviations of the deposition velocities during the rapidly changing conditions usually found in this seasonal category indicates that these differences are relatively insignificant.

The situation is somewhat reversed during the summertime seasonal category (1), when the inferential technique produces significantly larger estimates of deposition velocities for SO_2 and O_3 at ARG, BON, OAK, and PAN than does the module. These larger estimates can also be seen in the appropriate four pairs of figures in Appendix III (between ordinal days of approximately 120 and 270) and are associated with the clusters of points beneath the 1:1 line of Figures 2a and 2b for ARG, BON, OAK, and PAN. In general, one would expect the inferential technique to produce smaller stomatal resistances and thus larger deposition velocities than the module, because the inferential technique in its present configuration assumes that water stress is negligible. The module, on the other hand, only indirectly assumes characteristic soil moisture conditions because the estimates of stomatal resistance are based primarily on fragmentary experimental evidence in which soil water conditions were not measured directly. An additional source of scatter is the fact that the module does not consider the differences in the stomatal resistances of various plant species that might occur within each landuse type.

Overall, the inferential technique and the modified module produce estimates of seasonal average deposition velocities within ±30% of each other for SO_2 and O_3, if we neglect the strong differences that occur during seasonal categories 3 and 4 when the inferential technique probably overestimates surface resistances. This relative uncertainty of ±30% could

be lessened if the algorithms for stomatal resistance in the module were tailored for individual plant species and the algorithms in the inferential method were altered slightly to assume a small amount of soil moisture stress. Such changes in the algorithms for the purposes of reducing uncertainty, however, would be best justified by comparison to experimental data.

The differences shown in Table IV for HNO_3 deposition velocities have already been shown to result from the methods of computing gas-phase resistances, where the inferential technique assumes that they are the same for different types of surface cover at each site, while the modified module attempts to alter these resistances in a manner similar to that used in the RADM module. Comparison of values of ΔV_d (difference in deposition velocity, expressed as a percent of the mean) to values of σ shows that the differences are often quite significant, as is also evident in Figure 2c. The values in Table IV do not show a seasonal variation in these differences that is repeated from site to site. Hence, changes in the differences in v_d computed by each of the two techniques are apparently mostly due to variations of the distributions of landuse types used in the module. Overall, it appears that the estimates of seasonal averages of deposition velocities for HNO_3 have a relative uncertainty of about ±30%. Both approaches as used here, however, assume that no significant effects are caused by nonuniform terrain, edges between types of vegetation, and other surface irregularities that might increase atmospheric mixing, reduce gas-phase resistances, and thus increase deposition velocities. Wind sheltering by surface obstacles might have the opposite effect in some locations. Thus, the estimate of ±30% is probably smaller than the real limits of accuracy.

The absolute values of Δv_d for SO_4^{2-} in Table IV are very small and thus may have very little impact on calculations that could be made on sulfur removal from the atmosphere and deposition on the surface. As was discussed above, the modified module tends to estimate smaller deposition velocities for SO_4^{2-} than the inferential technique, because of differences in the algorithms that process the observational data. While a repeated seasonal variation in the differences is not evident, particularly large values of ΔV_d are seen for seasonal categories 2, 3, and 4 for WST. These large relative differences correspond to the points farthest beneath the 1:1 line of Figure 2d. Overall, the relative uncertainty in seasonal averages in the deposition velocities for SO_4^{2-} appears to be approximately ±50%.

AVERAGES OVER LARGER AREAS

Deposition velocities estimated with the module using the local site landuse distributions are compared in Table V with results from the module using the landuse types for RADM grid cells. For BON, the differences are extremely small because the landuse distributions for the two areas of different size are nearly identical (Table III). The change in landuse distributions for PSU appears to be minor, but the effect on v_d for HNO_3 is rather large because the change involves a shift between agricultural land and deciduous forest, which have quite different surface roughness lengths (Table 1). In general, small alterations in landuse distributions that might occur when the size of the area addressed is expanded or reduced around the measurement location appear capable of altering weekly averages of v_d for HNO_3 by approximately ±30%. Perhaps the second most significant effect evident in Table V is that greater amounts of urban and water areas increase the deposition velocities for SO_2 during nonsummer conditions at ARG and WST. For SO_4^{2-}, these two landuse types are associated with smaller deposition velocities. For O_3 at WST, the effects of increased urban and water areas notably decrease deposition velocities during the summer and spring (seasonal categories 1 and 5).

When one ignores the strong sensitivity of v_d for HNO_3 to landuse types of different surface roughnesses and the effects of changing the amounts of urban and water areas, the computed seasonally averaged deposition velocities for the RADM grid squares encompassing these seven measurement stations are fairly typical of the velocities computed for the local sites, usually within ±20%. This conclusion should not be taken as generally valid at other measurement sites where changes in landuse distributions with increasing area are different than at the seven sites, because the variation of deposition velocities with changes in landuse types is often very strong, as is illustrated in Appendix II.

TABLE V

Differences between weekly averaged deposition velocities computed with the module using the landuse types for RADM grid cells (subscript R) and those found with the module using local site landuse types (subscript s).

			SO_2				O_3				HNO_3				SO_4^{2-}			
	C	n	Δv_d	ΔV_d	σ_s	σ_R	Δv_d	ΔV_d	σ_s	σ_R	Δv_d	ΔV_d	σ_s	σ_R	Δv_d	ΔV_d	σ_s	σ_R
ARG:	1	23	-0.06	-14	18	16	0.04	10	15	10	0.36	17	11	12	0.04	30	20	15
	2	4	-0.10	-33	54	40	-0.04	-16	23	21	0.46	22	12	12	0.00	3	16	17
	3,4	15	-0.12	-44	48	46	-0.02	-11	48	48	0.52	25	14	16	0.01	12	43	30
	5	4	-0.17	-38	12	3	0.01	2	11	5	0.51	19	5	7	0.08	44	16	10
BON:	1	16	0.00	1	12	12	0.01	1	10	10	-0.01	-1	10	10	0.00	1	22	23
	2	3	0.00	0	27	27	0.00	1	17	18	-0.03	-2	19	18	0.00	0	20	20
	3,4	25	0.00	0	41	40	0.00	1	68	67	-0.03	-3	20	20	0.00	0	48	48
	5	3	0.00	1	8	8	0.01	2	2	2	-0.03	-2	18	18	0.00	2	22	20
OAK:	1	24	-0.01	-4	24	22	-0.03	-13	15	14	0.14	14	20	21	0.01	13	26	25
	2	3	0.02	6	8	9	-0.04	-29	5	10	0.25	20	28	25	0.01	14	20	13
	3,4	20	-0.02	-9	57	37	-0.04	-28	19	18	0.37	25	13	13	0.01	23	21	20
	5	3	-0.04	-18	12	6	-0.04	-16	14	9	0.26	20	19	16	0.02	20	11	8
PAN:	1	25	-0.02	-5	15	16	-0.02	-8	16	15	0.11	9	24	24	0.01	14	28	26
	2	4	-0.04	-10	8	15	-0.04	-25	10	12	0.20	14	28	26	0.00	4	17	10
	3,4	16	-0.03	-12	36	28	-0.03	-18	16	14	0.26	18	21	21	0.01	14	30	26
	5	5	-0.02	-6	12	11	-0.02	-9	7	6	0.20	14	22	21	0.02	19	16	16
PSU:	1	17	0.04	9	11	12	0.05	14	12	14	-0.21	-10	9	8	-0.01	-4	15	18
	2	6	0.03	16	8	9	0.06	28	10	9	-0.32	-14	16	16	0.01	8	16	15
	3,4	25	0.06	31	33	37	0.04	27	59	54	-0.53	-21	16	14	0.00	-1	50	51
	5	3	0.08	22	7	15	0.08	20	5	6	-0.41	-14	3	5	-0.03	-11	21	21
WST:	1	18	-0.01	-2	12	11	0.10	40	19	12	0.40	24	25	26	0.05	52	38	30
	2	5	-0.14	-49	23	11	-0.02	-13	7	4	0.41	24	22	23	0.01	12	17	17
	3,4	25	-0.17	-90	50	36	-0.01	-8	44	36	0.54	24	15	15	0.01	16	30	19
	5	3	-0.08	-22	33	6	0.09	35	9	2	0.51	24	27	28	0.08	62	28	27
WHT:	1	15	0.00	1	26	20	0.04	17	14	11	0.23	12	20	20	0.01	10	20	18
	2	5	-0.05	-25	43	20	0.00	-2	4	4	0.24	13	26	26	-0.01	-18	24	24
	3,4	29	-0.05	-45	69	55	0.00	5	70	66	0.32	14	25	25	-0.02	-24	24	27
	5	3	0.00	1	4	6	0.04	17	20	20	0.22	13	22	23	0.01	9	31	34

Symbols are as in Table IV.

SECTION 5

OTHER CONSIDERATIONS

FLUXES

The fluxes at the measurement stations can be computed as the products of deposition velocity and concentration. Weekly averages of these two variables are used here because weekly averages of the concentrations measured with a filterpack system are readily available (Hosker and Womack, 1986). The resulting flux estimates might be slightly biased because of correlations between the diurnal trends of deposition velocity and concentrations (e.g., see Meyers and Yuen, 1987). We will ignore this source of error, which could make some of the weekly SO_2 flux estimates too small by as much as 30%, in order to provide a limited demonstration of the type of deposition computations that can be made. Future work at the Atmospheric Turbulence and Diffusion Division of NOAA's Air Resources Laboratory will include applying the inferential technique at many sites in a more rigorous manner (Dr. T. P. Meyers, private communication, 1988).

Examples of weekly dry deposition amounts computed with the inferential technique and with the modified module using the landuse distribution for the local site (ARG) are shown in Figure 3. The peak in SO_2 deposition rate occurs in late spring, when both the deposition velocity (Figure III.2) and concentrations of SO_2 are fairly high. Most of the major variations in HNO_3 flux are caused by changes in concentration, because the weekly averaged deposition velocities are fairly steady throughout the year. As is expected, the fluxes of SO_4^{2-} are small compared to the SO_2 fluxes. The differences between the fluxes estimated by the two approaches are caused entirely by the differences in the computed deposition velocity, which have already been discussed. For example, the SO_2 fluxes found with the inferential technique for summer are larger than those found with the modified module, but are smaller for the winter. Since the absolute differences in the SO_2 fluxes are greatest during the summertime, the net effect of the seasonal differences in deposition velocity is that significantly greater annual SO_2 dry deposition is computed with the inferential technique.

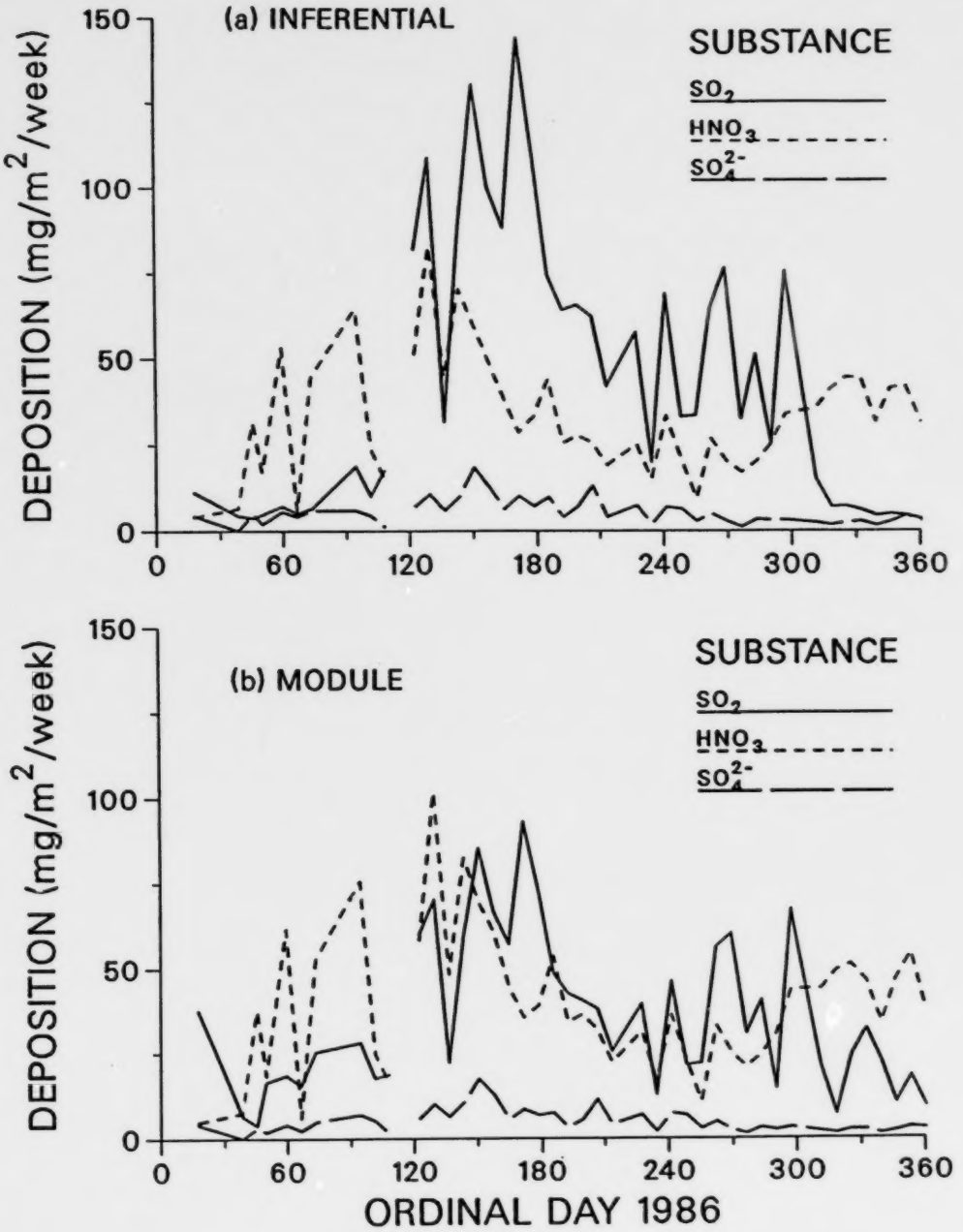

Fig. 3. Estimates of of SO_2, HNO_3, and SO_4^{2-} deposition at ARG, computed as the product of weekly averages of deposition velocities and concentrations.

OTHER SUBSTANCES

The deposition velocities for ten additional substances can be estimated with the RADM module (Wesely, 1988), a capability that is carried over to the modified module. Graphs of such deposition velocities are provided in Appendix IV for each of the seven sites, where the module has been applied with the landuse distributions for the local sites. If the concentrations of these substances were known at the measurement stations, the modified module could be used to make preliminary computations of the fluxes. Fairly large deposition velocities are shown for NO_2, NH_3, HNO_2, and formic acid (ORA, organic acid). For most of the substances, however, these deposition velocities at present are only predictions that have little, if any, supporting experimental evidence. Also, emissions from the soil or vegetation are not taken into account, although future research might indicate how this could be done.

SECTION 6

CONCLUSIONS

The dry deposition module of the Regional Acid Deposition Model (RADM) has been successfully adapted to use site-specific data obtained at dry deposition stations such as the CORE satellite sites. The data inputs for the modified module include those used by the inferential technique: hourly observations of mean wind speed, the standard deviation of the horizontal direction, solar irradiation, air temperature, relative humidity, and the presence and cause of surface wetness. In addition, the fraction of maximum leaf area (LAI, leaf area index) reported once every week for the vegetation in the area surrounding the measurement station is used to determine the seasonal category, which must be specified for the module. The modified module can be executed with any assumed distribution of the 11 landuse types used in the RADM module, including the distribution that corresponds best to the relative amounts of the species of vegetation found at the local site. In the inferential technique, the fraction of maximum LAI and the coverage by various vegetative species are used to provide relatively detailed parameterizations of dry deposition by vegetative species. This detailed information on vegetation amounts and types certainly suffices for determining the module landuse types for the local site.

The coding for the inferential technique and the data for seven sites for 1986 were provided by the Atmospheric Turbulence and Diffusion Division of NOAA's Air Resources Laboratory. This information was applied to compute the deposition velocities for SO_2, O_3, HNO_3, and SO_4^{2-} both by the inferential technique and by the modified module using three different landuse distributions. In addition to a landuse distribution conforming to the local site conditions, distributions were used for the smallest cells (approximately 20 km square) of the computerized landuse map and for the RADM grid squares (approximately 80 km square) encompassing the measurement stations.

The module was originally written to use more complete local micrometeorological information than is included in the parameters listed above, so considerable manipulation of the coding was needed in the RADM module in order to accept these inputs. Perhaps the least exact formulations in the modified module are those that deal with estimating atmospheric stability, but uncertainties introduced by the compromised equations are probably overshadowed by the fact that most of the sites are located in areas with surface properties insufficiently uniform, or with terrain insufficiently flat, to allow very precise micrometeorological calculations. The algorithms in the modified module to compute crucial parameters such as aerodynamic resistance above the surface and friction velocity are quite similar to those used in the inferential technique. Some notable differences exist, however. One is that the modified module attempts to mimic the RADM module by computing changes in the gas-phase resistances for surfaces identified by landuse types different from the dominant landuse type for the local site. At most of the sites, this alteration produces smaller aerodynamic resistances and larger friction velocities averaged over the areas surrounding the site, and thus increases the deposition velocities for HNO_3. The deposition velocities for other substances do not seem to be significantly affected because their surface resistances are usually much larger than the aerodynamic and gas-phase sublayer resistances (which depend on friction velocity).

The algorithms used in the modified module to compute the bulk surface resistance, usually the most important term for determining deposition velocities, are the same as those used in the RADM module. Some changes had to be made in the parameterizations of the SO_4^{2-} gas-phase sublayer resistance, which strongly controls SO_4^{2-} deposition velocity, but the changes conform with interpretation of the field experiments on which the parameterizations are based. The inferential technique is configured somewhat differently and appears to overestimate the deposition velocity for SO_4^{2-} in some situations. The module, however, tends to underestimate when the standard deviation of the horizontal wind direction is not measured very well.

The most striking difference between the results of the module and the inferential technique is the much smaller estimates made with inferential technique for SO_2 and O_3 deposition velocities during nonsummer conditions. These are probably underestimates caused by overly restrictive assumptions on the surface resistances of bare soil and sparse vegetation during nonsummer seasons, which could easily be adjusted by changing the values of a few numerical coefficients used in the inferential technique.

While the algorithms for surface resistance in the modified module are based on a more complex and versatile set of multiple surface resistances to various portions of the surface than the algorithms used in the current version of the inferential technique, the module is strongly limited by the fact that the surface can be described by only 11 landuse types. The inferential technique employs description of vegetation by species and tailors the surface resistances more precisely than the module to describe the physiological responses to environmental parameters such as solar irradiation and temperature. An additional feature that may be desirable is a factor to take into account soil moisture stress on the stomatal resistances of healthy vegetation during the daytime, because the current version of the inferential technique assumes no soil moisture stress and the module is effectively tuned to a small amount of moisture stress. As a result, the deposition velocities of substances such as SO_2 and O_3 that are strongly influenced by stomatal resistances are slightly larger when computed by the inferential technique than with the modified module.

For the weekly averages of deposition velocities computed for 1986 at the seven sites, the inferential technique and the modified module produce estimates within about ±30% of each other for SO_2 and O_3, if we neglect the strong differences that occur during nonsummer conditions at surfaces with bare soil or sparse vegetative canopies. Likewise, the differences for HNO_3 and SO_4^{2-} deposition velocities are usually about ±30% and ±50%, respectively. These relative uncertainties could probably be reduced somewhat if suggestions made above were adopted.

Estimates of deposition velocities over large areas are easily computed with the modified module by use of the appropriate landuse distributions. Of course, if the areas are very large, the observations of meteorological conditions at the measurement stations might not be sufficiently representative. Some trial runs involving the 20-km squares of the landuse map cell and the 80-km RADM cells at the seven measurement sites show that the estimates of weekly averaged deposition velocities for SO_2, O_3, and SO_4^{2-} are fairly sensitive to the amounts of urban and water areas included in landuse distributions. Aside from this effect, the deposition velocities calculated for these three substances over the RADM grid cells are usually within ±20% of those for the local site descriptions. These limits should not be taken as generally valid at sites other than the seven examined in this study, because different meteorological conditions and altered combinations of landuse types could cause larger changes in deposition velocities. For HNO_3, minor changes in the assumed landuse distributions often cause rather large changes, easily ±30%, in deposition velocities.

We conclude that the differences in deposition velocity estimates caused by scaling from local site conditions to RADM grid cells are often slightly smaller than the relative uncertainties of the deposition velocities estimated with the modified module and the inferential technique. Hence, inferences of deposition velocities for the local conditions at carefully chosen sites appear to be reasonably representative of areas extending at least to sizes of RADM grid squares. Nevertheless, adjustments for changes in surface conditions are clearly desirable, and extrapolation to types of surfaces that have notably different properties can be made only at the cost of considerably greater uncertainty. By use of a computerized landuse map or, preferably, a more detailed description of surface conditions, one should be able to estimate weekly averaged dry deposition amounts for sulfur, nitric acid, and ozone to within about ±30% over some fairly large areas.

The above number of 30% is not the true uncertainty or accuracy. An assessment of accuracy would require experiments designed specifically for dry deposition, because a number of factors can cause additional uncertainty. For example, one must determine how representative the local meteorological measurements actually are. The relatively low wind speeds measured at OAK and

PAN (Figure 1) suggest that proper exposure of instruments in a forested, hilly area might be difficult. In addition, measurements taken at sites not representative of any one surface or influenced by local aerodynamic obstacles might not be suitable for application of the algorithms used in the inferential and the module approaches. Finally, these algorithms do not directly consider the effects of surface nonuniformities in the area considered, including hills, isolated surface irregularities, and edges associated with changes in height of surface cover. The aerodynamic resistances could be strongly altered by surface nonuniformities, and stomatal resistances could be altered by varying degrees of shading of sunlight by hills and other vegetation.

REFERENCES

Hales, J. M., Hicks, B. B., and Miller, J. M.: 1987, The role of research measurement networks as contributors to federal assessments of acid deposition. *Bull. Am. Meteorol. Soc.* **68**, 216-225.

Hicks, B. B., Baldocchi, D. D., Meyers, T. P., Hosker, R. P., Jr., and Matt, D. R.: 1988, A preliminary multiple resistance routine for deriving dry deposition velocities from measured quantities. *Water, Air, and Soil Pollut.* **36**, 311-330.

Hicks, B. B., Baldocchi, D. D. Hosker, R.P., Jr., Hutchison, B. A., McMillen, R. T., and Satterfield, L. C.: 1985, *On the Use of Monitored Air Concentrations to Infer Dry Deposition (1985)*, NOAA Technical Memorandum ERL ARL-141, 65 pp.

Hosker, R. P. Jr. and Womack, J. D.: 1986, Simple meteorological and chemical filter pack monitoring system for estimating dry deposition of gaseous pollutants. In *Proceedings of the 5th Annual National Symposium on Recent Advances in the Measurement of Air Pollutants*, Raleigh, North Carolina, 14-16 May 1985, EPA/600/9-85/029 (Available from NTIS, Springfield, VA), pp. 23-29.

Meyers, T. P. and Yuen, T. S.: 1987, An assessment of averaging strategies associated with day/night sampling of dry-deposition fluxes of SO_2 and O_3. *J. Geophys. Res.* **92**, 6705-6712.

Monteith, J. L.: 1973, *Principles of Environmental Physics*, American Elsevier Publishing Company, Inc., New York.

Panofsky, H. A. and Dutton, J. A.: 1984, *Atmospheric Turbulence*, John Wiley & Sons, New York.

Sheih, C. M., Wesely, M. L., and Walcek, C. J.: 1986, *A Dry Deposition Module for Regional Acid Deposition*, U.S. Environmental Protection Agency Report, EPA/600/3-86/037, (Available as PB86218104 from NTIS, Springfield, VA) 63 pp.

Walcek, C. J., Brost, R. A., Chang, J. S., and Wesely, M. L.: 1986, SO_2, sulfate and HNO_3 deposition velocities computed using regional landuse and meteorological data. *Atmos. Environ.* **20**, 949-964.

Wesely, M. L.: 1988, *Improved Parameterizations for Surface Resistance to Gaseous Dry Deposition in Regional-Scale Numerical Models*, U.S. Environmental Protection Agency Report (available from NTIS, Springfield, VA) (in press).

Wesely, M. L., Cook, D. R., Hart, R. L., and Spear, R. E.: 1985, Measurements and parameterization of particulate sulfur over grass. *J. Geophys. Res.* **90**, 2131-2143.

Appendix I

Coding for the modified module.

```
C     MODDEP2.FOR
C*** This is for computing deposition velocities for specific
C     sites, surrounding immediate areas, and surrounding grid
C     squares for selected routine measurement sites.
C
C*** The deposition velocities are computed  for (1) SO2,
C     (2) O3, (3) NO2, (4) NO, (5) HNO3, (6) H2O2, (7) ALD
C     actually acetaldehyde, (8) HCHO, (9) OP actually methyl
C     hydroperoxide, (10) PAA, (11) ORA actually formic acid,
C     (12) NH3, (13) PAN, (14) HNO2, and (15) SO4.
C*** No estimates are made of surface emissions.
C
C*** This program was constructed by M. L. Wesely and
C     B. M. Lesht, with earlier imput by C. M. Sheih, at
C     Argonne National laboratory.
C
C*** Observed parameters are JDAY,---, and RAIN as defined below:
C     JDAY = Julian date;
C     U = average wind speed (m/s);
C     STHETA = standard deviation of wind direction;
C     RG = solar irradiation (W/m**2);
C     TA = air temperature;
C     RH = relative humicity (%);
C     CWET = canopy wetness (0-1)
C     RAIN = rainfall (mm)
C*** Some derived or additional input parameters are:
C     INIT= 1 (yes) or 0 (no) for initialization of parameters;
C     ISESN = 1, midsummer, with lush vegetation
C             2, autumn, with unharvested cropland
C             3, late autumn after frost, no snow
C             4, winter, with snow on ground
C             5, transitional spring with partial green coverage;
C     VDSMAX = maximum permissable surface SO4 deposition
C     velocity for various landuse types and seasons;
C     HSTAR = Henry's Law constant for substances 1 through 14,
C             for water pH near 7;
C     F0 = measure of reactivity for substances 1 through 14,
C          relative to O3;
C     DIFRAT = ratio of molecular diffusivity for substances 1
C              through 14 in air to diffusivity for water vapor;
C*** Computed parameters.
C     HV = virtual heat flux (W/m**2);
C     RA = aerodynamic resistance (s/m);
C     USTAR = friction velocity (m/s);
C     R = bulk surface (non-gaseous) resistances.
C     VDSITE = deposition velocity (m/s) for site;
C     VDAREA = deposition velocity for area given by smallest
C              increment of longitude and latitude for site;
C     VDSQAR =   deposition velocity for grid square of
C                approximately 100 km square centered on site;
C
C*** Resistances and deposition velocities are computed for
C     specific landuse types obtained from a landuse map,
C     derived from surface landuse and land cover inventory
C     by S. H. Page of Lockheed Engineering and Management
C     Services Inc., Remote Sensing Laboratory, Las Vegas,
C     Nevada 89114.
C*** There are eleven landuse types as follows:
C      1, urban land, almost no vegetation;
C      2, agricultural land, usually well watered;
C      3, range land, usually with low soil moisture;
C      4, deciduous forest;
C      5, coniferous forest;
C      6, mixed forest including wetland;
C      7, water, sea water assumed but used for fresh water also;
C      8, barren land, mostly desert;
C      9, non-forested wetland;
C     10, mixed agricultrual and range land;
C     11, rocky open areas occupied by low-growing shrubs.
C
C
```

```
      IMPLICIT INTEGER*2 (I-N)
      INTEGER TIME,JDBRK(20),PCTBRK(20)
      LOGICAL*1 COM(70),DUMMY(70)
      LOGICAL LAST
      CHARACTER*16 FNAME
      CHARACTER*36 STATION
      CHARACTER*12 OUTFILE
      DIMENSION IUSE(11),ISQUSE(11),IZO(11),ZO(11),RA(11),USTAR(11),
     1 VDSMAX(11),HSTAR(14),FO(14),DIFRAT(14),DC(14),XRI(11),
     2 XRLU(11),XRAC(11),XRGSS(11),XRGSO(11),XRCLS(11),XRCLO(11),
     3 RI(11),RLU(11),RAC(11),RGSS(11),RGSO(11),RCLS(11),RCLO(11),
     4 R(15,11),RSUM(14),VDSITE(15),VDAREA(15),VDSQAR(15),
     5 VDSUM(3,15),VDSSUM(3,15),VMEAN(3,15),VSTD(3,15),VDDAY(3,15),
     6 DAYSUM(3,15),VARG(3,15)
C
C*** Initialize some parameters.
      ISNOW=0
C
C*** Open file for values of maximum SO4 deposition velocities.
C     (VDSMAX), surface roughness lengths (IZO), and surface
C     components (RI, RLU, RAC, RGSS, RGSO, RCLS, RCLO).
        OPEN(UNIT=5,FILE='MODINP.DAT',RECORDTYPE='VARIABLE',
     1STATUS='OLD',FORM='FORMATTED')
C
C*** Open file for landuse inputs.
        OPEN(UNIT=6,FILE='LUSE.DAT',RECORDTYPE='VARIABLE',
     1STATUS='OLD',FORM='FORMATTED')
C
C*** Set values for substance chemical and physical properties.
      DATA HSTAR/1.0E+05,0.01,.01,.003,1.0E+14,1.0E+05,15.,6000.,240.
     1,540.,4.0E+06,20000.,3.6,1.0E+05/
      DATA FO/0.,1.,.1,0.,0.,1.,0.,0.,.1,.1,0.,0.,.1,0./
      DATA DIFRAT/1.9,1.6,1.6,1.3,1.9,1.4,1.6,1.3,1.6,2.0,1.6,.97,
     1 2.6,1.6/
C
C     THETA is the terrain slope, assumed to be zero radians for RADM
      THETA=0.
C
C*** Get the station index number from the input data file.
      READ(*,*) NSTIN
C*** Get the JDAYS for determining ISESN.
C     NBPTS is the number of points input; PCTBRK is the
C     integer percentage, for which the first and last values
C     should be zero.
      READ(*,*) NBPTS
      READ(*,*) (JDBRK(IKAY),PCTBRK(IKAY),IKAY=1,NBPTS)
      IBRK=1
C*** Open file to read station name.
      OPEN(7,FILE='STATION.DAT',STATUS='OLD')
      DO 1 I=1,NSTIN
    1 READ(7,*) INDEX,STATION,X1,X2,L1,L2,X3,X4,L3,L4,L5,L6,X5
      CLOSE(7)
C
C*** Read in local landuse category and landuse data for immediate
C     area.
      DO 2 II=1,NSTIN
      READ(6,900) INDEX,NSITE,IUSITE,NSIT,IUSIT,(IUSE(N),N=1,11)
  900 FORMAT(5I3,9X,11I4)
C*** Read in landuse date for local grid square, approximately
C     100 km square.
    2 READ(6,910) (ISQUSE(N),N=1,11)
  910 FORMAT(24X,11I4)
      CLOSE(6)
C
C*** Get the name of the current met data file.
 4000 READ(*,3,END=4001) FNAME
    3 FORMAT(A)
      NREC=0
C
C
```

```
C*** Initialize counters and accumulators.
      INUST=0
      INSTN=0
      USUM=0.0
      ICWET=0
      NDAY=0
      DO 4 I=1,3
      DO 4 J=1,15
      VDSUM(I,J)=0.0
      VDSSUM(I,J)=0.0
      VDDAY(I,J)=0.0
    4 DAYSUM(I,J)=0.0
C*** Read input data from file.
      OPEN(8,FILE=FNAME,STATUS='OLD')
C*** Skip header records.
      DO 5 I=1,3
    5 READ(8,3)
C
      ISES=0
C*** ISES=0 so that INIT=1 defined intially in  to permit
C    reading of MONINP.DAT  only once for each seasonal
C    category and then set INIT=0 to bypass initialization.
C
      DO 100 II=1,10000
C
      READ(8,*,END=500)JDAY,TIME,U,STHETA,RG,TA,RH,CWET,RAIN
C*** Save starting day and time for this file.
      IF(II.EQ.1) THEN
        IFDAY=JDAY
        IDDAY=JDAY
        ITIME=TIME
        IDTIME=TIME
        NDREC=0
        LAST=.FALSE.
      ENDIF
C*** Check for missing met data.
      IF(U.GE.99.9.OR.STHETA.GE.99.9.OR.RG.GE.9999.9.OR.
     1 TA.GE.999.9.OR.RH.GE.999.9.OR.CWET.GE.9.99.OR.
     2 RAIN.GE.999.90) GOTO 100
C    Check for negative solar irradiation.
      IF (RG.LT.0.0) RG=0.0
C    Check for low value of STHETA
      IF (STHETA.LT.1.0) STHETA=1.0
C
C*** Check to see if the day accumulators need to be updated.
  600 INDAY=IDDAY+1
      IF(INDAY.GT.365) INDAY=INDAY-365
      IF((JDAY.GE.INDAY.AND.TIME.GE.IDTIME).OR.(LAST)) THEN
        IDDAY=JDAY
        IDTIME=TIME
        IF(NDREC.GE.20) THEN
          NDAY=NDAY+1
          DO 6 IALI=1,3
          DO 6 JALI=1,15
          DAYSUM(IALI,JALI)=DAYSUM(IALI,JALI)+
     1    VDDAY(IALI,JALI)/FLOAT(NDREC)
     6    VDSSUM(IALI,JALI)=VDSSUM(IALI,JALI)+
     1    (VDDAY(IALI,JALI)/FLOAT(NDREC))**2
        ELSE
          DO 7 IALI=1,3
          DO 7 JALI=1,15
     7    VDDAY(IALI,JALI)=0.0
        ENDIF
        NDREC=0
        IF(LAST) GOTO 700
      ELSE
        NDREC=NDREC+1
      ENDIF
C*** End of input file.
      NREC=NREC+1
      USUM=USUM+U
C
```

```
C*** Use JDAY to find ISESN
    8 IF((IBRK.LT.NBPTS).AND.(JDAY.GT.JDBRK(IBRK+1))) THEN
       IBRK=IBRK+1
       GOTO 8
      ENDIF
      IF(RAIN.GT.0..AND.TA.LT.0.5) ISNOW=1
      IF(TA.GT.5.) ISNOW=0
      IF(PCTBRK(IBRK).GE.90) THEN
        ISESN=1
      ELSE
        IF(PCTBRK(IBRK).GE.25..AND.PCTBRK(IBRK).LT.90) THEN
          IF(JDAY.LE.181) ISESN=5
          IF(JDAY.GT.181) ISESN=2
        ENDIF
        IF(PCTBRK(IBRK).LT.25) THEN
           IF(ISNOW.EQ.0) ISESN=3
           IF(ISNOW.EQ.1) ISESN=4
        ENDIF
      ENDIF
      IF(ISESN.NE.ISES) INIT=1
      ISES=ISESN
C
C*** READ IN MODINP.DAT
      IF(INIT.NE.1) GOTO 25
C*** Read in maximum permissible SO4 deposition velocities.
C*** I is landuse type.
C*** Read a dummy line first.
      READ(5,1000) DUMMY
      READ(5,1000) DUMMY
 1000 FORMAT(70A1)
      DO 16 L=1,5
      IF(L.NE.ISESN) GOTO 14
      READ(5,1100) COM,(VDSMAX(I),I=1,11)
 1100 FORMAT(70A1/(11F6.3))
      GOTO 16
   14 READ(5,1100) COM,(C1,I=1,11)
   16 CONTINUE
C*** Read a dummy line.
      READ(5,1000) DUMMY
C*** Read IZO (surface roughness) of proper season.
      DO 22 L=1,5
      IF(L.NE.ISESN) GOTO 20
      READ(5,1200) COM,(IZO(I),I=1,11)
 1200 FORMAT(70A1/11I6)
      GOTO 22
   20 READ(5,1200) COM,(IC1,I=1,11)
   22 CONTINUE
C*** Read a dummy line.
      READ(5,1000) DUMMY
C*** Read in inital values of surface resistance components.
      L=0
   23 L=L+1
      READ(5,1000) COM
      READ(5,1300) (XRI(I),I=1,11)
      READ(5,1300) (XRLU(I),I=1,11)
      READ(5,1300) (XRAC(I),I=1,11)
      READ(5,1300) (XRGSS(I),I=1,11)
      READ(5,1300) (XRGSO(I),I=1,11)
      READ(5,1300) (XRCLS(I),I=1,11)
      READ(5,1300) (XRCLO(I),I=1,11)
 1300 FORMAT(5X,11F6.0)
      IF(L.NE.ISESN) GOTO 23
      REWIND 5
C*** Convert to appropriate units.
      DO 24 I=1,11
      ZO(I)=IZO(I)*1.E-4
   24 CONTINUE
      INIT=0
      STHCUT=1.1/(ALOG(10./ZO(NSITE)))
   25 CONTINUE
C
```

```
C*** Compute USTAR.
C     Convert STHETA to radians.
      STHETA=STHETA*0.01745
C     Sigma theta cutoff if value exceeds specified limit.
      IF(STHETA.GT..5) STHETA=0.5
C     If neutral or stable, cut off STHETA.
      IF((RG.LT.10.).AND.(STHETA.GT.STHCUT)) STHETA=STHCUT
C*** Check stability, wind speed, and solar irradiation.
      IF (U.EQ.0.0) U=0.12
      IF((U.LT..2).AND.(RG.LE.100.)) THEN
        U=0.12
        IF(RG.LE.100) THEN
          RAA=1000.
          INSTN=INSTN+1
        ELSE
          RAA=25.
          INUST=INUST+1
        ENDIF
        DO 26 NI=1,11
   26   RA(NI)=RAA
      ELSE
C     Compute aerodynamic resistance.
        RA(NSITE)=1./(STHETA*STHETA*U)
        IF(STHETA.GT.STHCUT.AND.(RG.GT.100)) THEN
          RA(NSITE)=9.*RA(NSITE)
          INUST=INUST+1
        ELSE
          RA(NSITE)=4.*RA(NSITE)
          INSTN=INSTN+1
        ENDIF
C*** Compute RAs for different landuse types.
        DO 27 NI=1,11
   27   RA(NI)=RA(NSITE)*
     1  (ALOG(10./Z0(NI))/ALOG(10./Z0(NSITE)))**1.5
      ENDIF
C     Determine USTAR from RA and U.
C
      USTAR(NSITE)=(U/RA(NSITE))**0.5
      DO 28 NI=1,11
   28  USTAR(NI)=USTAR(NSITE)*
     +  (ALOG(10./Z0(NSITE))/ALOG(10./Z0(NI)))**0.5
C
C*** Determine if dew or rain-wetted surface exists,
C     based in part on Monteith (1973).
      IDEW=0
      IRAIN=0
      IF(((100.-RH)*(U+0.6)).LT.19.) THEN
        ICFLG=1
      ELSE
        ICFLG=0
      ENDIF
      IF((CWET.GT..5).AND.(CWET.LT.1)) CWET=1
      IF(RH.GT.95) CWET=1
      IF((CWET.GT.0.).AND.(RAIN.GT.0)) THEN
       IRAIN=1
      ELSE
       IF(ICFLG.EQ.1) THEN
         ICWET=ICWET+1
         IDEW=1
       ENDIF
      ENDIF
C
C     Initialize variables.
      C1=(273.+TA)/273.
      C2=C1**1.75*1.0E-04
      DO 31 K=1,15
      VDSITE(K)=0.
      VDAREA(K)=0.
      VDSQAR(K)=0.
      IF(K.NE.15) DC(K)=0.219*C2/DIFRAT(K)
   31 CONTINUE
      XNU=0.151*C1**1.77*1.0E-04
C
```

```
C*** Compute bulk surface resistances for gases.
C*** Adjust external surface resistances for temperature.
      RT=1000.*EXP(-TA-4.)
      DO 40 N=1,11
      RI(N)=XRI(N)
      RLU(N)=XRLU(N)+RT
      RAC(N)=XRAC(N)
      RGSS(N)=XRGSS(N)+RT
      RGSO(N)=XRGSO(N)+RT
      RCLS(N)=XRCLS(N)+RT
   40 RCLO(N)=XRCLO(N)+RT
      DO 44 N=1,11
C*** Set initial max. and min. values for resistance components.
      IF(RI(N).GE.9999.) RI(N)=100000.
      IF(RLU(N).GE.9999.) RLU(N)=100000.
      IF(RAC(N).GE.9999.) RAC(N)=100000.
      IF(RGSS(N).GE.9999.) RGSS(N)=100000.
      IF(RGSO(N).GE.9999.) RGSO(N)=100000.
      IF(RCLS(N).GE.9999.) RCLS(N)=100000.
      IF(RCLO(N).GE.9999.) RCLO(N)=100000.
      IF(RAC(N).LT.1.) RAC(N)=1.
      IF(RGSS(N).LT.1.) RGSS(N)=1.
      GFACTOR=100.
      RIX=RI(N)
C*** Adjust stomatal resistances for insolation and temp.
      IF(RI(N).GE.9999.) GOTO 42
      IF(TA.LE.0..OR.TA.GE.40.) GOTO 41
      GFACTOR=400./TA/(40.-TA)
C
   41 RGPP1=RG+0.1
C
      RIX=RI(N)*(1.+(200./RGPP1)**2.)*GFACTOR
C*** Adjust stomatal resistances for liquid water coverage.
      IF(IDEW.EQ.1.OR.IRAIN.EQ.1) RIX=3.*RIX
C*** Compute aerodynamic resistance to lower elements in lower
C     part of canopy or structure.
   42 RDC=100.*(1.+1000./(RG+10.))/(1.+1000.*THETA)
C*** Compute resistances for SO2.
      X=1./(3.*RLU(N))
      RLUX=RLU(N)
C     Adjust for effects of dew and rain.
      IF(TA.GT.0.5) THEN
        IF(RLUX.LT.9999..AND.IDEW.EQ.1) RLUX=100.
        IF(RLUX.LT.9999..AND.IRAIN.EQ.1) RLUX=1./(1./5000.+X)
        IF(N.EQ.1.AND.(IDEW+IRAIN).GE.1) RLUX=50.
      ENDIF
      R(1,N)=1./(1./(DIFRAT(1)*RIX)+1./RLUX+1./(RAC(N)+RGSS(N))
     1 +1./(RDC+RCLS(N)))
C*** Compute resistance for O3.
      RLUX=RLU(N)
C     Adjust for effects of dew and rain.
      IF(TA.GT.0.5) THEN
        IF(RLUX.LT.9999..AND.IDEW.EQ.1) RLUX=1./(1./3000.+X)
        IF(RLUX.LT.9999..AND.IRAIN.EQ.1) RLUX=1./(1./1000.+X)
      ENDIF
      R(2,N)=1./(1./(DIFRAT(2)*RIX)+1./RLUX+1./(RAC(N)+RGSO(N))
     1 +1./(RDC+RCLO(N)))
C*** Compute resistances for (3) NO2,(4) NO, (5) HNO3, AND (4-12)
C     other substances for which solubility, aqueous redox, and
C     diffusivity ratio relative to water vapor in air are specified.
      DO 43 K=3,14
      RIXX=RIX*DIFRAT(K)+1./(HSTAR(K)/3000.+100*F0(K))
      RLUXX=RLU(N)/(HSTAR(K)/1.0E+5 + F0(K))
C     Adjust for effects of dew or rain.
      IF((IDEW+IRAIN).GE.1.AND.TA.GT.0.5.AND.RLU(N).LT.9999.)
     1 RLUXX=1./(1./(3.*RLUXX)+HSTAR(K)/1.0E+07+F0(K)/RLUX)
      RGSX=1./(HSTAR(K)/1.0E+05/RGSS(N)+F0(K)/RGSO(N))
      RCLX=1./(HSTAR(K)/1.0E+05/RCLS(N)+F0(K)/RCLO(N))
      R(K,N)=1./(1./RIXX+1./RLUXX+1./(RAC(N)+RGSX)
     1 +1./(RDC+RCLX))
   43 CONTINUE
   44 CONTINUE
C
C
```

```
C*** Set max. and min. values for bulk surface resistances.
      DO 45 K=1,14
      DO 45 N=1,11
      IF(R(K,N).GT.9999.)R(K,N)=9999.
   45 IF(R(K,N).LE.1.)R(K,N)=10.
C
C
C*** LOOP THROUGH DIFFERENT LANDUSE TYPES.
      DO 70 N=1,11
      IF((IUSE(N).EQ.0).AND.(ISQUSE(N).EQ.0).AND.
     1 (N.NE.NSITE).AND.(N.NE.NSIT)) GOTO 70
      IF(N.NE.7) GOTO 50
C*** Set values of roughness length for water. (This assumes
C    that NSITE is not equal to 7.)
      Z0(7)=1.4E-02*USTAR(7)*USTAR(7)/9.8+1.1E-01*XNU/USTAR(7)
   50 CONTINUE
C*** Compute SO4 surface deposition velocities.
      VDS=0.002*USTAR(N)
      IF((STHETA.GT.STHCUT).AND.(RG.GT.250.).AND.
     1 (Z0(N).GT.0.001)) THEN
        ZIFE=(2.*(STHETA*U/USTAR(NSITE))**3.-24.)**0.667
        VDS=0.0009*USTAR(N)*ZIFE
      ENDIF
C*** Set VDS to be less than VDSMAX.
      CVDS=VDS
      IF(CVDS.GT.VDSMAX(N)) CVDS=VDSMAX(N)
      DO 64 K=1,14
C*** Compute deposition velocities for each grid point.
C*** VDs are converted to cm/s.
       RSUB=1.75*(DIFRAT(K))**0.667/(0.4*USTAR(N))
   64 RSUM(K)=RA(N)+R(K,N)+RSUB
      DO 65 K=1,14
      IF(N.EQ.NSITE) VDSITE(K)=VDSITE(K)+IUSITE/RSUM(K)
      IF(N.EQ.NSIT) VDSITE(K)=VDSITE(K)+IUSIT/RSUM(K)
      VDAREA(K)=VDAREA(K)+IUSE(N)/RSUM(K)
   65 VDSQAR(K)=VDSQAR(K)+ISQUSE(N)/RSUM(K)
      IF(N.EQ.NSITE) VDSITE(15)=VDSITE(15)+
     1 IUSITE/(1./CVDS+RA(N))
      IF(N.EQ.NSIT) VDSITE(15)=VDSITE(15)+
     1 IUSIT/(1./CVDS+RA(N))
      VDAREA(15)=VDAREA(K)+IUSE(N)/(1./CVDS+RA(N))
      VDSQAR(15)=VDSQAR(15)+ISQUSE(N)/(1./CVDS+RA(N))
   70 CONTINUE
C*** THIS ENDS THE MAIN COMPUTATIONAL LOOP FOR DEP. VELOCITIES.
      DO 80 JJ=1,15
      VDSUM(1,JJ)=VDSUM(1,JJ)+VDSITE(JJ)
      VDSUM(2,JJ)=VDSUM(2,JJ)+VDAREA(JJ)
      VDSUM(3,JJ)=VDSUM(3,JJ)+VDSQAR(JJ)
      VDDAY(1,JJ)=VDDAY(1,JJ)+VDSITE(JJ)
      VDDAY(2,JJ)=VDDAY(2,JJ)+VDAREA(JJ)
   80 VDDAY(3,JJ)=VDDAY(3,JJ)+VDSQAR(JJ)
  100 CONTINUE
C*** THIS COMPLETES PROCESSING OF ONE WEEK OF DATA.
C
C
```

```
C*** Calculate the mean and standard deviation for the week.
  500 LAST=.TRUE.
      CLOSE(8)
      GOTO 600
  700 DO 101 I=1,3
      DO 101 J=1,15
      VMEAN(I,J)=VDSUM(I,J)/FLOAT(NREC)
      IF(NDAY.GT.1.) THEN
        VARG(I,J)=(VDSSUM(I,J)-
     1  (DAYSUM(I,J)*DAYSUM(I,J)/FLOAT(NDAY)))/FLOAT(NDAY-1)
      ELSE
        VARG(I,J)=0.0
      ENDIF
      IF(VARG(I,J).GE.0.0) THEN
        VSTD(I,J)=SQRT(VARG(I,J))
      ELSE
        VSTD(I,J)=0.0
      ENDIF
  101 CONTINUE
C
C
C*** WRITE OUTPUTS.
      UMEAN=USUM/FLOAT(NREC)
C*** outputs for SO2, O3, HNO3, SO4, H2O2:  M=1
C*** Open the output files.
C     In "*.XNM", X=A refers to averages, X=S refers to standard
C      deviations and counters; N=1,2,3 refers to site, area, and
C      grid square average, respectively, of variables; M=1,2,3
C      refers to which set of five substances.
C     Open files for first set of substances.
      OUTFILE=STATION(1:8)//'.A11'
      OPEN(1,FILE=OUTFILE,STATUS='UNKNOWN',ACCESS='APPEND')
      OUTFILE=STATION(1:8)//'.S11'
      OPEN(11,FILE=OUTFILE,STATUS='UNKNOWN',ACCESS='APPEND')
      OUTFILE=STATION(1:8)//'.A21'
      OPEN(2,FILE=OUTFILE,STATUS='UNKNOWN',ACCESS='APPEND')
      OUTFILE=STATION(1:8)//'.S21'
      OPEN(12,FILE=OUTFILE,STATUS='UNKNOWN',ACCESS='APPEND')
      OUTFILE=STATION(1:8)//'.A31'
      OPEN(3,FILE=OUTFILE,STATUS='UNKNOWN',ACCESS='APPEND')
      OUTFILE=STATION(1:8)//'.S31'
      OPEN(13,FILE=OUTFILE,STATUS='UNKNOWN',ACCESS='APPEND')
      DO 102 I=1,3
C     for site, area, and grid square:  *.*1M, *.*2M, *.*3M
      II=I+10
C     for averages (*.ANM) and other statistics (*.SNM)
      WRITE(I,3000)FNAME,IFDAY,ITIME,JDAY,TIME,VMEAN(I,1),
     1 VMEAN(I,2),VMEAN(I,5),VMEAN(I,15),VMEAN(I,6),NREC
      WRITE(II,3010)FNAME,IFDAY,ITIME,JDAY,TIME,VSTD(I,1),
     1 VSTD(I,2),VSTD(I,5),VSTD(I,15),VSTD(I,6),UMEAN,
     2 INSTN,INUST,ICWET,NREC,NDAY
      CLOSE(I)
      CLOSE(II)
  102 CONTINUE
C
C*** outputs for NO, NO2, PAN, NH3, HNO2; M=2
C     Open files for second set of substances.
      OUTFILE=STATION(1:8)//'.A12'
      OPEN(1,FILE=OUTFILE,STATUS='UNKNOWN',ACCESS='APPEND')
      OUTFILE=STATION(1:8)//'.S12'
      OPEN(11,FILE=OUTFILE,STATUS='UNKNOWN',ACCESS='APPEND')
      OUTFILE=STATION(1:8)//'.A22'
      OPEN(2,FILE=OUTFILE,STATUS='UNKNOWN',ACCESS='APPEND')
      OUTFILE=STATION(1:8)//'.S22'
      OPEN(12,FILE=OUTFILE,STATUS='UNKNOWN',ACCESS='APPEND')
      OUTFILE=STATION(1:8)//'.A32'
      OPEN(3,FILE=OUTFILE,STATUS='UNKNOWN',ACCESS='APPEND')
      OUTFILE=STATION(1:8)//'.S32'
      OPEN(13,FILE=OUTFILE,STATUS='UNKNOWN',ACCESS='APPEND')
```

```
      DO 103 I=1,3
C     for site, area, and grid square:  *.*1M, *.*2M, *.*3M
      II=I+10
C     for averages (*.ANM) and other statistics (*.SNM)
      WRITE(I,3000)FNAME,IFDAY,ITIME,JDAY,TIME,VMEAN(I,4),
     1 VMEAN(I,3),VMEAN(I,13),VMEAN(I,12),VMEAN(I,14),NREC
      WRITE(II,3010)FNAME,IFDAY,ITIME,JDAY,TIME,VSTD(I,4),
     1 VSTD(I,3),VSTD(I,13),VSTD(I,12),VSTD(I,14),UMEAN,
     2 INSTN,INUST,ICWET,NREC,NDAY
      CLOSE(I)
      CLOSE(II)
  103 CONTINUE
C
C*** outputs for ALD, HCHO, OP, PAA, ORA; M=3
C     Open files for third set of substances.
      OUTFILE=STATION(1:8)//'.A13'
      OPEN(1,FILE=OUTFILE,STATUS='UNKNOWN',ACCESS='APPEND')
      OUTFILE=STATION(1:8)//'.S13'
      OPEN(11,FILE=OUTFILE,STATUS='UNKNOWN',ACCESS='APPEND')
      OUTFILE=STATION(1:8)//'.A23'
      OPEN(2,FILE=OUTFILE,STATUS='UNKNOWN',ACCESS='APPEND')
      OUTFILE=STATION(1:8)//'.S23'
      OPEN(12,FILE=OUTFILE,STATUS='UNKNOWN',ACCESS='APPEND')
      OUTFILE=STATION(1:8)//'.A33'
      OPEN(3,FILE=OUTFILE,STATUS='UNKNOWN',ACCESS='APPEND')
      OUTFILE=STATION(1:8)//'.S33'
      OPEN(13,FILE=OUTFILE,STATUS='UNKNOWN',ACCESS='APPEND')
      DO 104 I=1,3
C     for site, area, and grid square:  *.*1M, *.*2M, *.*3M
      II=I+10
C     for averages (*.ANM) and other statistics (*.SNM)
      WRITE(I,3000)FNAME,IFDAY,ITIME,JDAY,TIME,VMEAN(I,7),
     1 VMEAN(I,8),VMEAN(I,9),VMEAN(I,10),VMEAN(I,11),NREC
      WRITE(II,3010)FNAME,IFDAY,ITIME,JDAY,TIME,VSTD(I,7),
     1 VSTD(I,8),VSTD(I,9),VSTD(I,10),VSTD(I,11),UMEAN,
     2 INSTN,INUST,ICWET,NREC,NDAY
      CLOSE(I)
      CLOSE(II)
  104 CONTINUE
 3000 FORMAT(' ',1H',A16,1H',I4,I5,I6,I5,5F8.2,I5)
 3010 FORMAT(' ',1H',A16,1H',I4,I5,I6,I5,5F10.4,F6.2,5I5)
C
      GOTO 4000
 4001 CONTINUE
      STOP
      END
```

```
C    MODINP.DAT
C********** Maximum SO4 dep. velocities (m/s;11F6.3), types 1-11
C       1, Midsummer with lush vegetation
 0.001 0.01  0.01  0.01  0.01  0.01  0.001 0.01  0.01  0.01  0.01
C       2, Autumn with unharvested cropland
 0.001 0.01  0.01  0.001 0.008 0.004 0.001 0.01  0.01  0.01  0.01
C       3, Late autmn after frost, no snow
 0.001 0.01  0.01  0.001 0.008 0.004 0.001 0.01  0.01  0.01  0.01
C       4, Winter with snow on ground
 0.001 0.01  0.01  0.001 0.008 0.004 0.001 0.01  0.01  0.01  0.01
C       5, Transitional spring with partial green coverage
 0.001 0.01  0.01  0.01  0.01  0.01  0.001 0.01  0.01  0.01  0.01
C********** Values of Zo (1.E-4 m; 11I6), landuse types 1-11
C       1, Midsummer with lush vegetation
 10000  2500   500 10000 10000 10000     1    20  1500  1000  1000
C       2, Autumn with unharvested cropland
 10000  1000   500 10000 10000 10000     1    20  1000   800   800
C       3, Late autumn after frost, no snow
 10000    50   500 10000 10000 10000     1    20  1000   200   600
C       4, Winter with snow on ground
 10000    10    10 10000 10000 10000     1    20    10    10   400
C       5, Transitional spring with partial green coverage
 10000   300   200 10000 10000 10000     1    20  1000   300   600
C********** Values of surface resistance components (s/m)
C       1, Midsummer with lush vegetation
ri   9999.   60.  120.   70.  130.  100. 9999. 9999.   80.  100.  150.
rlu  9999. 2000. 2000. 2000. 2000. 2000. 9999. 9999. 2500. 2000. 4000.
rac   100.  200.  100. 2000. 2000. 2000.    0.    0.  300.  150.  200.
rgsS  400.  150.  350.  500.  500.  100.    0. 1000.    0.  220.  400.
rgs0  300.  150.  200.  200.  200.  300. 2000.  400. 1000.  180.  200.
rclS 9999. 2000. 2000. 2000. 2000. 2000. 9999. 9999. 2500. 2000. 4000.
rcl0 9999. 1000. 1000. 1000. 1000. 1000. 9999. 9999. 1000. 1000. 1000.
C       2, Autumn with unharvested cropland
ri   9999. 9999. 9999. 9999.  250.  500. 9999. 9999. 9999. 9999. 9999.
rlu  9999. 9000. 9000. 9000. 4000. 8000. 9999. 9999. 9000. 9000. 9000.
rac   100.  150.  100. 1500. 2000. 1700.    0.    0.  200.  120.  140.
rgsS  400.  200.  350.  500.  500.  100.    0. 1000.    0.  300.  400.
rgs0  300.  150.  200.  200.  200.  300. 2000.  400.  800.  180.  200.
rclS 9999. 9000. 9000. 9000. 2000. 4000. 9999. 9999. 9000. 9000. 9000.
rcl0 9999.  400.  400.  400. 1000.  600. 9999. 9999.  400.  400.  400.
C       3, Late autumn after frost, no snow
ri   9999. 9999. 9999. 9999.  250.  500. 9999. 9999. 9999. 9999. 9999.
rlu  9999. 9999. 9000. 9000. 4000. 8000. 9999. 9999. 9000. 9000. 9000.
rac   100.   10.  100. 1000. 2000. 1500.    0.    0.  100.   50.  120.
rgsS  400.  150.  350.  500.  500.  200.    0. 1000.    0.  200.  400.
rgs0  300.  150.  200.  200.  200.  300. 2000.  400. 1000.  180.  200.
rclS 9999. 9999. 9000. 9000. 3000. 6000. 9999. 9999. 9000. 9000. 9000.
rcl0 9999. 1000.  400.  400. 1000.  600. 9999. 9999.  800.  600.  600.
C       4, Winter with snow on ground
ri   9999. 9999. 9999. 9999.  400.  800. 9999. 9999. 9999. 9999. 9999.
rlu  9999. 9999. 9999. 9999. 6000. 9000. 9999. 9999. 9000. 9000. 9000.
rac   100.   10.   10. 1000. 2000. 1500.    0.    0.   50.   10.   50.
rgsS  100.  100.  100.  100.  100.  100.    0. 1000.  100.  100.   50.
rgs0  600. 3500. 3500. 3500. 3500. 3500. 2000.  400. 3500. 3500. 3500.
rclS 9999. 9999. 9999. 9000.  200.  400. 9999. 9999. 9000. 9999. 9000.
rcl0 9999. 1000. 1000.  400. 1500.  600. 9999. 9999.  800. 1000.  800.
C       5, Transitional spring with partial green coverage
ri   9999.  120.  240.  140.  250.  190. 9999. 9999.  160.  200.  300.
rlu  9999. 4000. 4000. 4000. 2000. 3000. 9999. 9999. 4000. 4000. 8000.
rac   100.   50.   80. 1200. 2000. 1500.    0.    0.  200.   60.  120.
rgsS  500.  150.  350.  500.  500.  200.    0. 1000.    0.  250.  400.
rgs0  300.  150.  200.  200.  200.  300. 2000.  400. 1000.  180.  200.
rgsS 9999. 4000. 4000. 4000. 2000. 3000. 9999. 9999. 4000. 4000. 8000.
rcl0 9999. 1000.  500.  500. 1500.  700. 9999. 9999.  600.  800.  800.
```

Appendix II

Graphs of v_d estimates for SO_2, O_3, HNO_3, SO_4^{2-} and H_2O_2 for various landuse types at PSU. All points represent averages for individual weeks of 1986.

Fig. II.1. Weekly average deposition velocity of SO_2 at The Pennsylvania State Univ. (PSU), calculated with the deposition module as a function of landuse type.

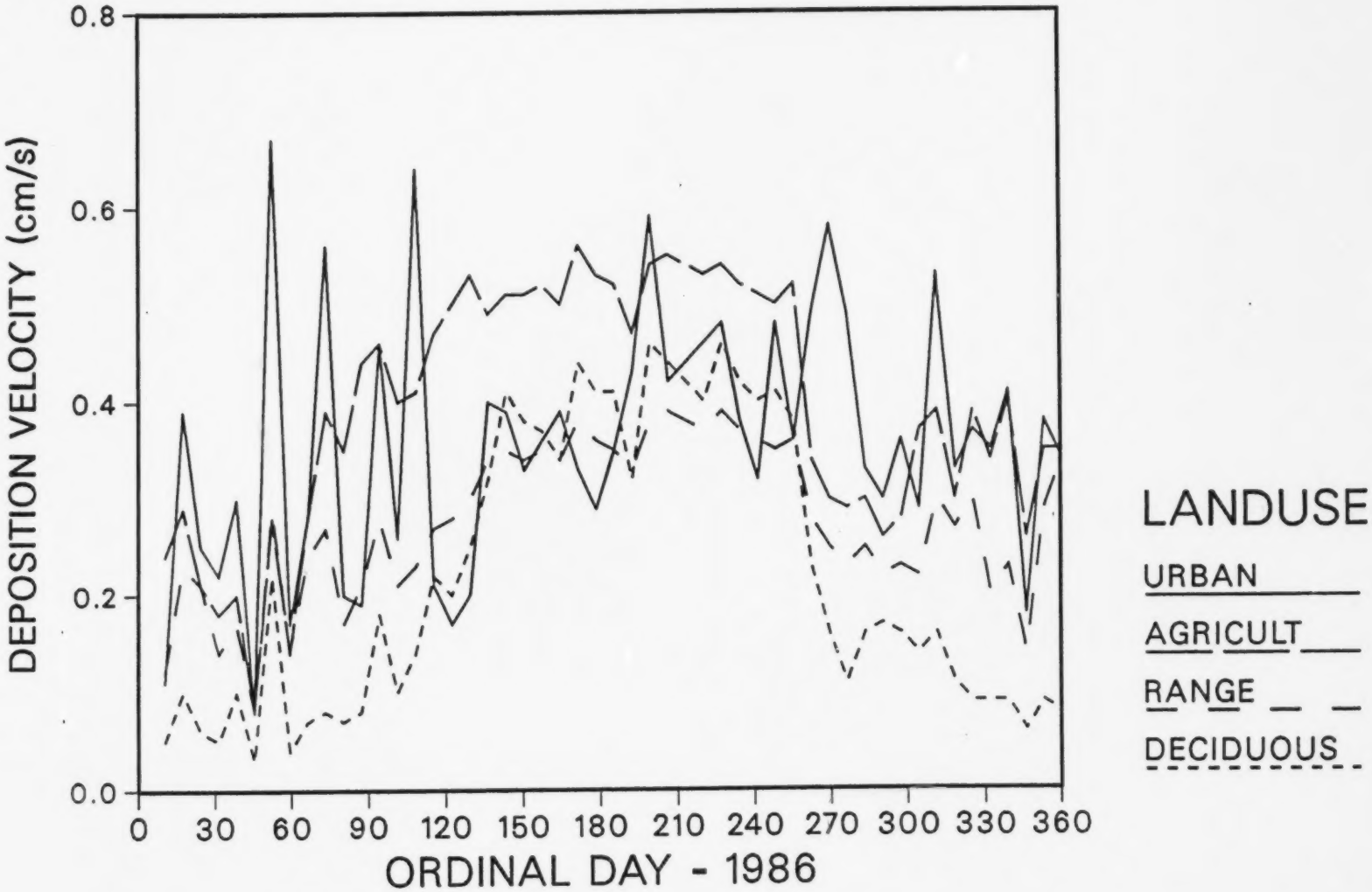

Fig. II.2. Weekly average deposition velocity of SO_2 at The Pennsylvania State Univ. (PSU), calculated with the deposition module as a function of landuse type.

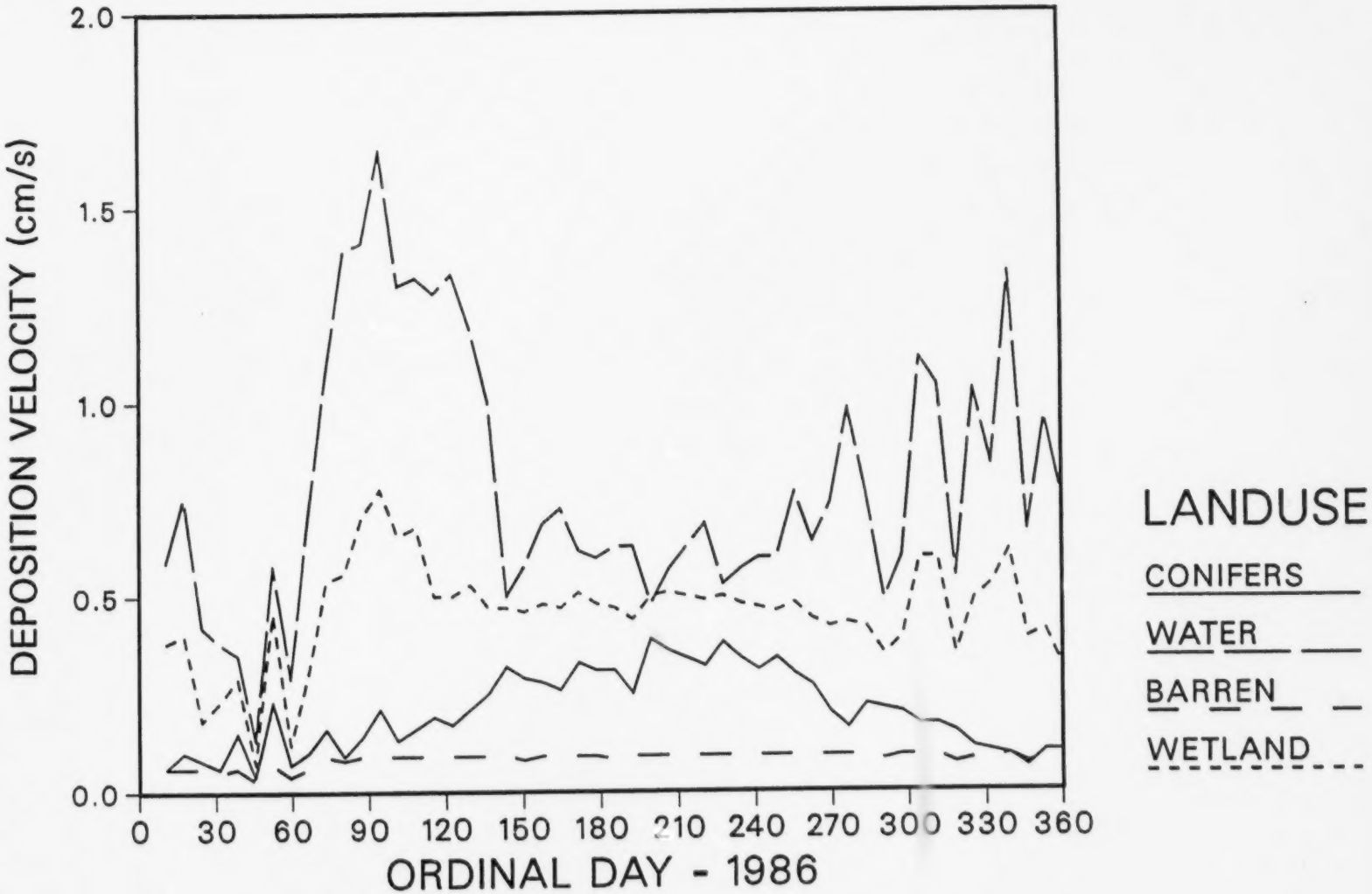

Fig. II.3. Weekly average deposition velocity of O_3 at The Pennsylvania State Univ. (PSU), calculated with the deposition module as a function of landuse type.

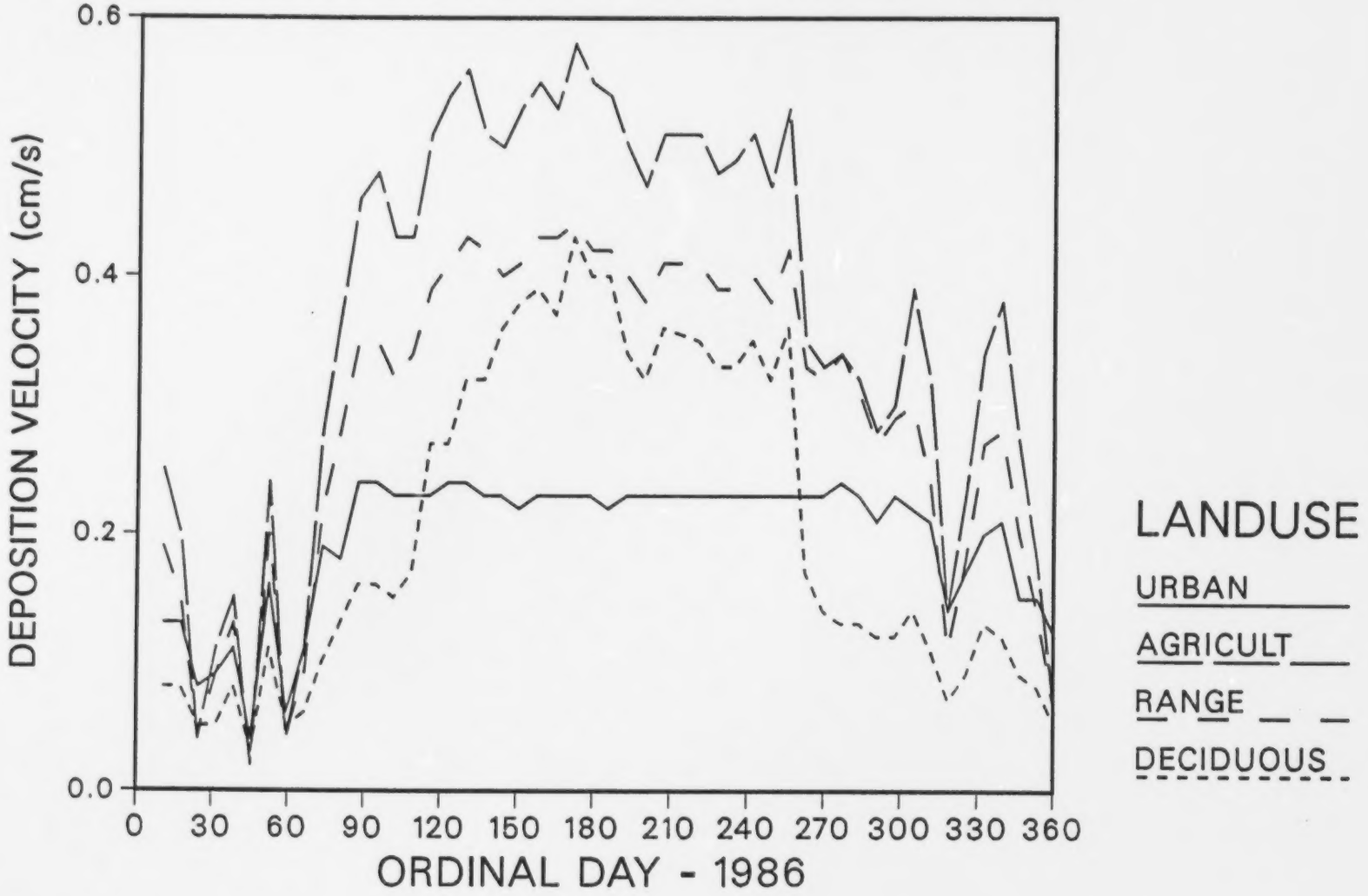

Fig. II.4. Weekly average deposition velocity of O_3 at The Pennsylvania State Univ. (PSU), calculated with the deposition module as a function of landuse type.

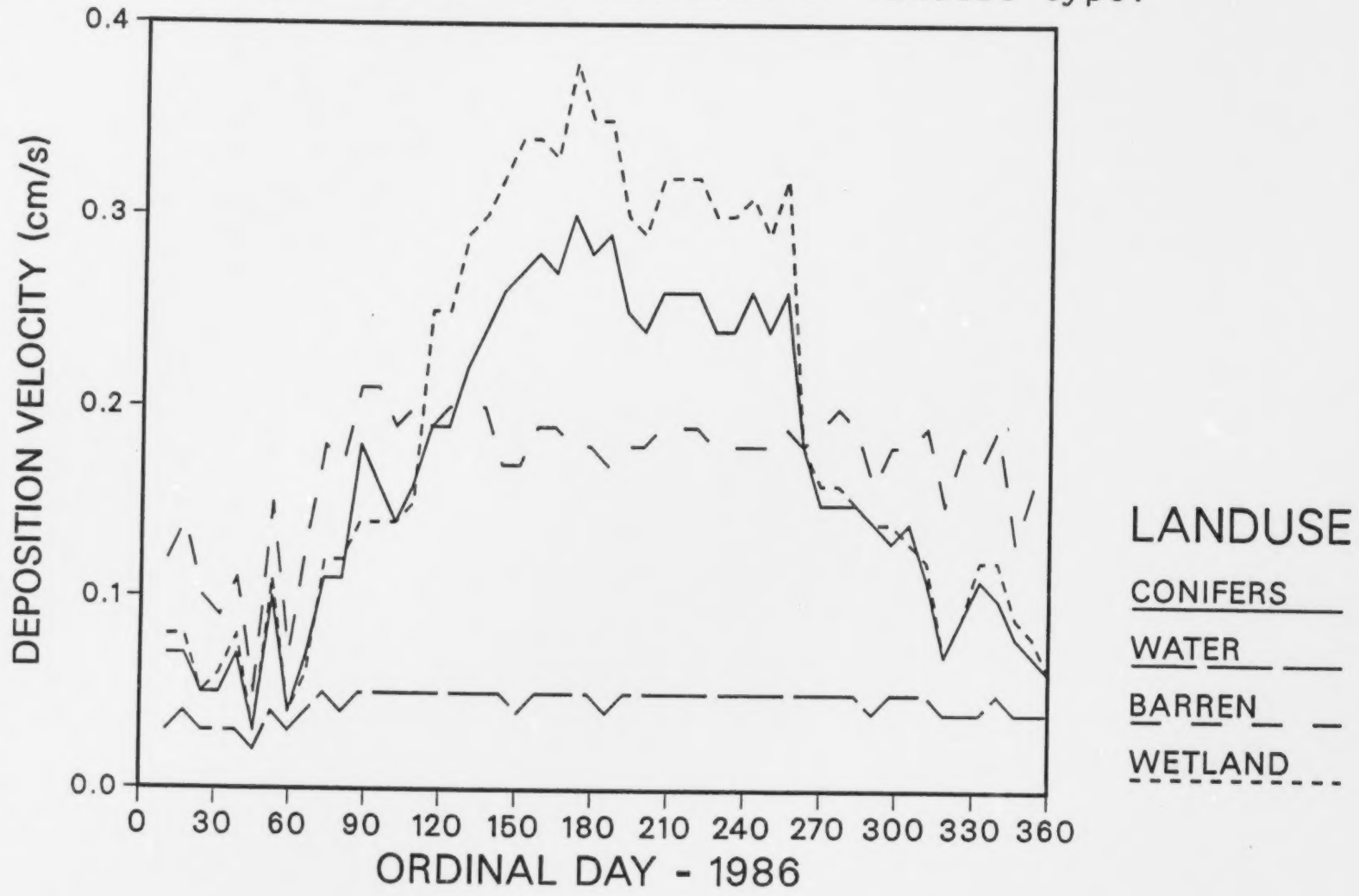

Fig. II.5. Weekly average deposition velocity of HNO_3 at The Pennsylvania State Univ. (PSU), calculated with the deposition module as a function of landuse type.

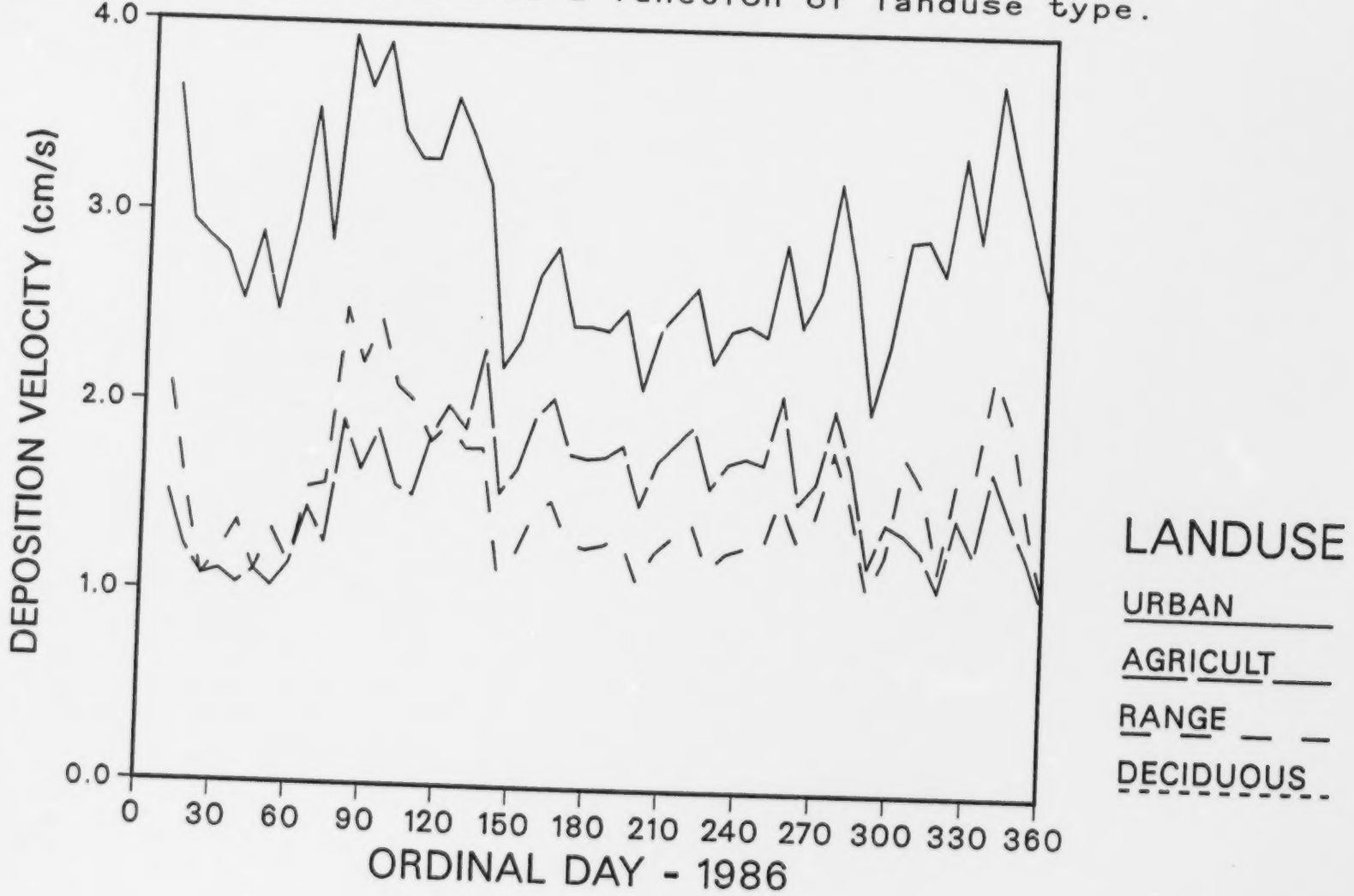

Fig. II.6. Weekly average deposition velocity of HNO_3 at The Pennsylvania State Univ. (PSU), calculated with the deposition module as a function of landuse type.

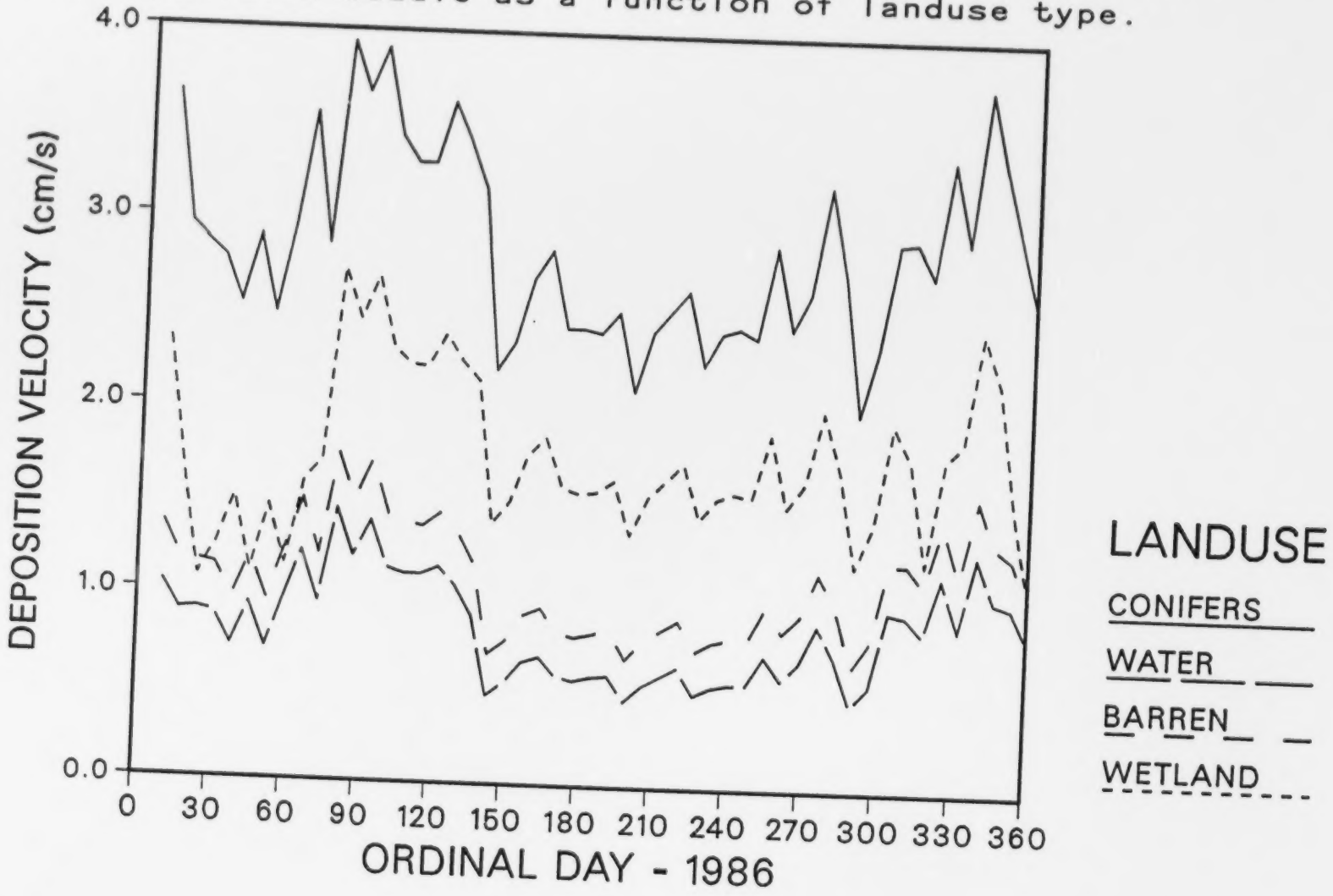

Fig. II.7. Weekly average deposition velocity of SO_4^{2-} at The Pennsylvania State Univ. (PSU), calculated with the deposition module as a function of landuse type.

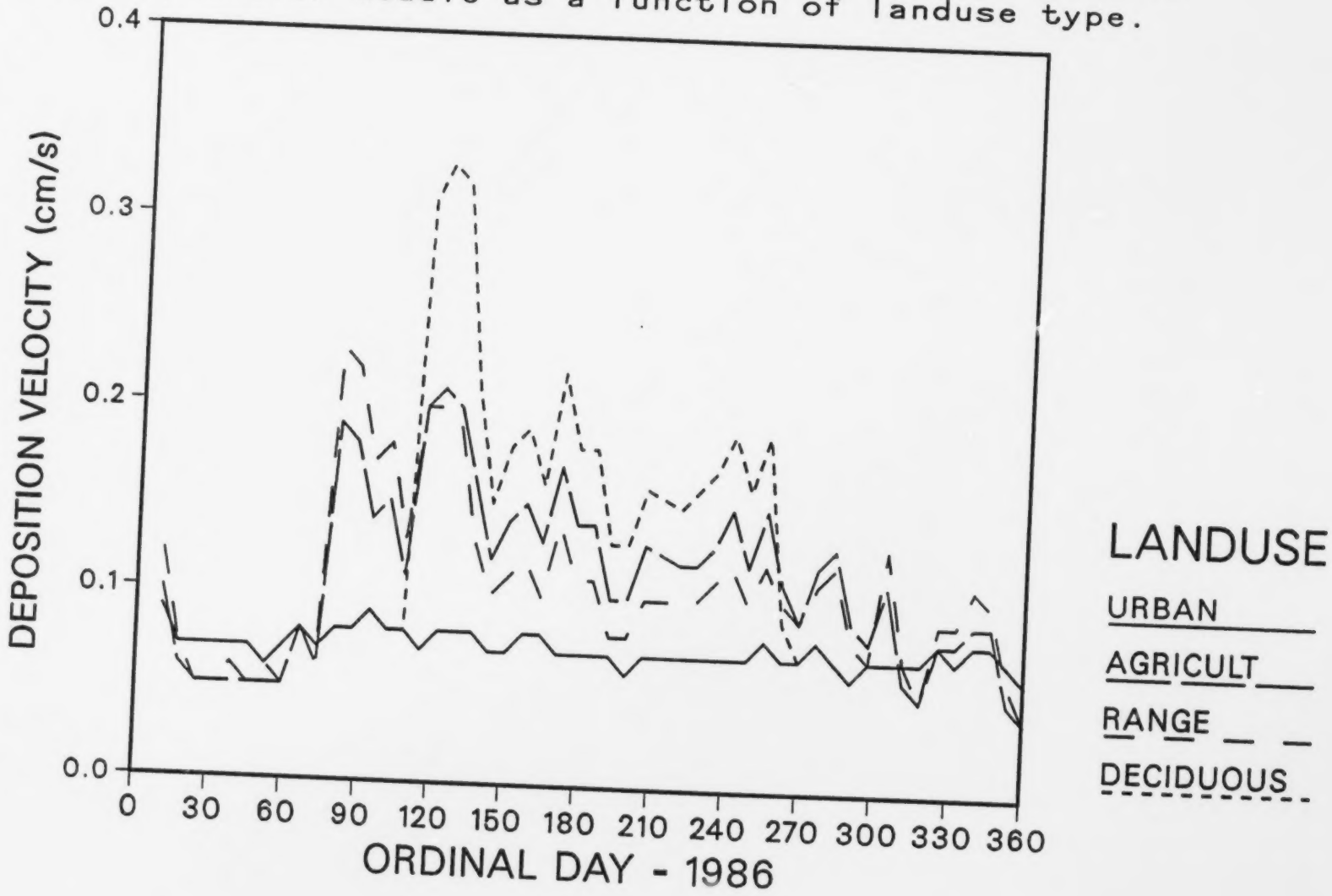

Fig. II.8. Weekly average deposition velocity of SO_4^{2-} at The Pennsylvania State Univ. (PSU), calculated with the deposition module as a function of landuse type.

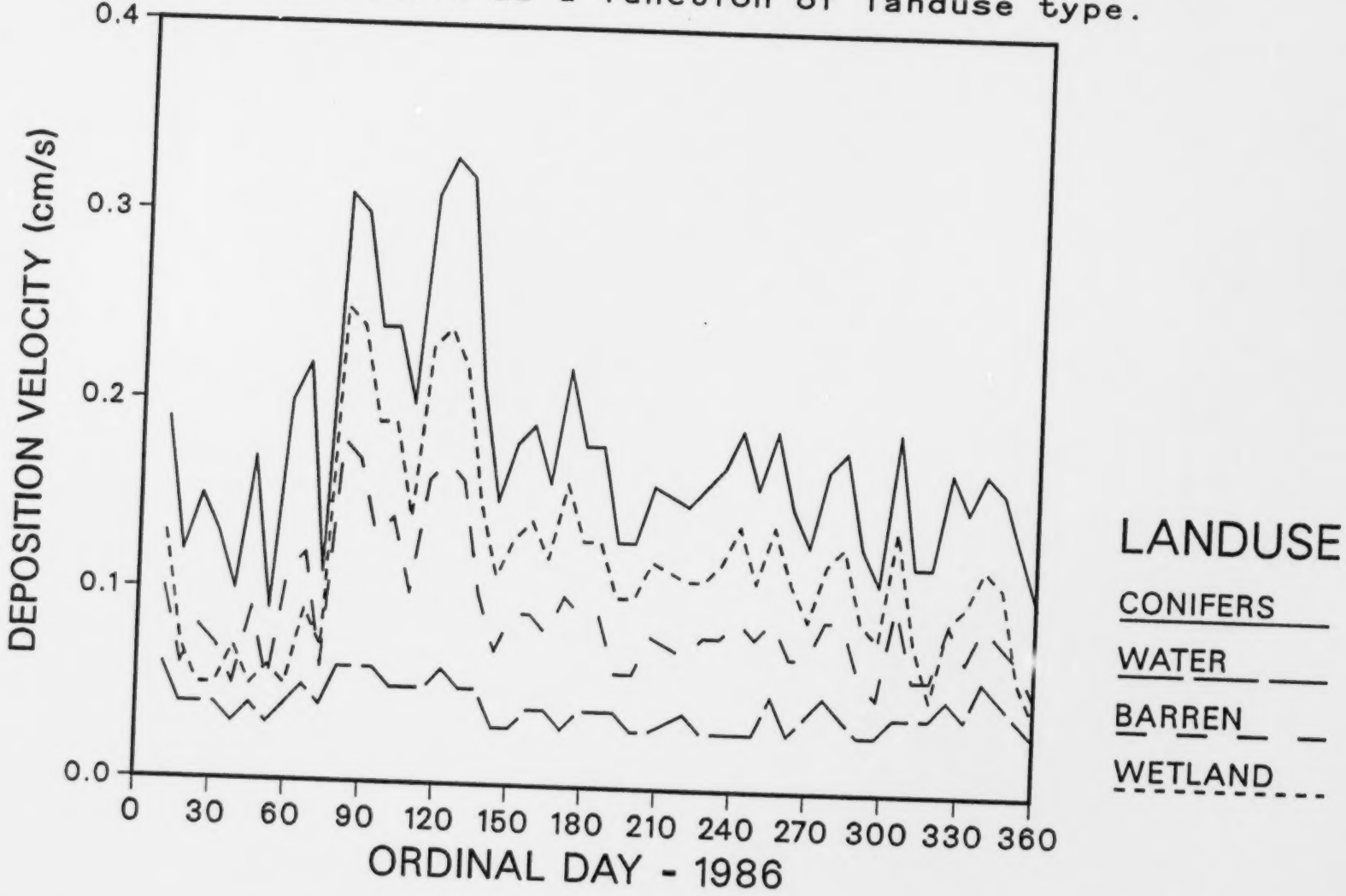

Fig. II.9. Weekly average deposition velocity of H_2O_2 at The Pennsylvania State Univ. (PSU), calculated with the deposition module as a function of landuse type.

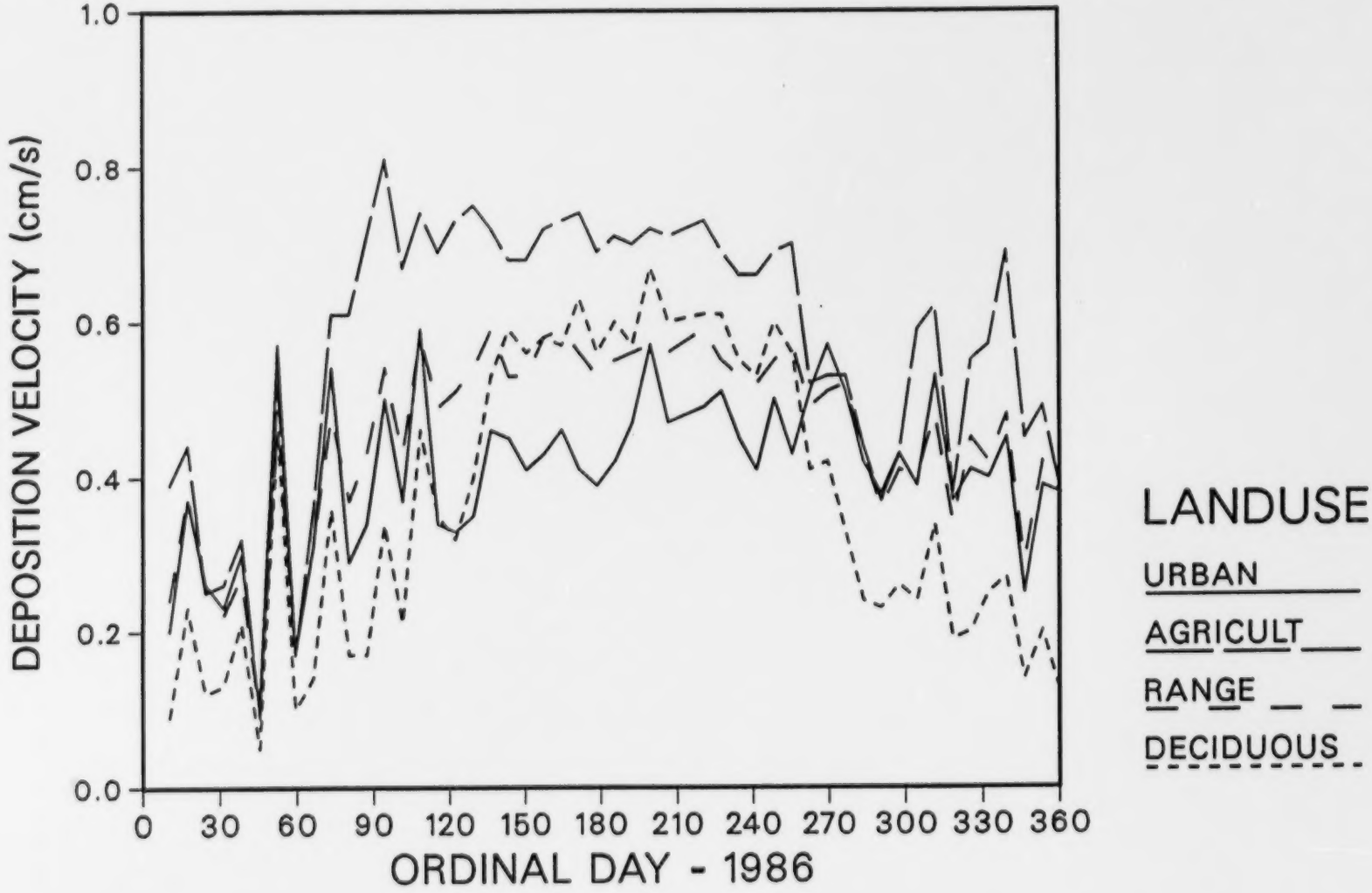

Fig. II.10. Weekly average deposition velocity of H_2O_2 at The Pennsylvania State Univ. (PSU), calculated with the deposition module as a function of landuse type.

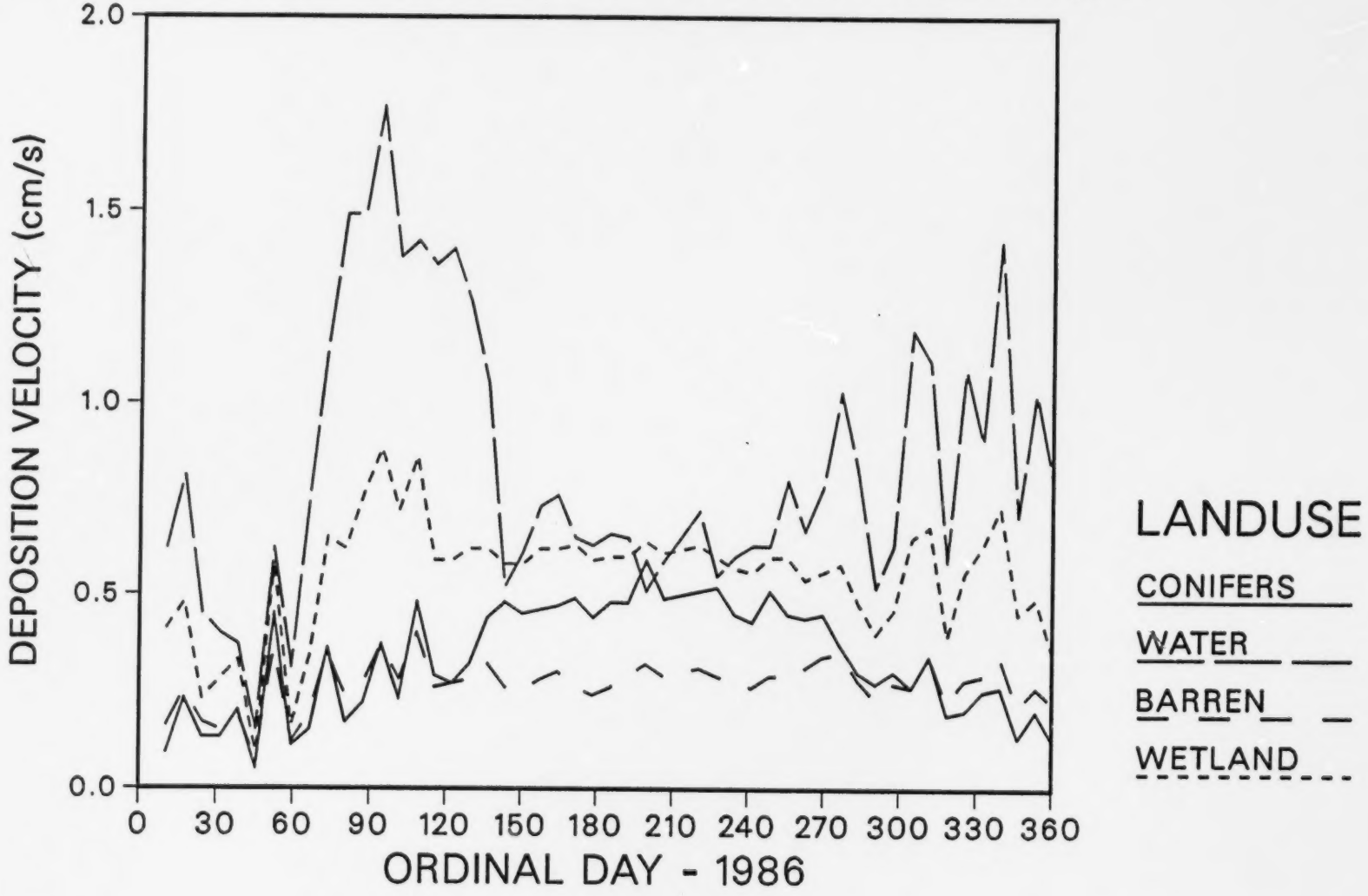

Appendix III

Plots of v_d estimates for 1986 for SO_2, O_3, HNO_3, and SO_4^{2-} at the seven sites by the inferential method and with the modified module using three different landuse distributions (as listed in Table III).

Fig. III.1. Weekly average deposition velocities at Argonne National Laboratory (ARG), calculated with the inferential method.

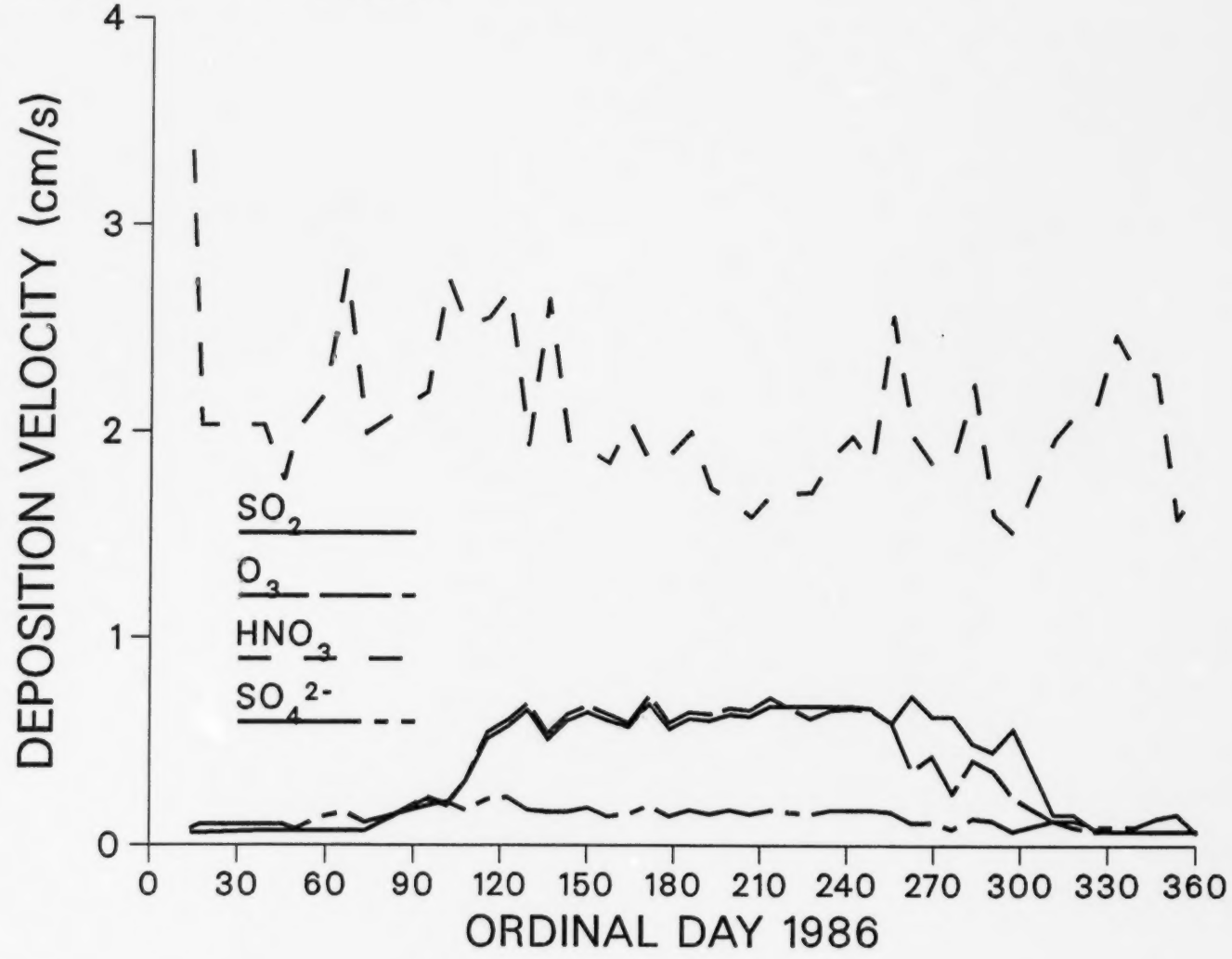

Fig. III.2. Weekly average deposition velocities at Argonne National Laboratory (ARG), calculated with the dry deposition module, for the local site.

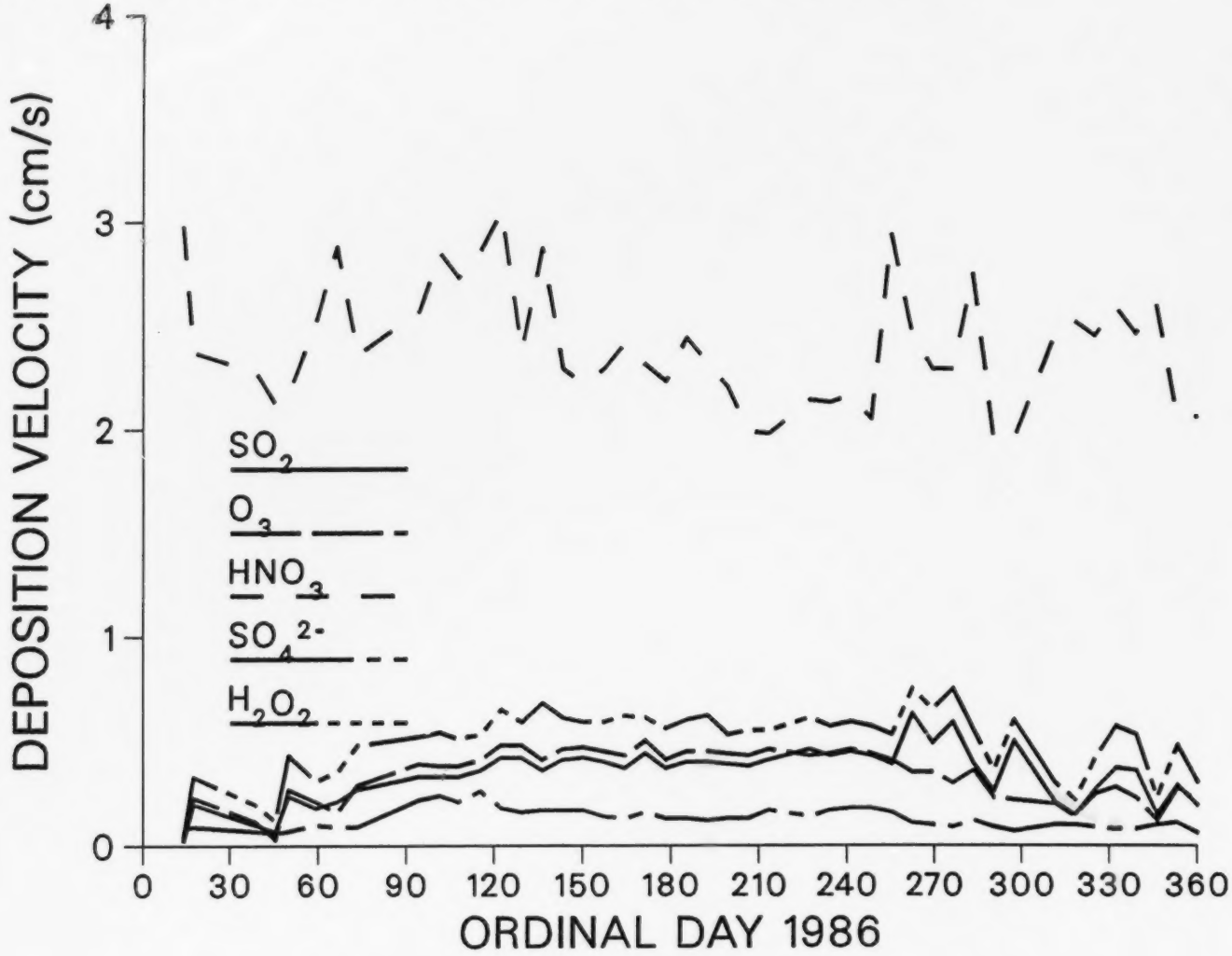

Fig. III.3. Weekly average deposition velocities at Argonne Nationa' Laboratory (ARG), calculated with the dry deposition module, for the landuse map cell.

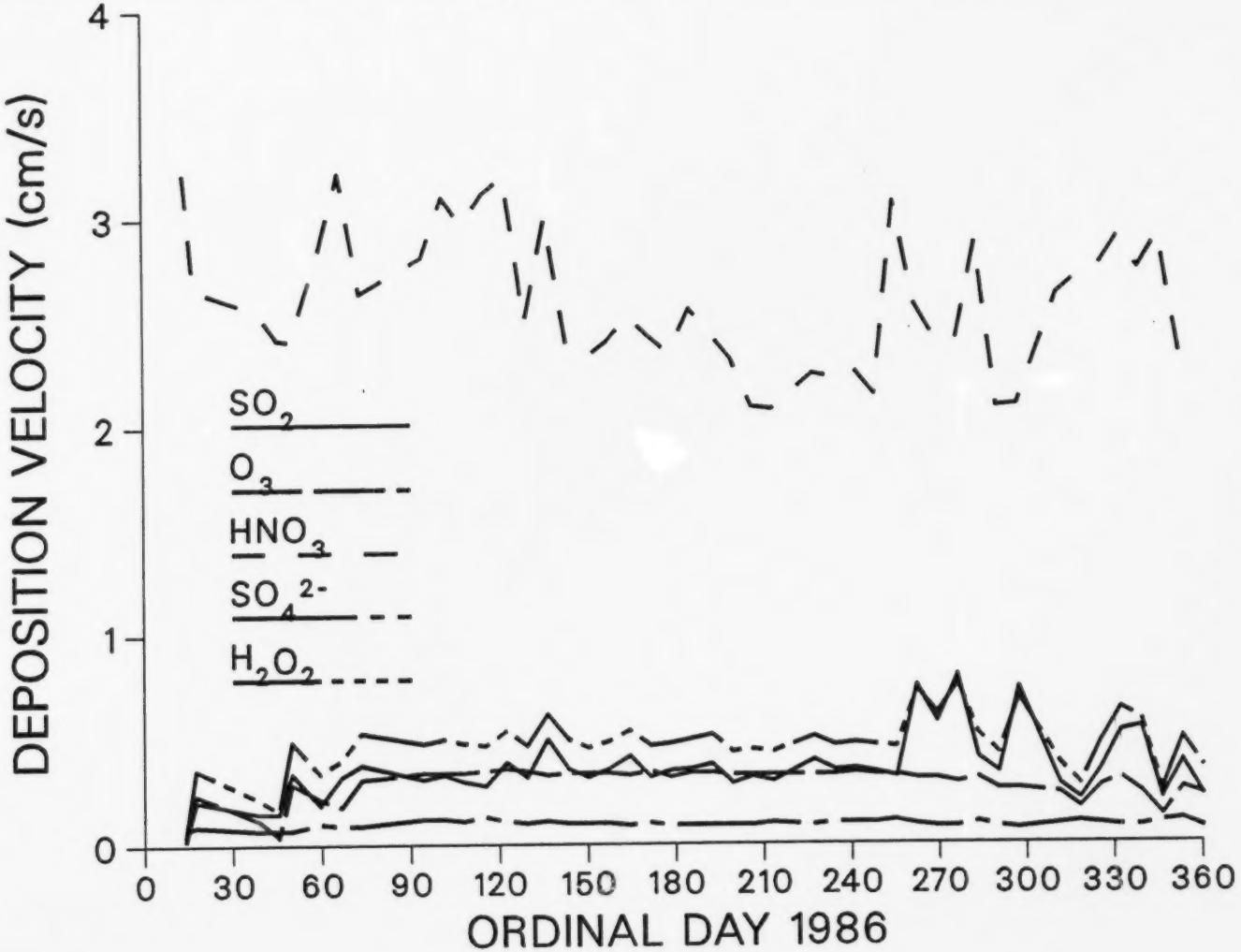

Fig. III.4. Weekly average deposition velocities at Argonne National Laboratory (ARG), calculated with the dry deposition module, for the RADM grid cell.

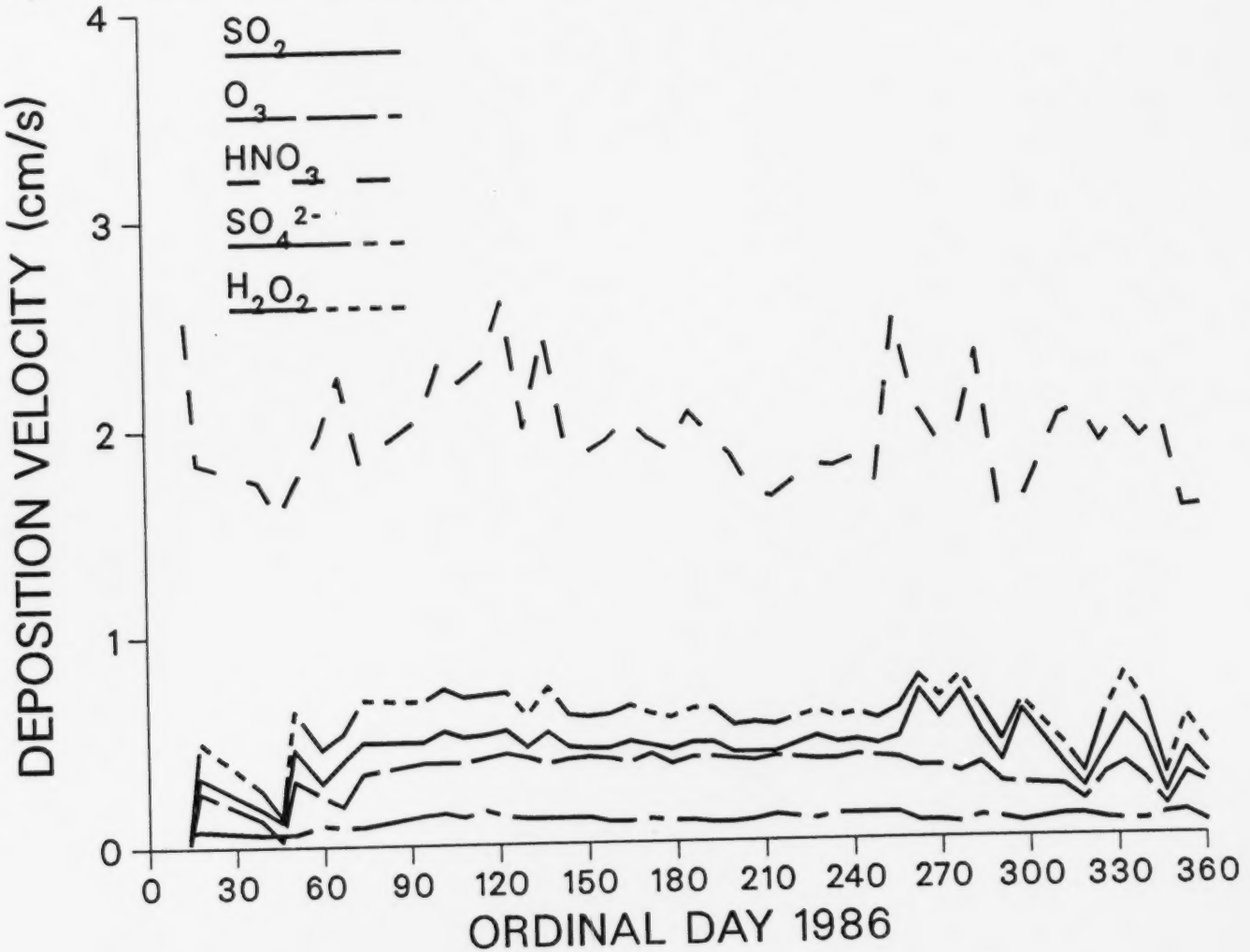

Fig. III.5. Weekly average deposition velocities at Bondville, IL (BON), calculated with the inferential method.

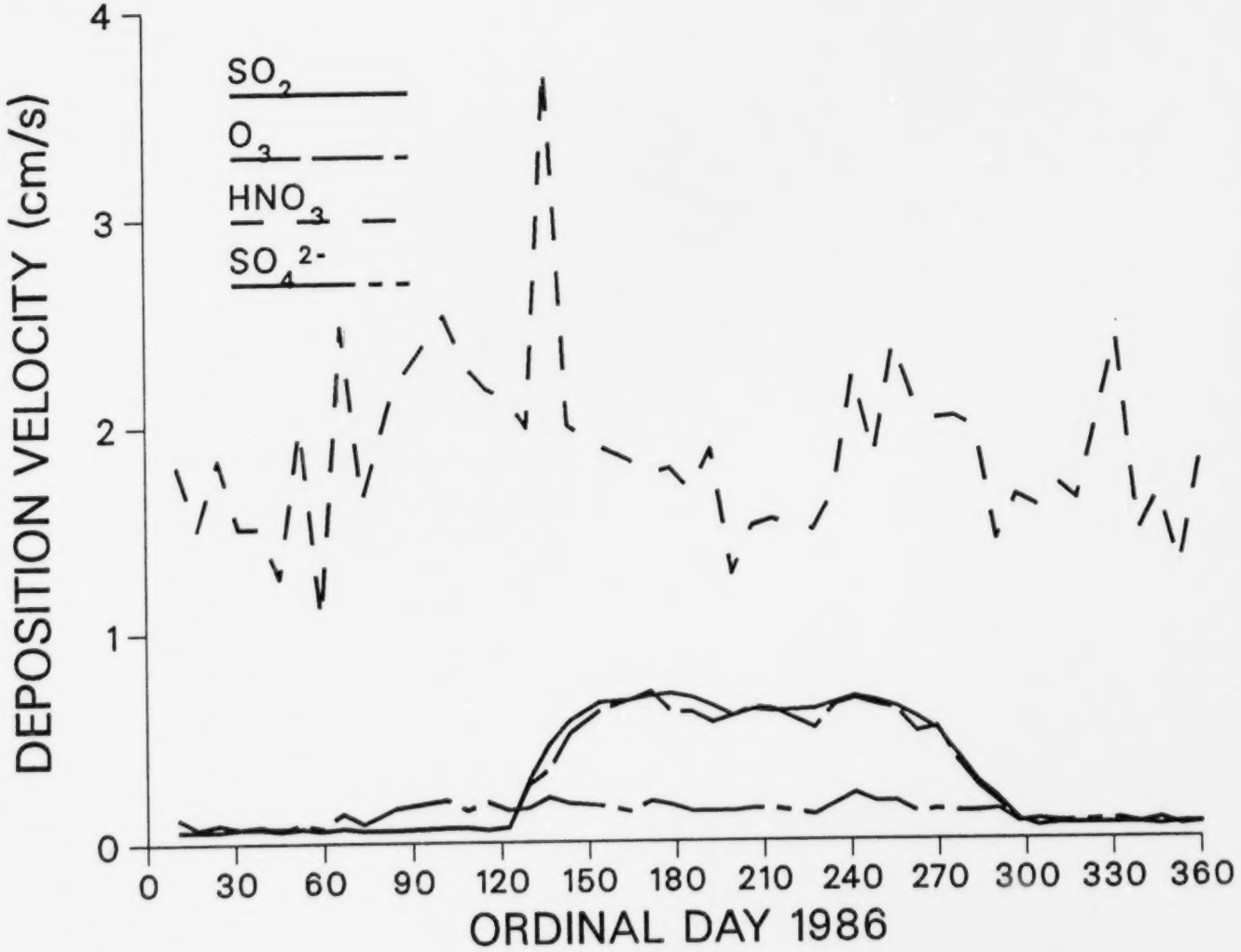

Fig. III.6. Weekly average deposition velocities at Bondville, IL (BON), calculated with the dry deposition module, for the local site.

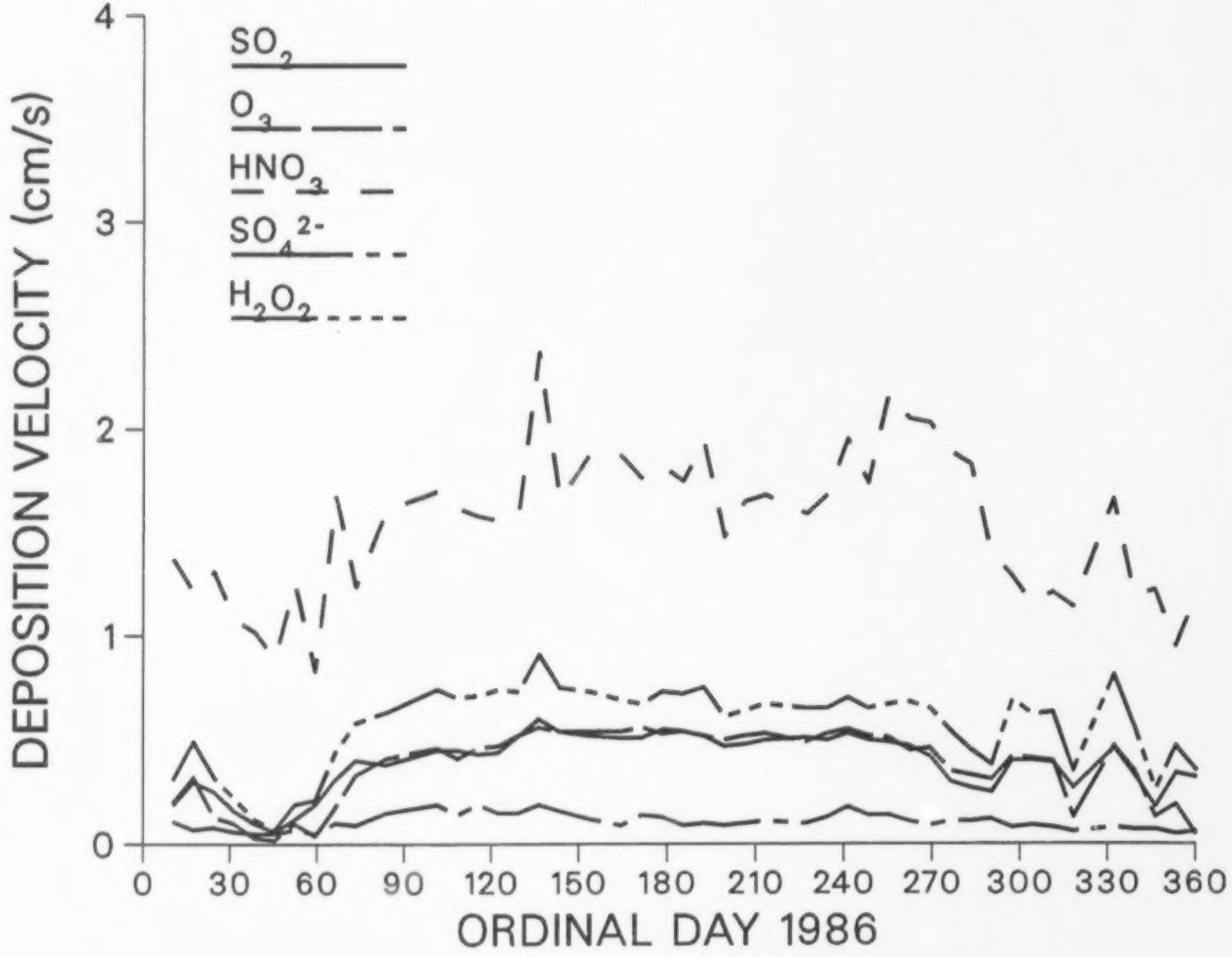

Fig. III.7. Weekly average deposition velocities at Bondville, IL (BON), calculated with the dry deposition module, for the landuse map cell.

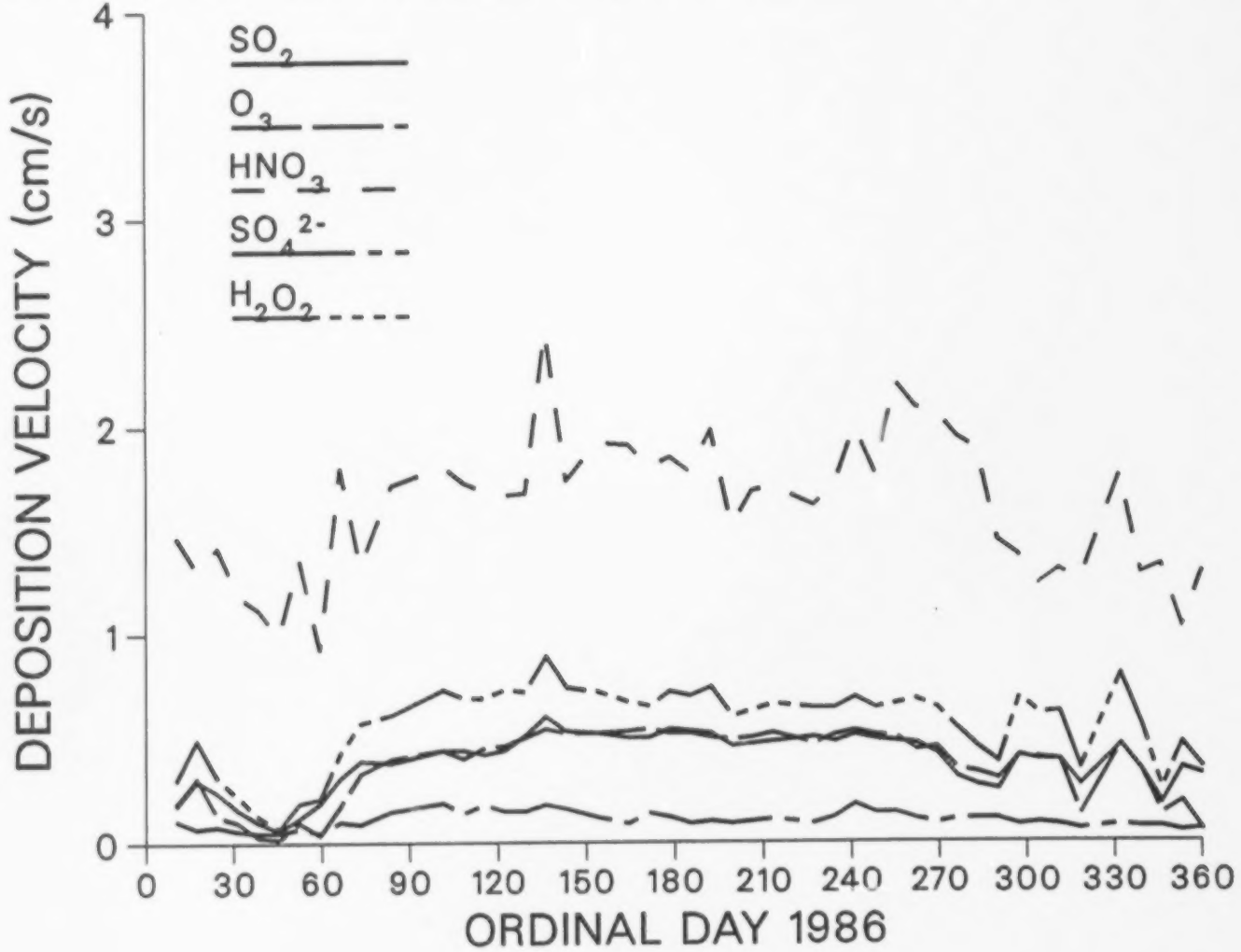

Fig. III.8. Weekly average deposition velocities at Bondville, IL (BON), calculated with the dry deposition module, for the RADM grid cell.

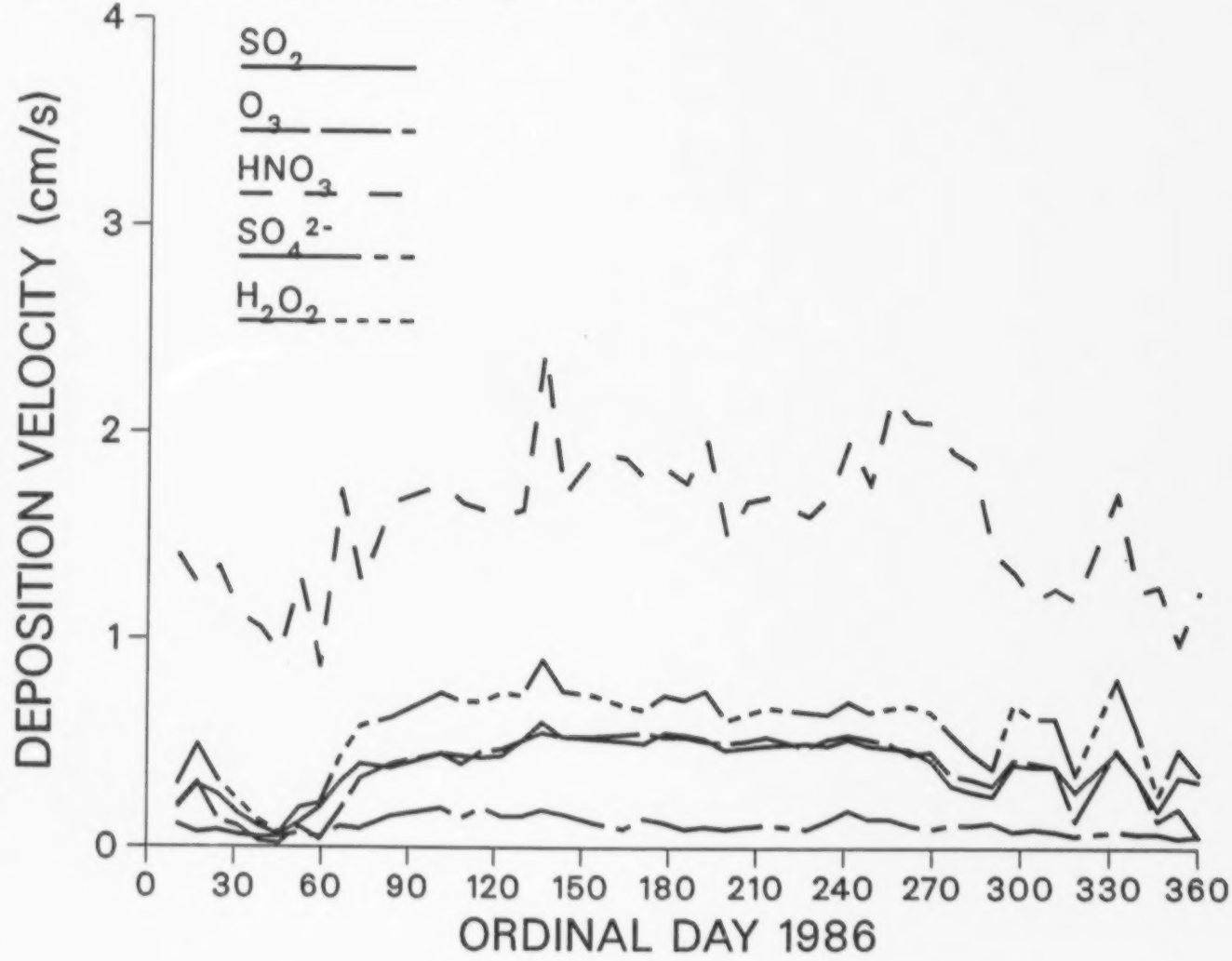

Fig. III.9. Weekly average deposition velocities at Oak Ridge, TN (OAK), calculated with the inferential method.

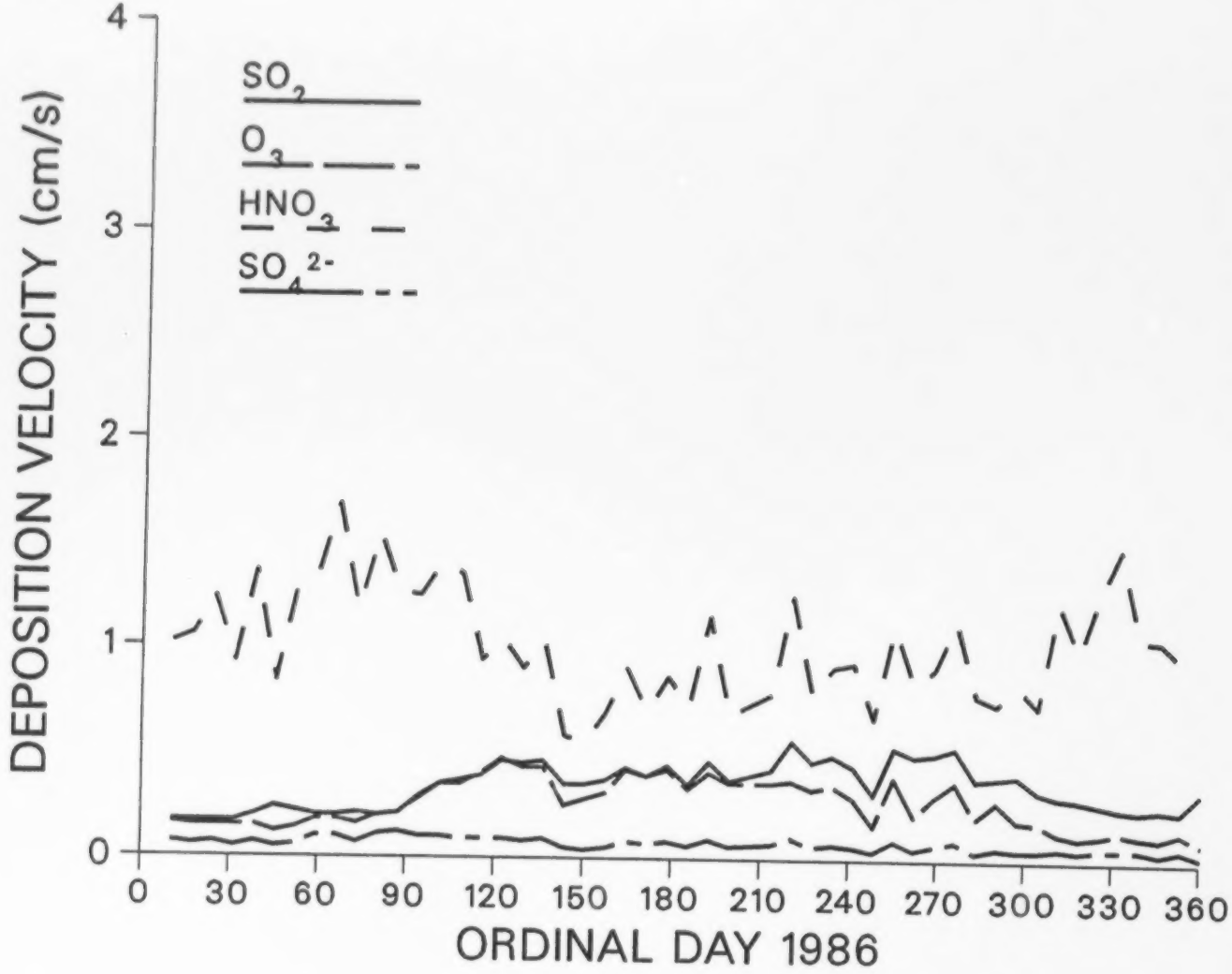

Fig. III.10. Weekly averaged deposition velocities at Oak Ridge, TN (OAK), calculated with the dry deposition module, for the local site.

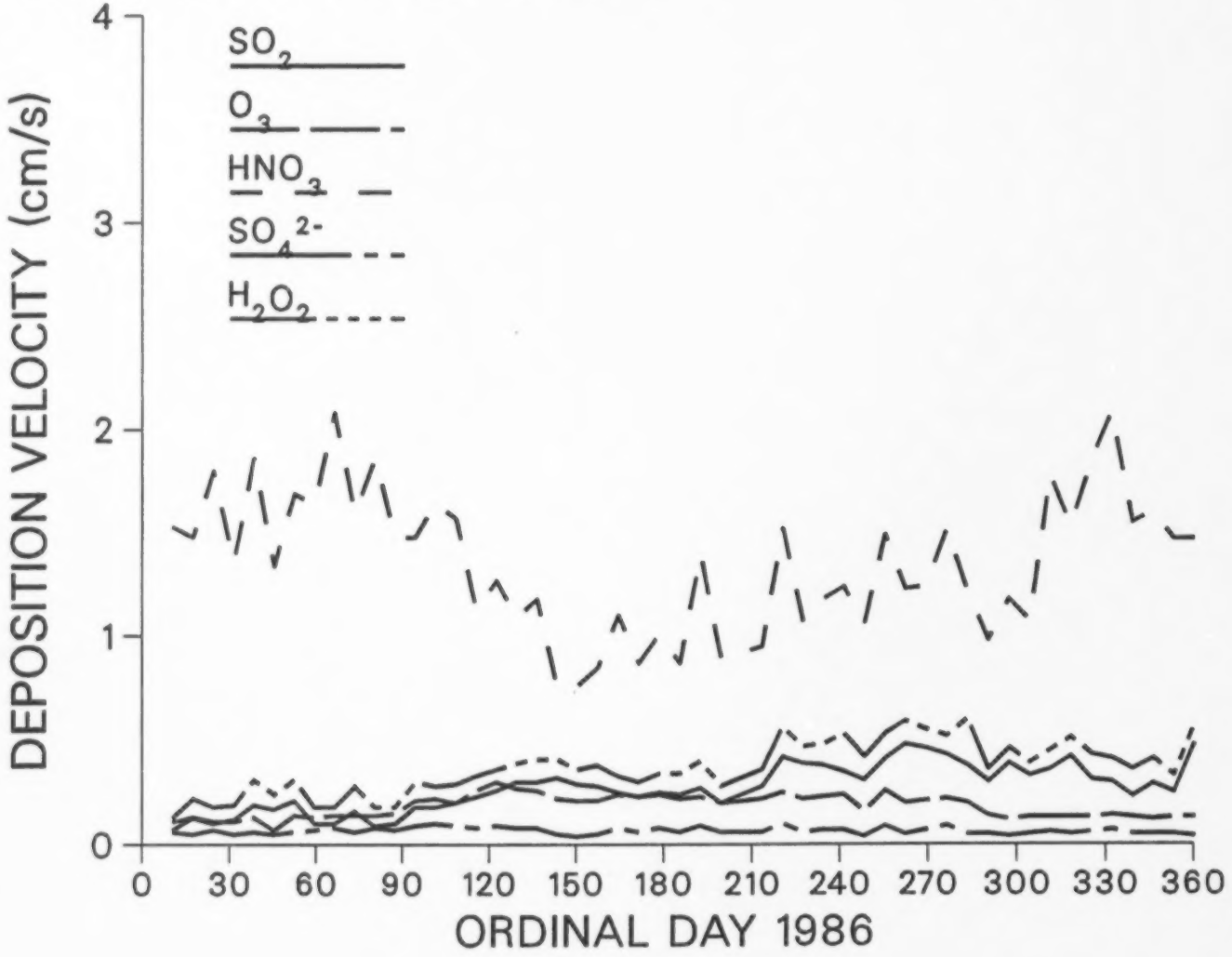

Fig. III.11. Weekly averaged deposition velocities at Oak Ridge, TN (OAK), calculated with the dry deposition module, for the landuse map cell.

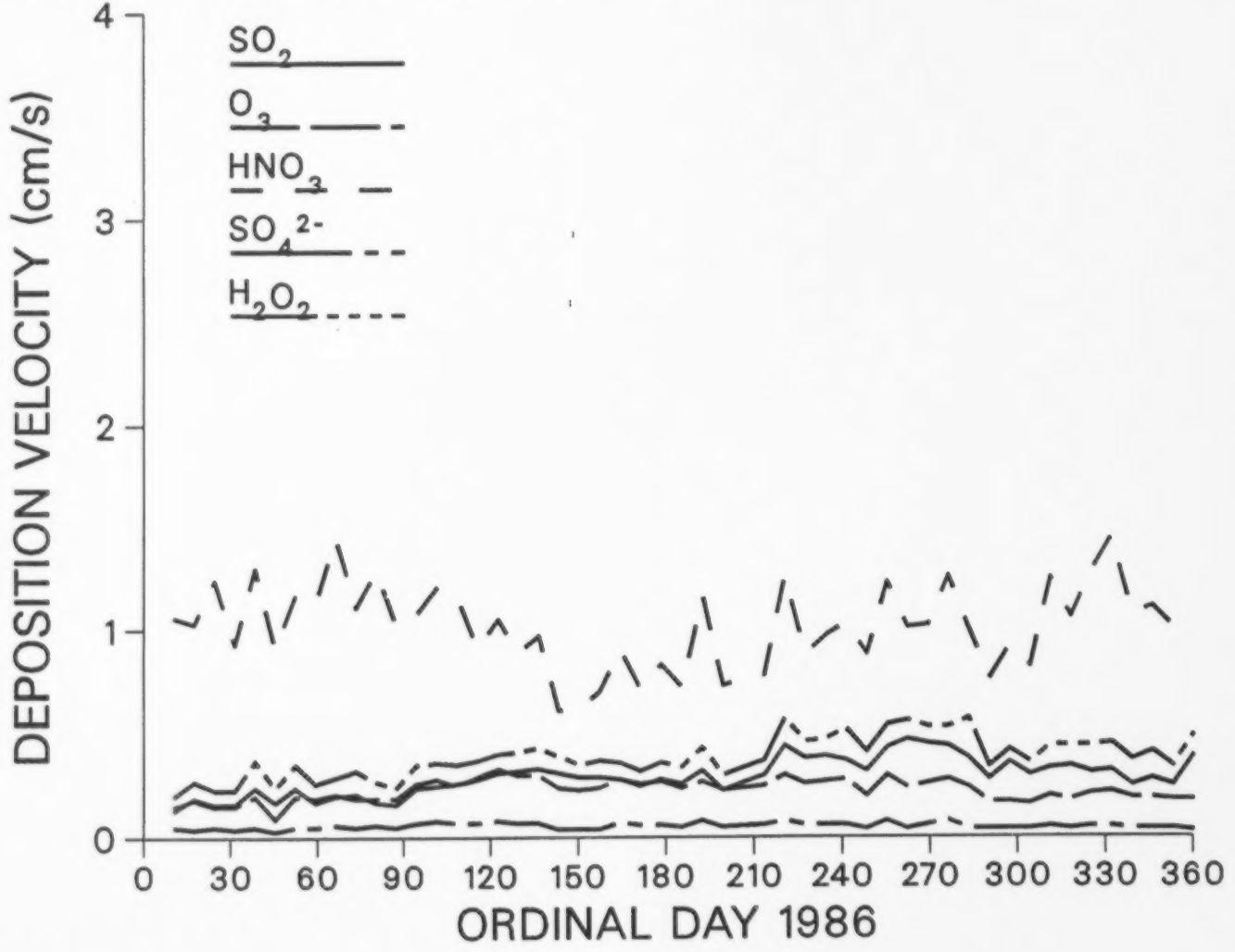

Fig. III.12. Weekly averaged deposition velocities at Oak Ridge, TN (OAK), calculated with the dry deposition module, for the RADM grid cell.

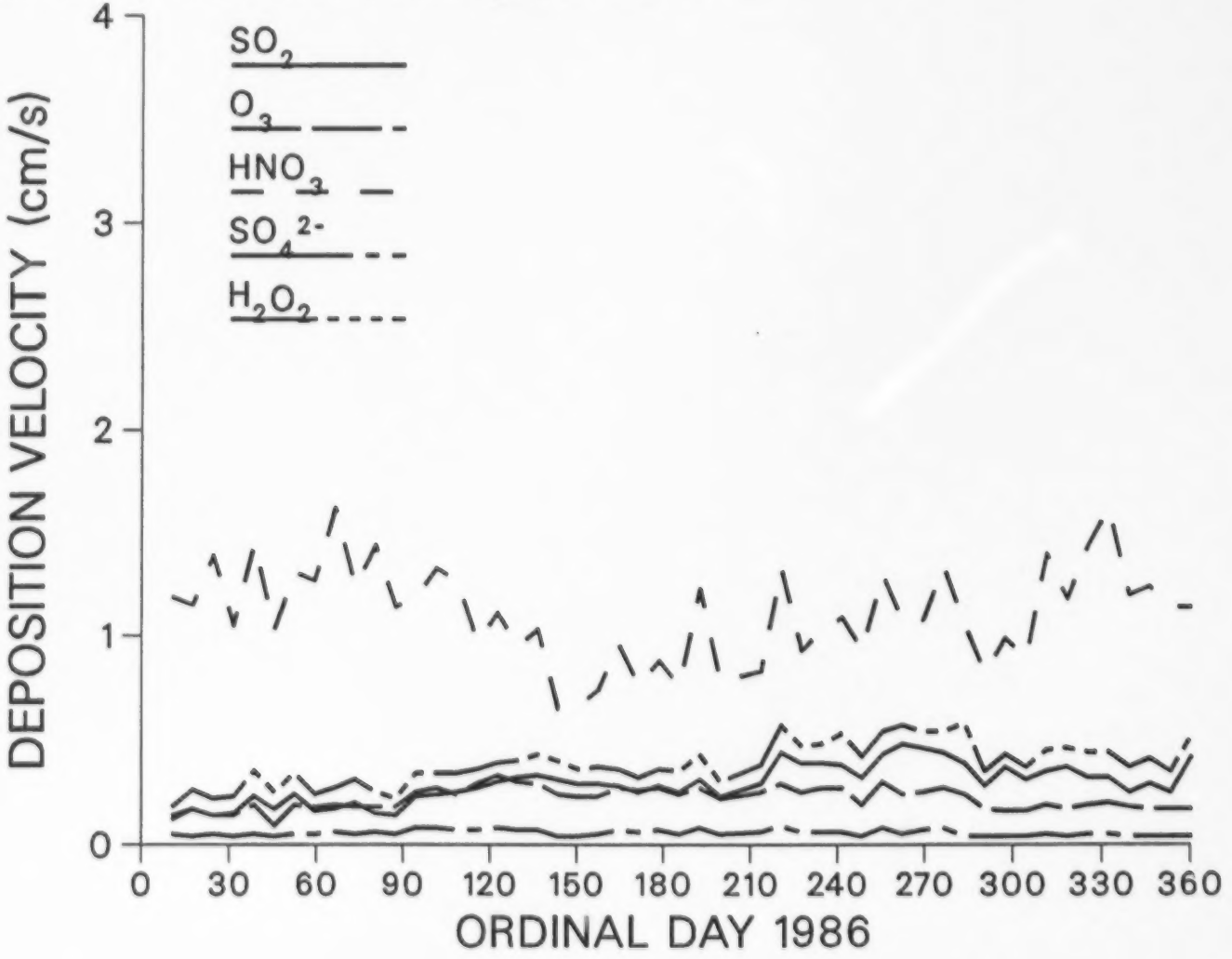

Fig. III.13. Weekly averaged deposition velocities at Panola State Park (PAN), calculated with the inferential method.

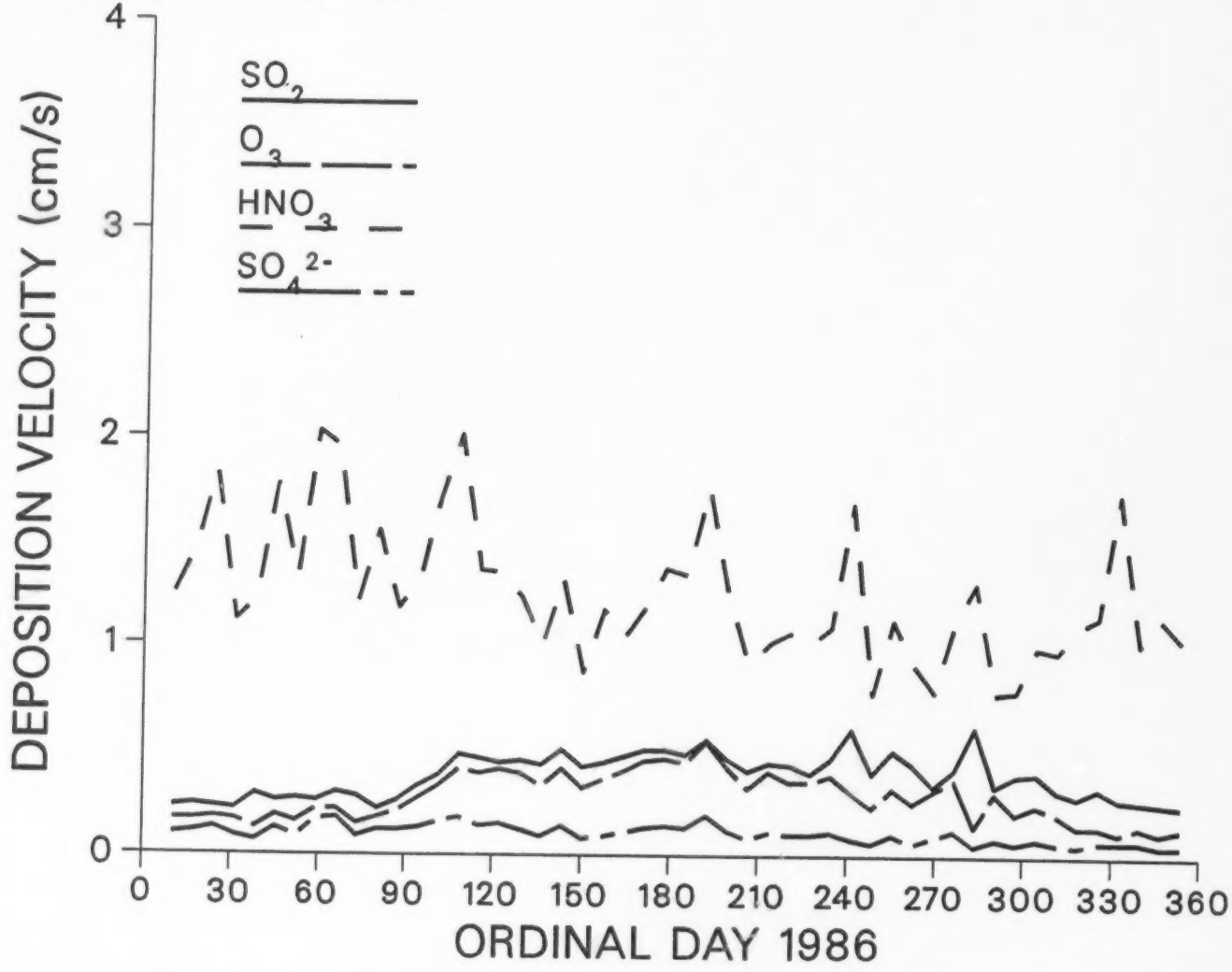

Fig. III.14. Weekly averaged deposition velocities at Panola State Park (PAN), calculated with the dry deposition module, for the local site.

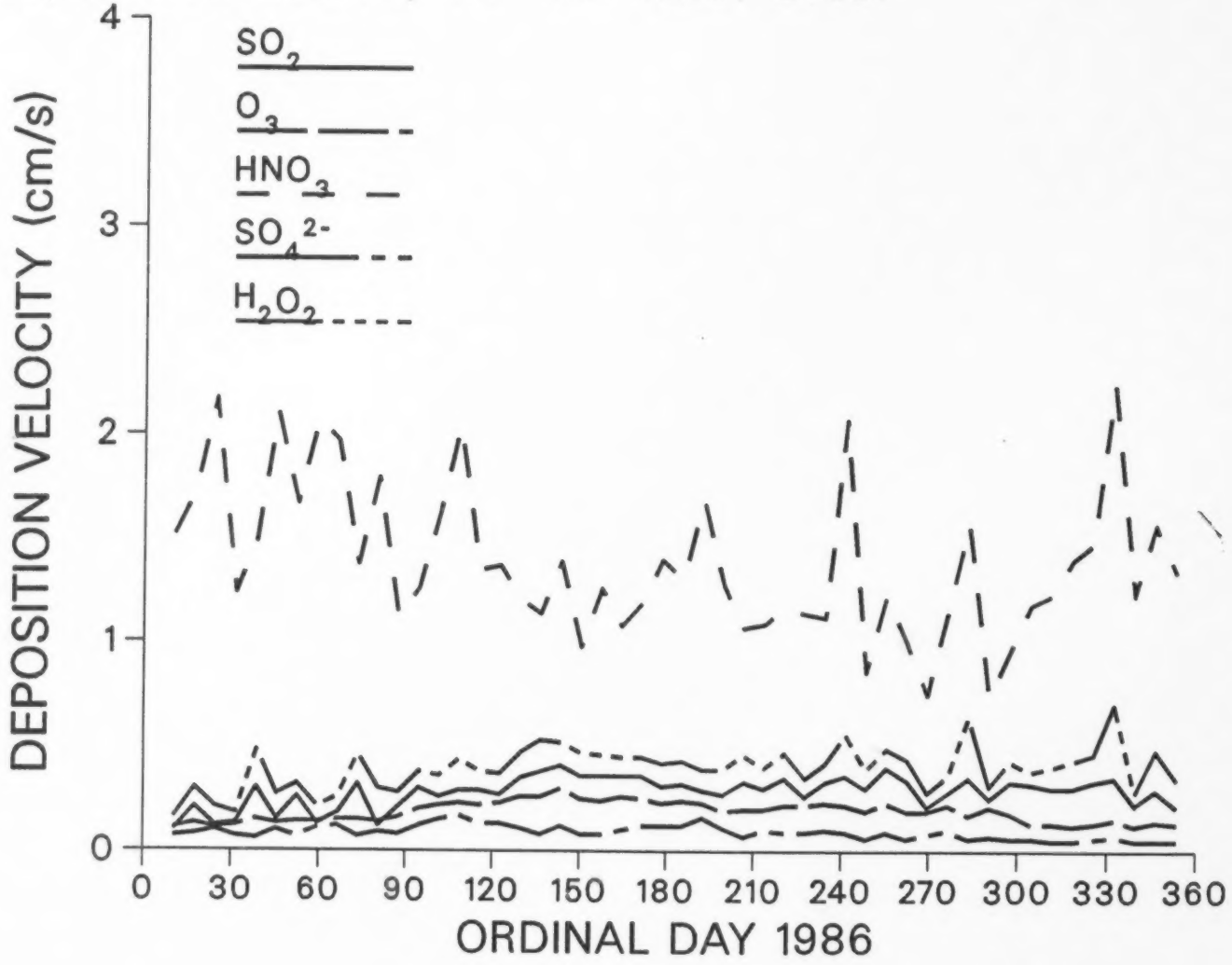

Fig. III.15. Weekly averaged deposition velocities at Panola State Park (PAN), calculated with the dry deposition module, for the landuse map cell.

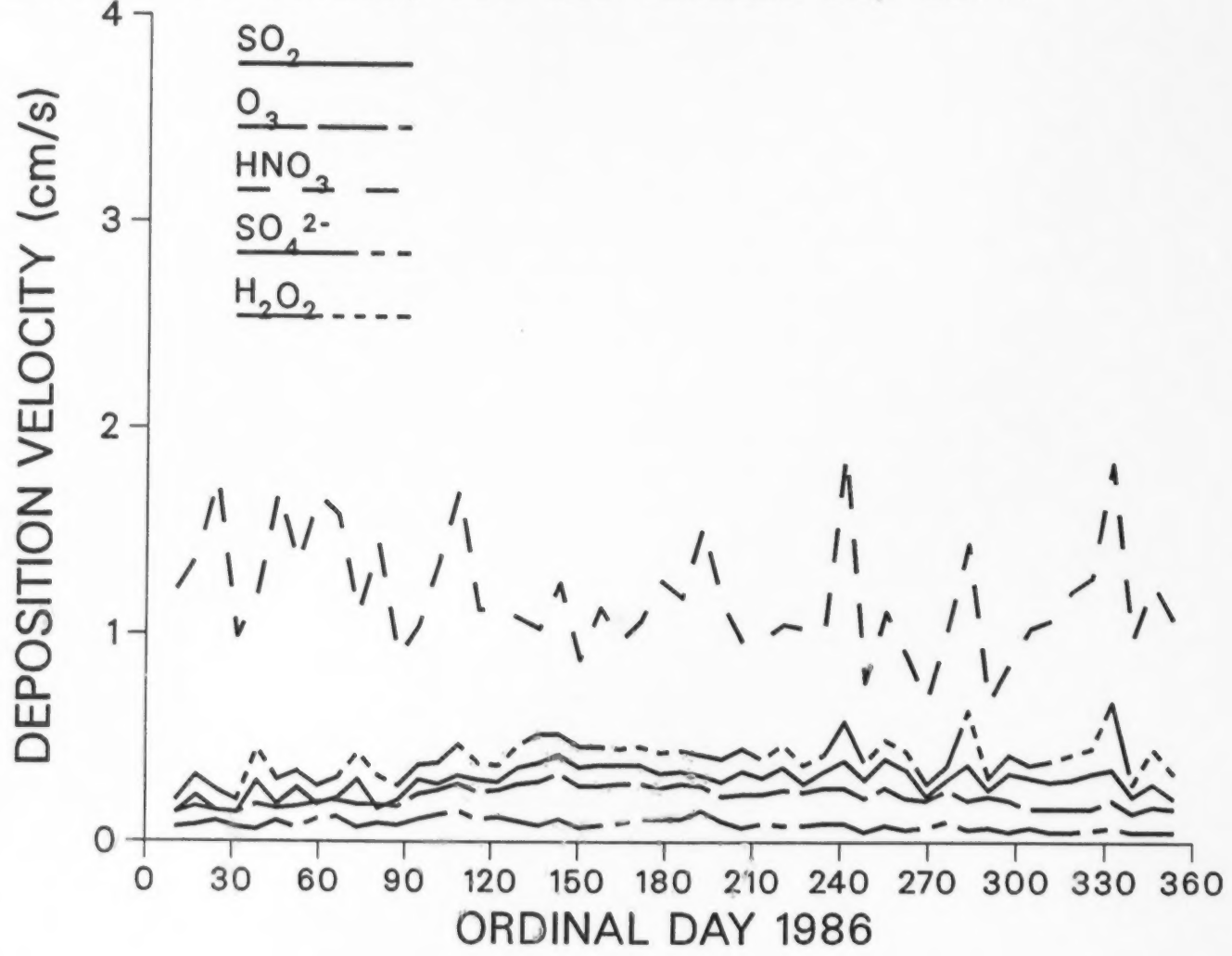

Fig. III.16. Weekly averaged deposition velocities at Panola State Park (PAN), calculated with the dry deposition module, for the RADM grid cell.

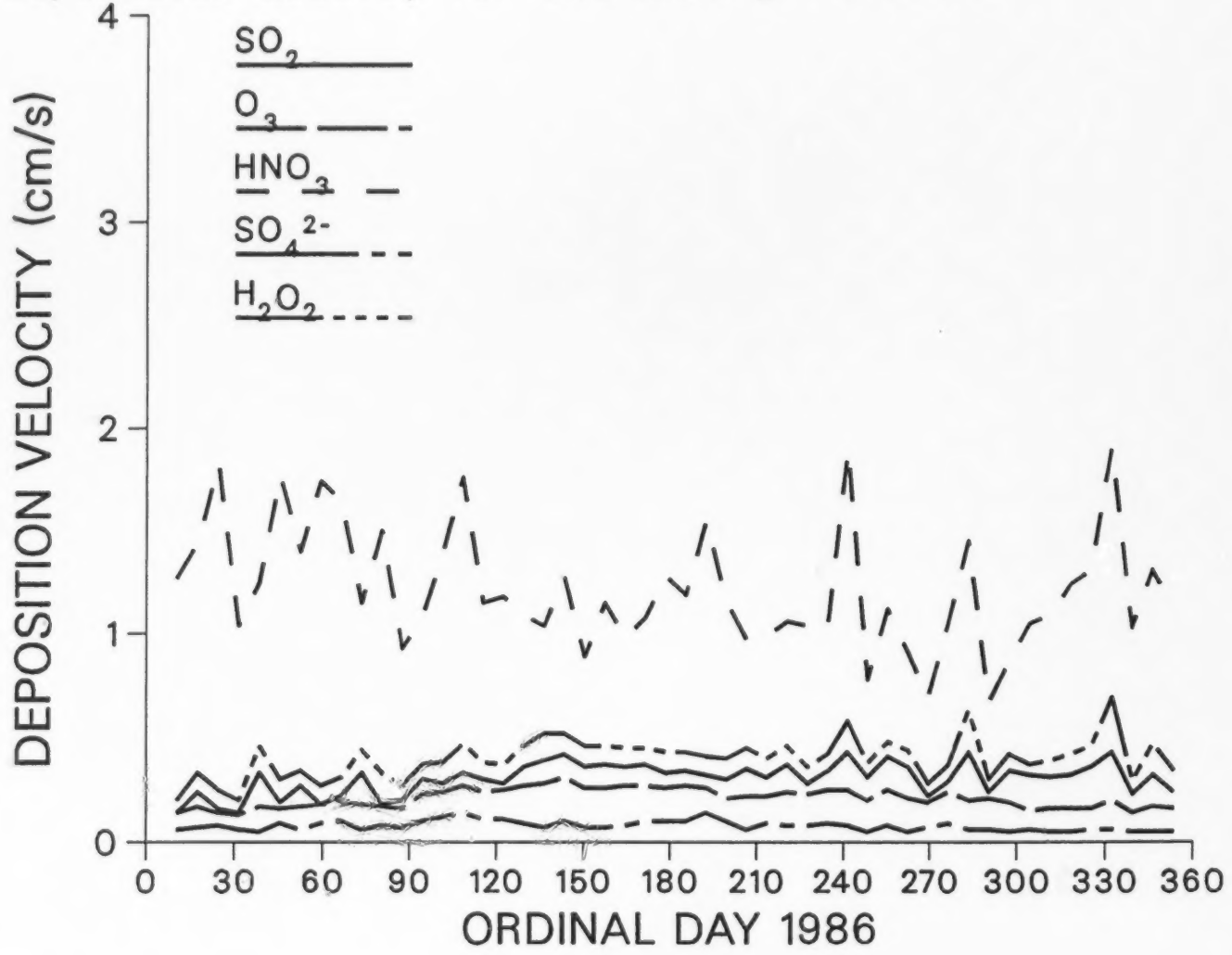

Fig. III.17. Weekly averaged deposition velocities at The Pennsylvania State Univ. (PSU), calculated with the inferential method.

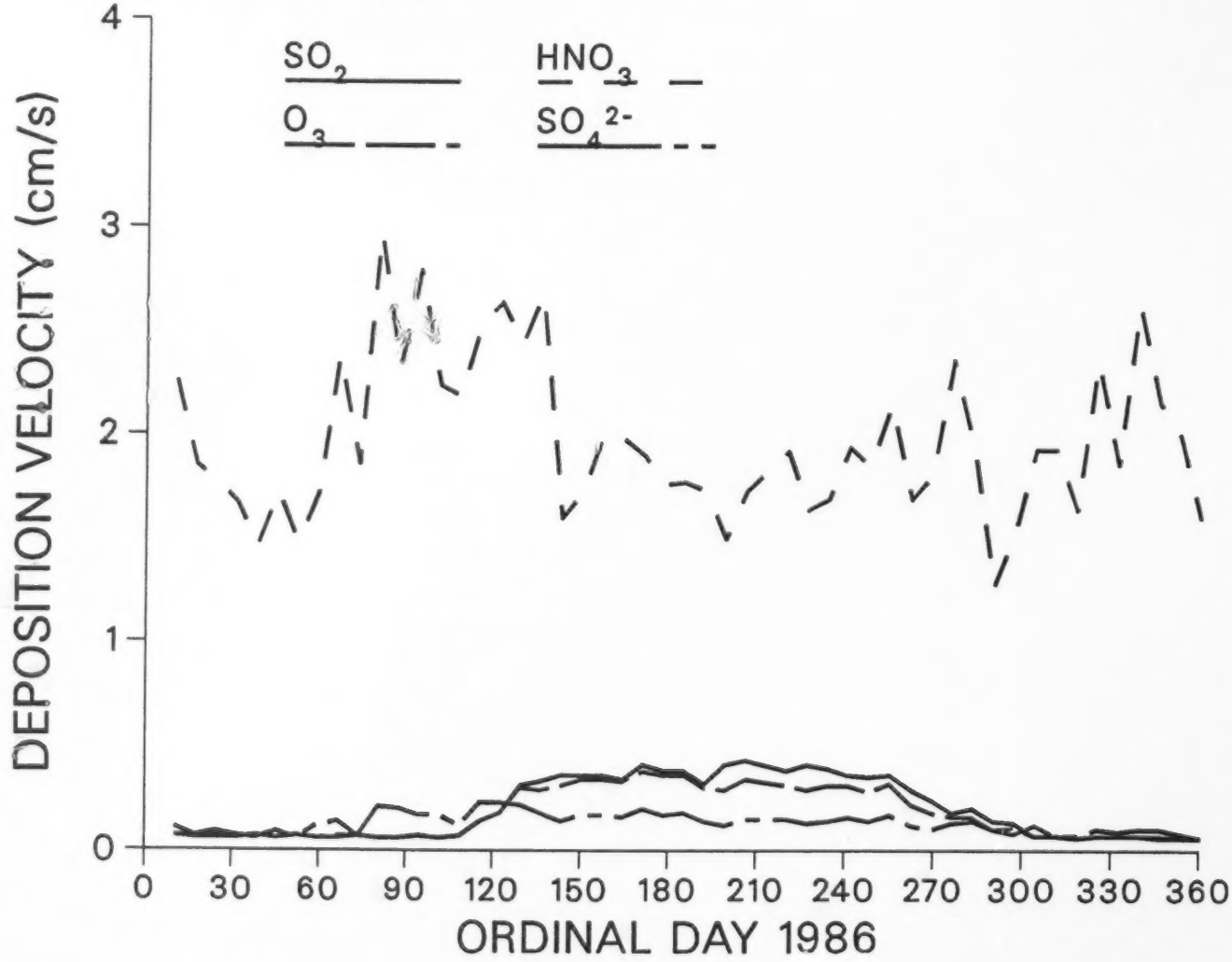

Fig. III.18. Weekly averaged deposition velocities at The Pennsylvania State Univ. (PSU), calculated with the dry deposition module, for the local site.

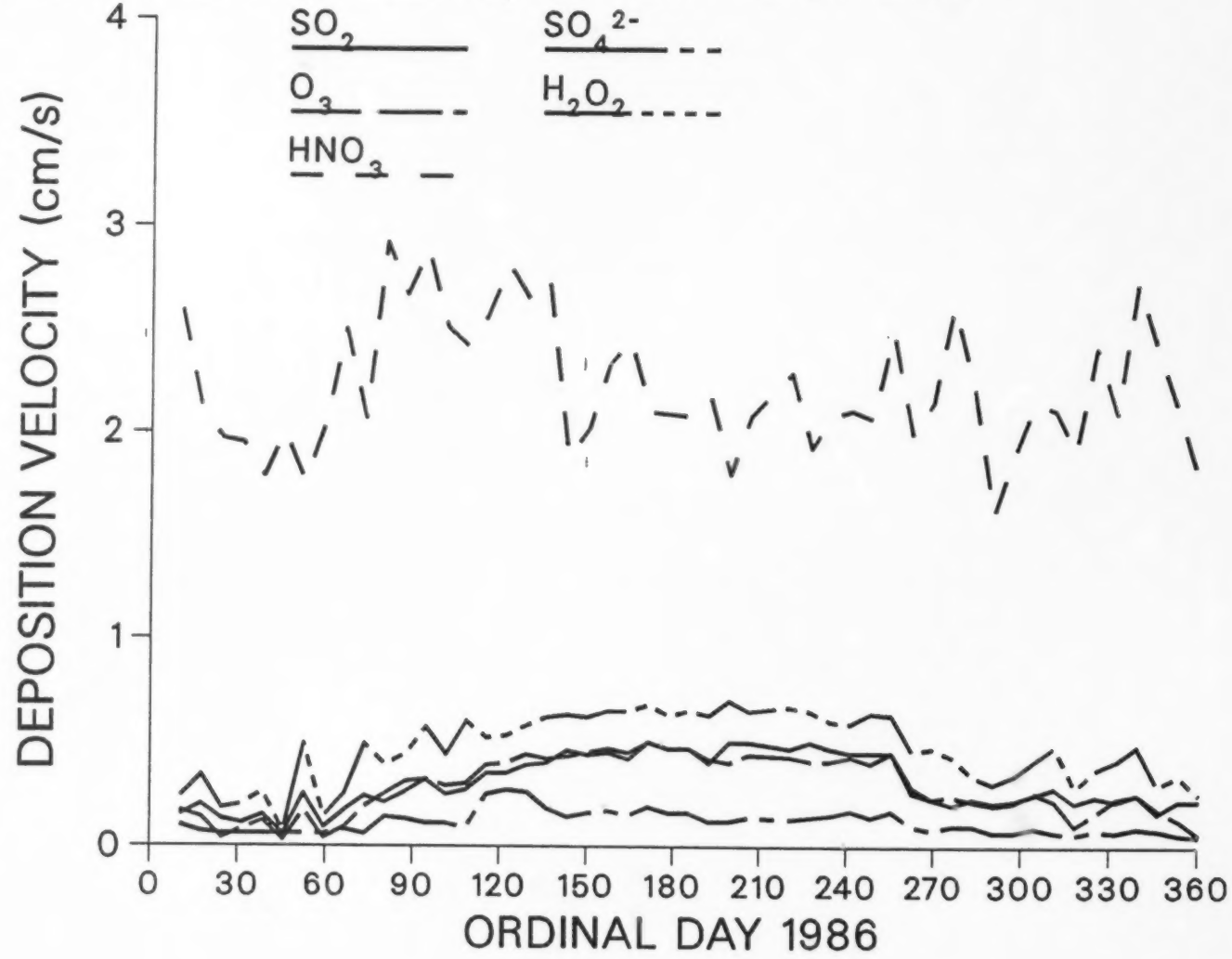

Fig. III.19. Weekly averaged deposition velocities at The Pennsylvania State Univ. (PSU), calculated with the dry deposition module, for the landuse map cell.

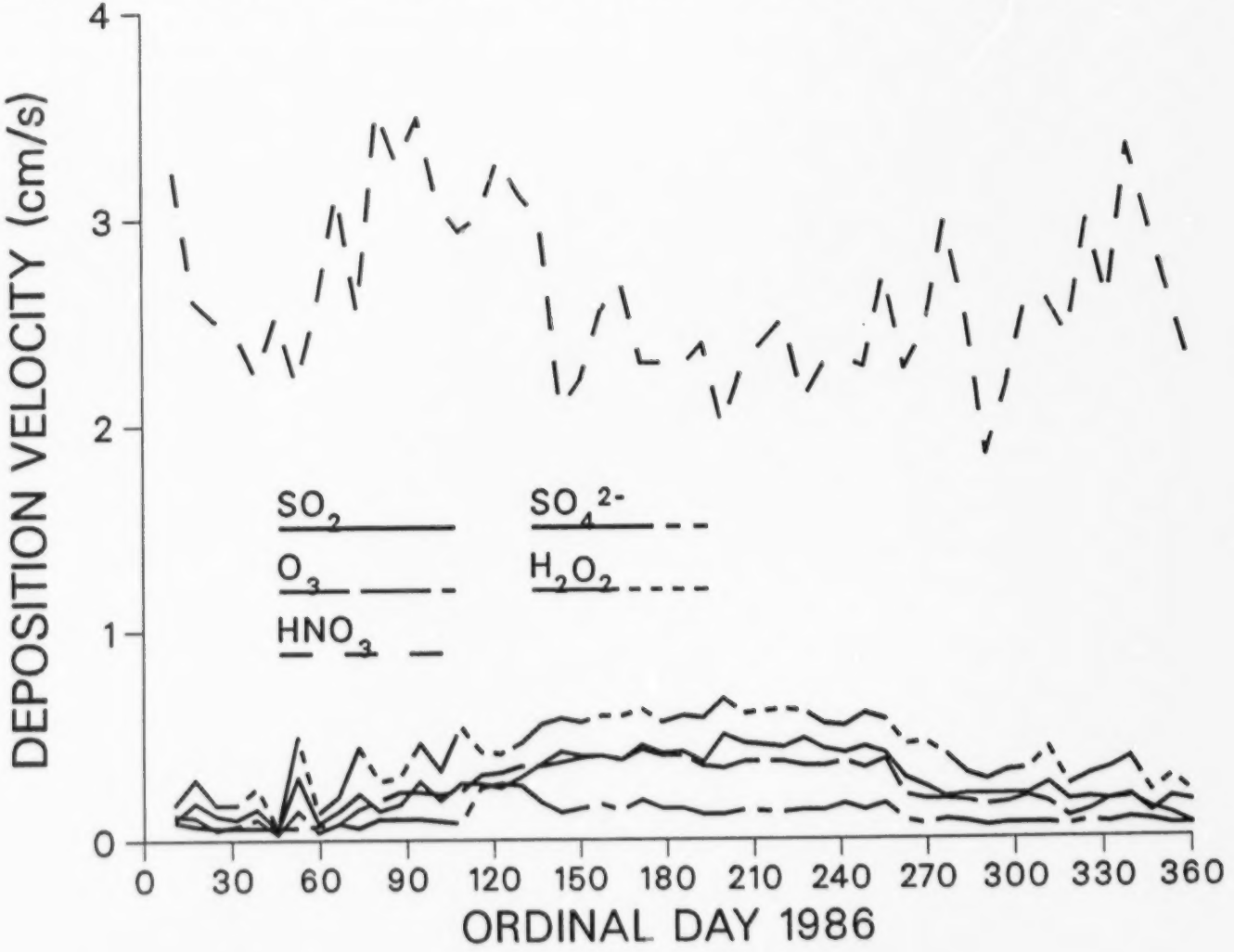

Fig. III.20. Weekly averaged deposition velocities at The Pennsylvania State Univ. (PSU), calculated with the dry deposition module, for the RADM grid cell.

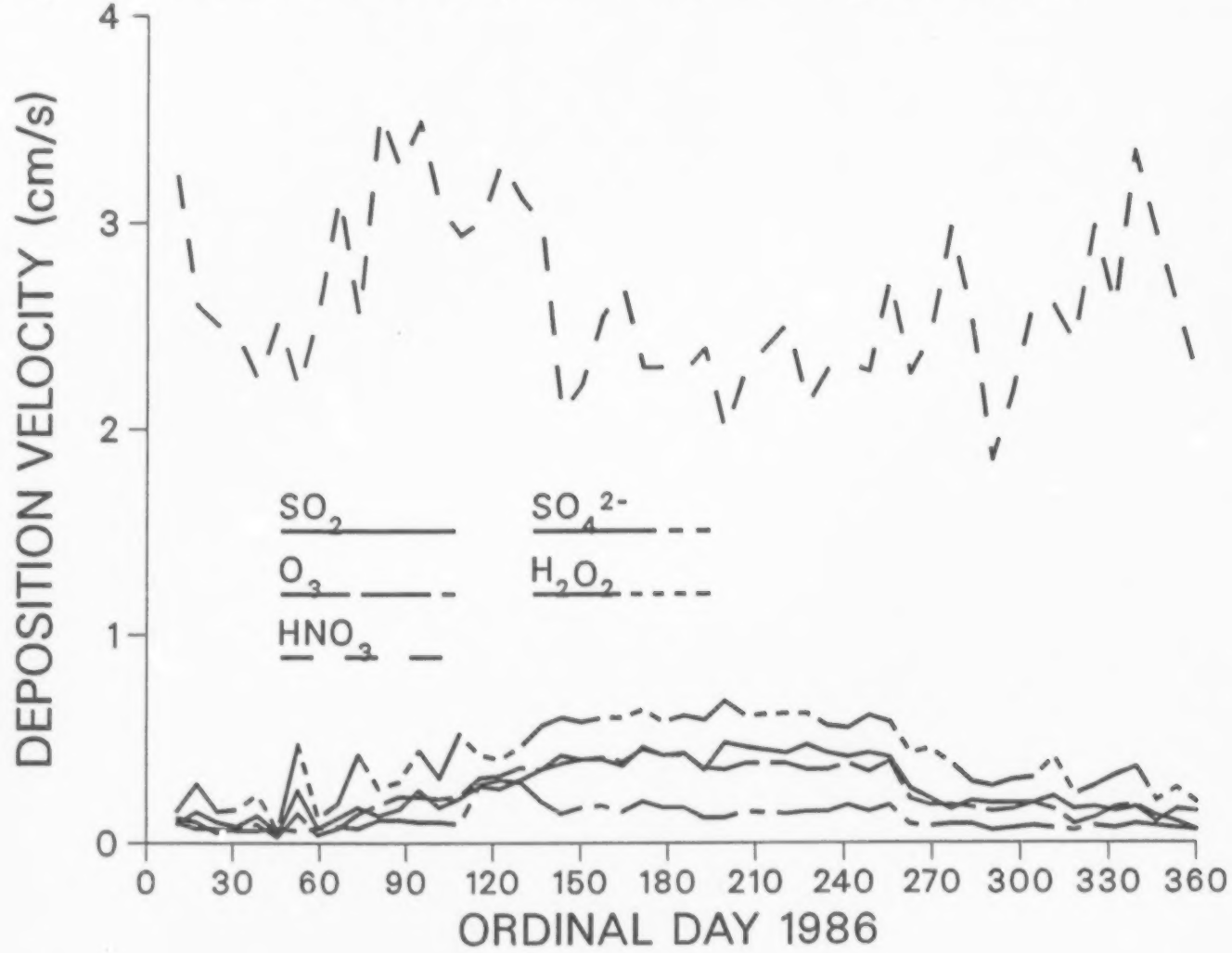

Fig. III.21. Weekly averaged deposition velocities at West Point, NY (WST), calculated with the inferential method.

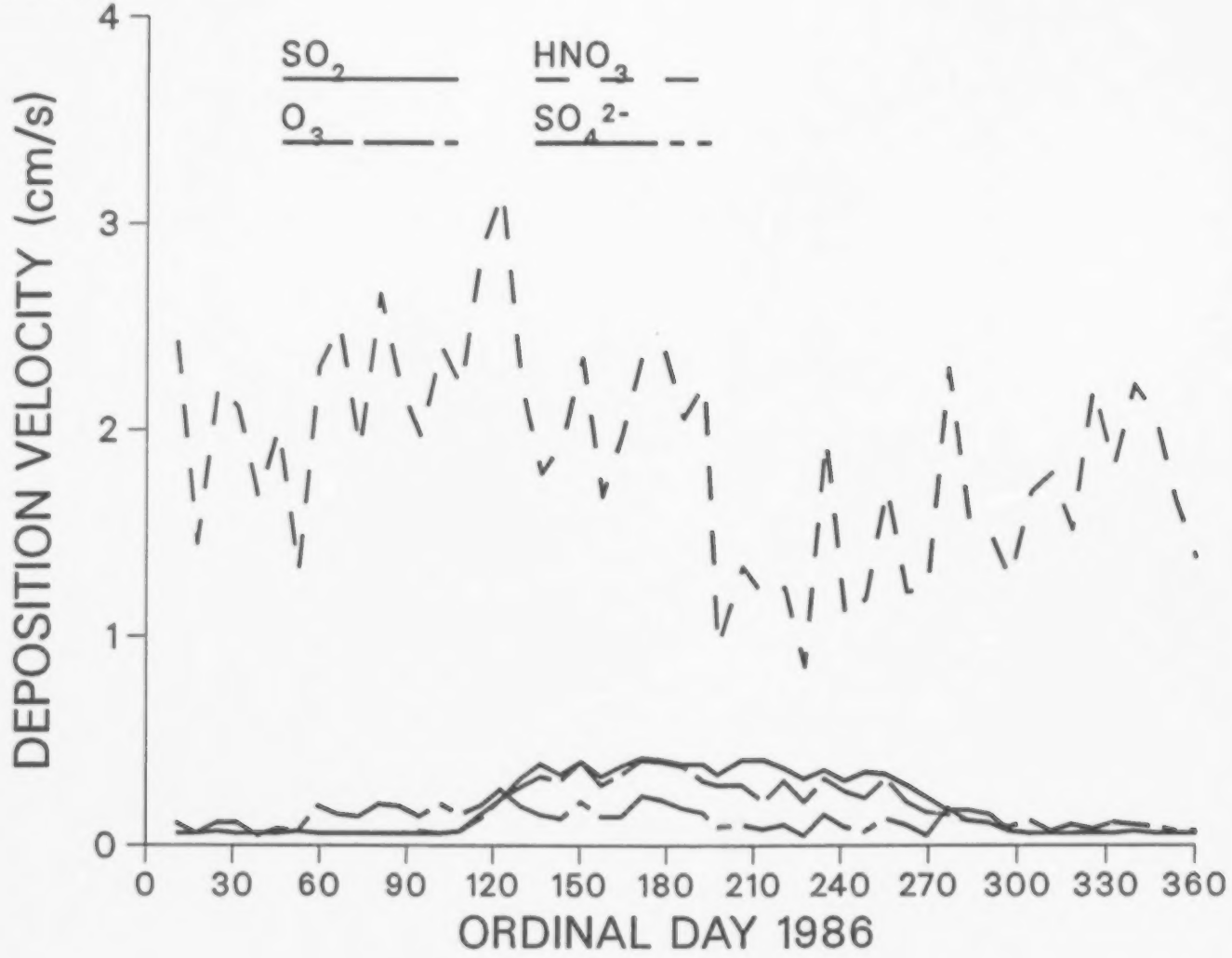

Fig. III.22. Weekly averaged deposition velocities at West Point, NY (WST), calculated with the dry deposition module, for the local site.

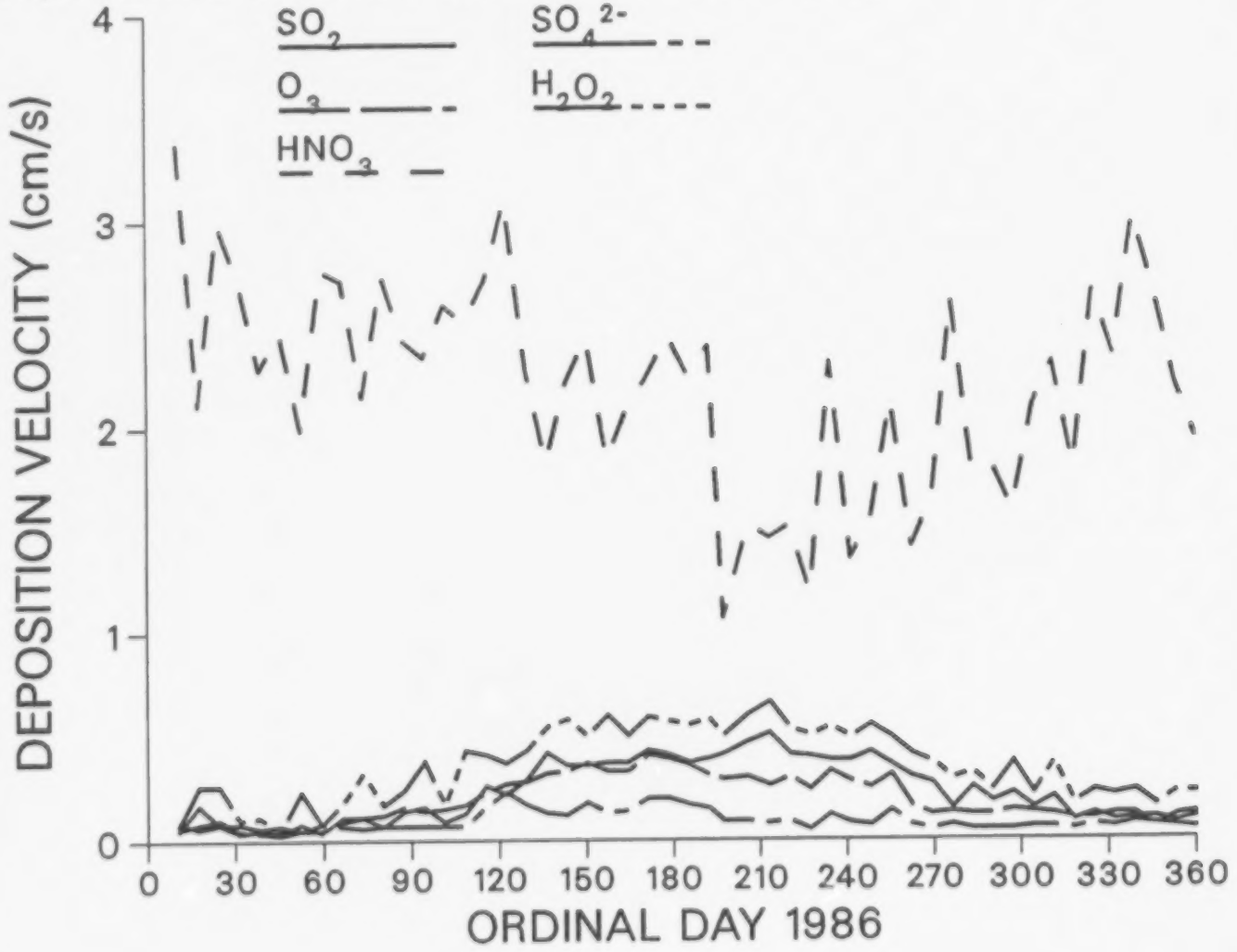

Fig. III.23. Weekly averaged deposition velocities at West Point, NY (WST), calculated with the dry deposition module, for the landuse map cell.

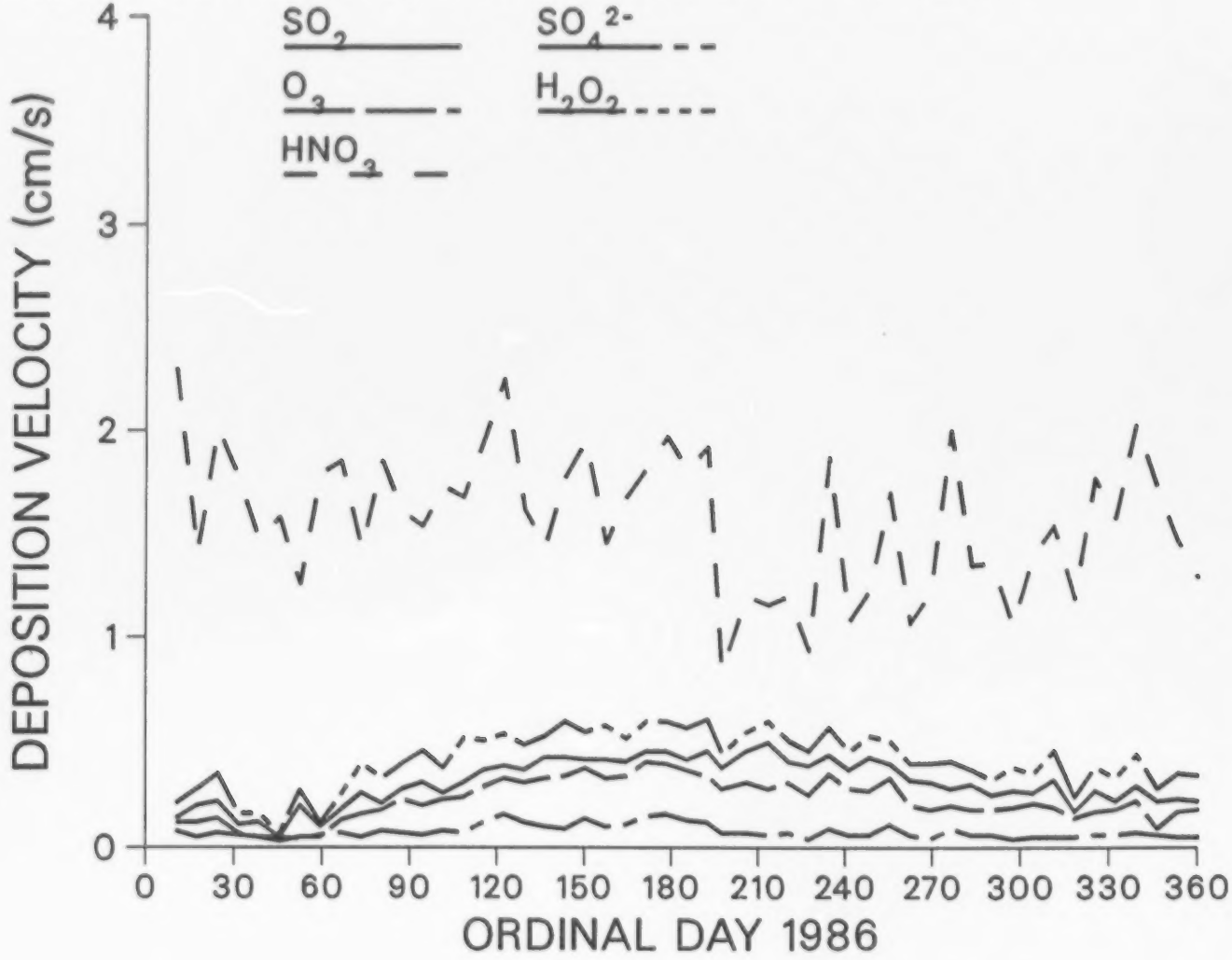

Fig. III.24. Weekly averaged deposition velocities at West Point, NY (WST), calculated with the dry deposition module, for the RADM grid cell.

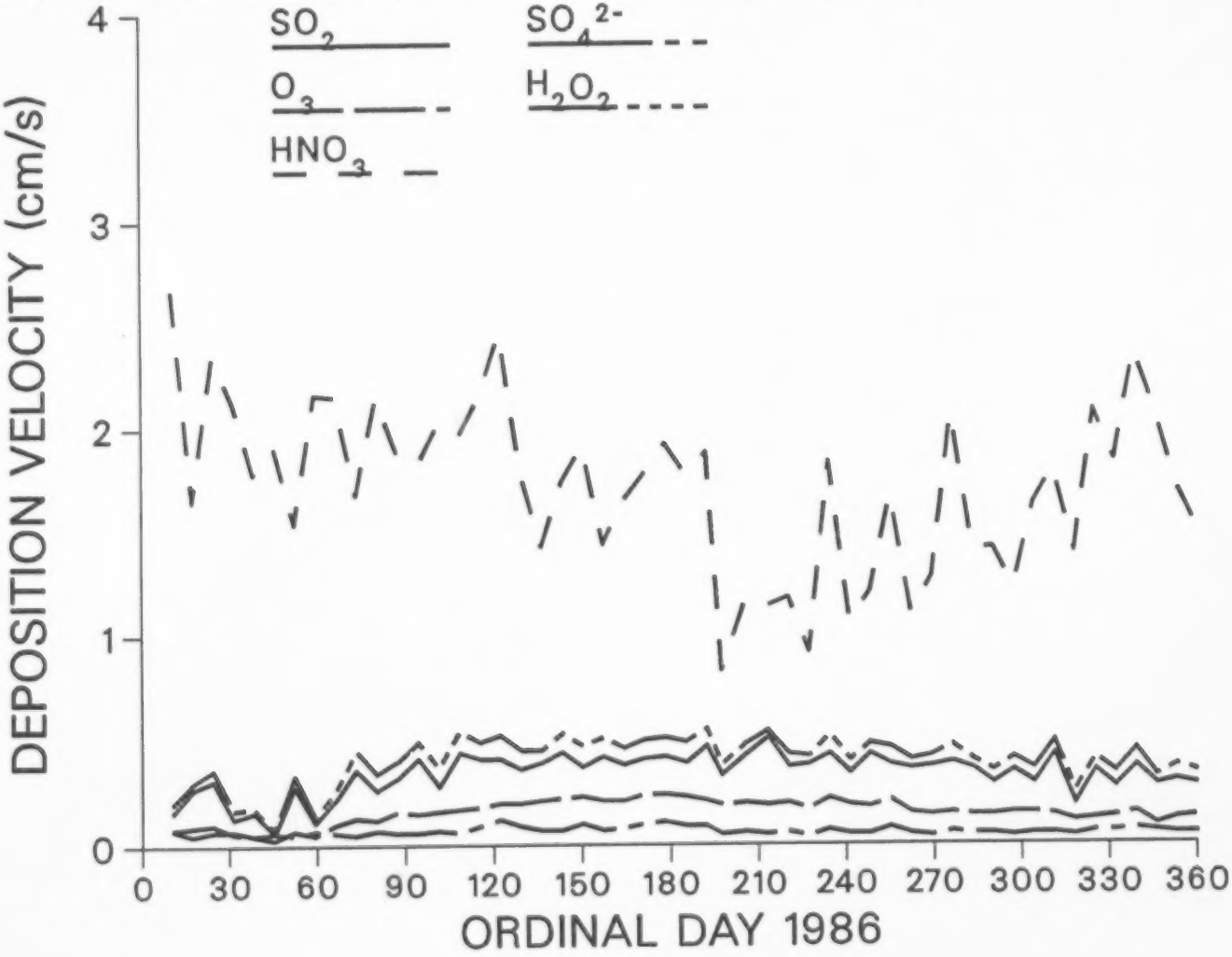

Fig. III.25. Weekly averaged deposition velocities at Whiteface Mountain (WHT), calculated with the inferential method.

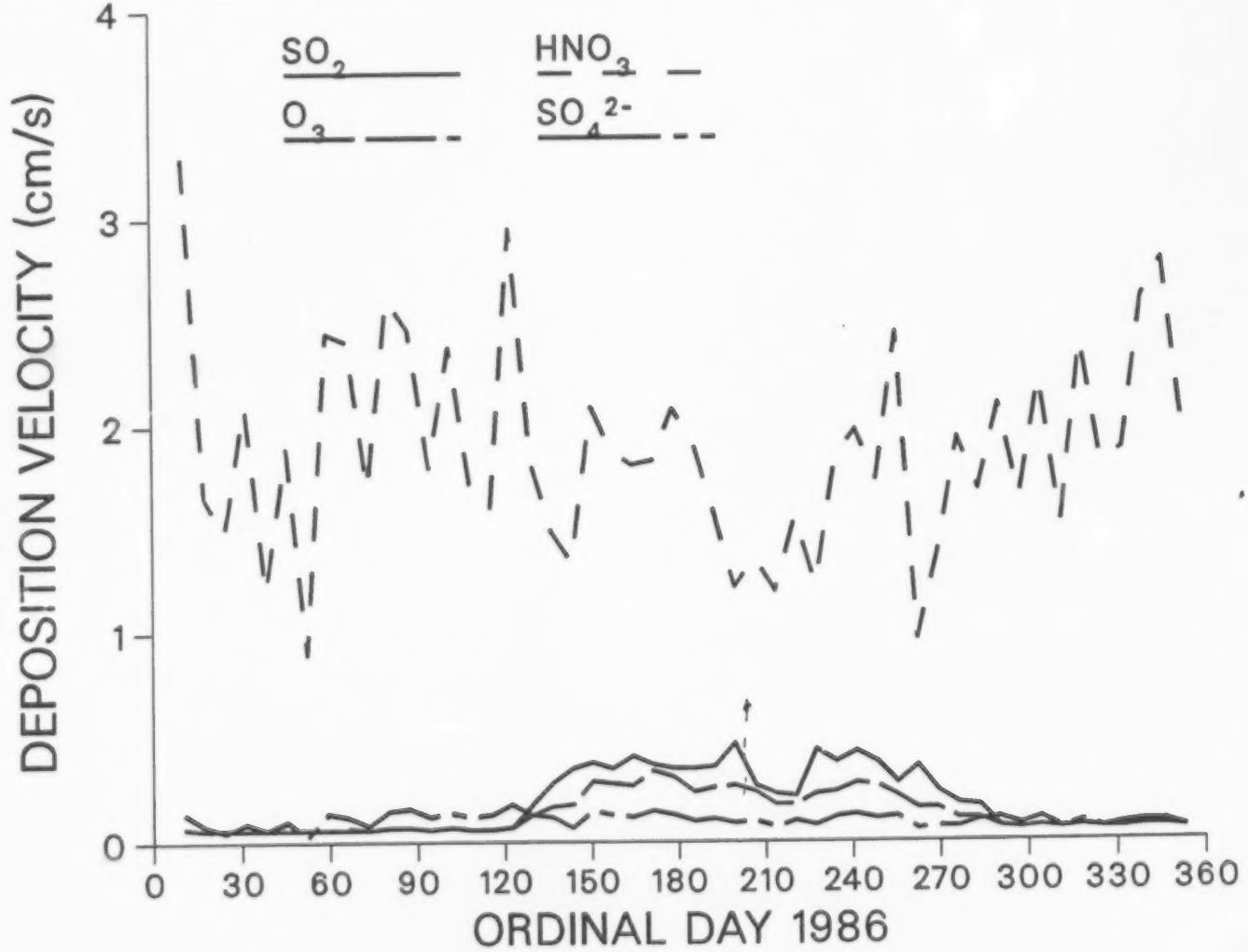

Fig. III.26. Weekly averaged deposition velocities at Whiteface Mountain (WHT), calculated with the dry deposition module, for the local site.

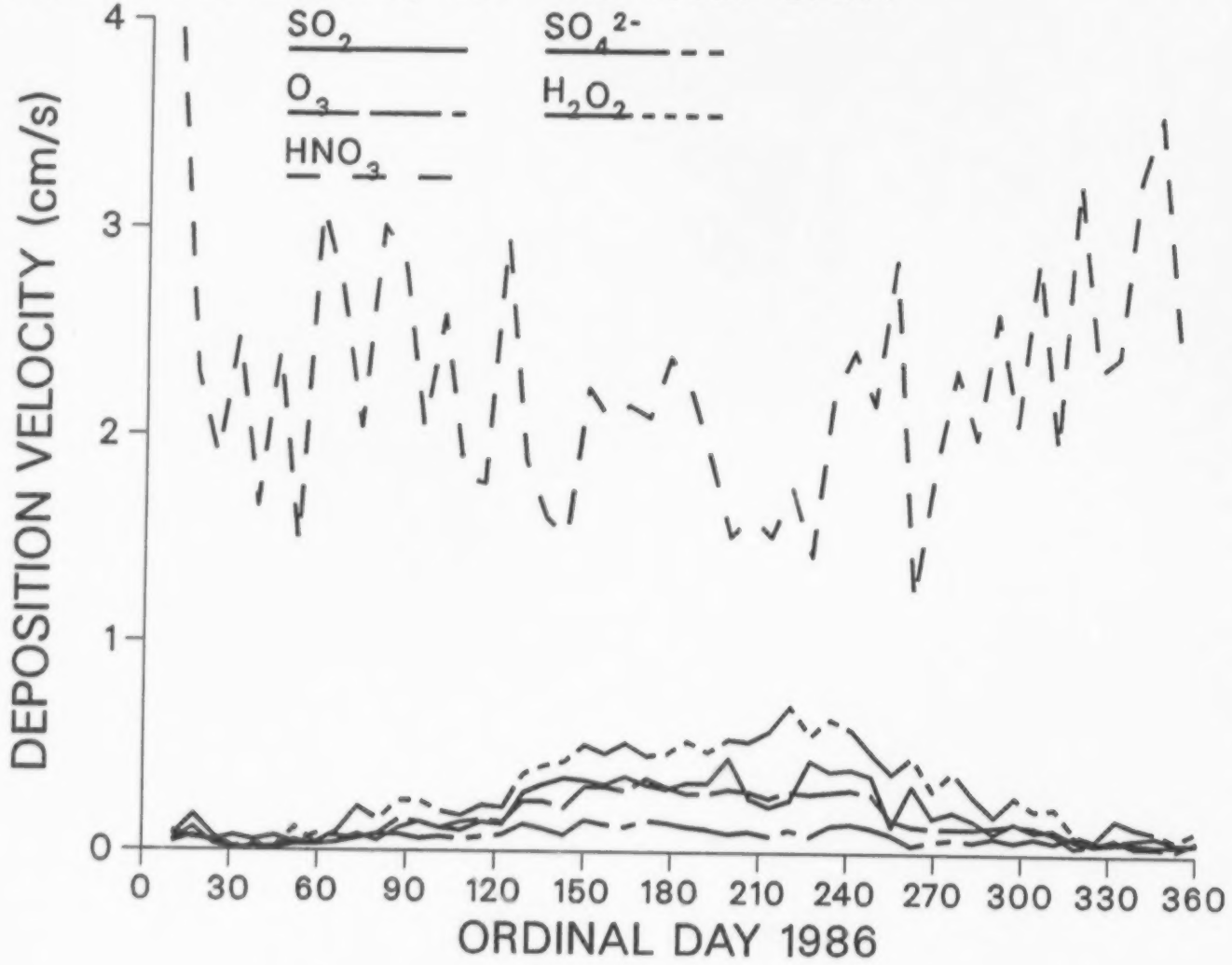

Fig. III.27. Weekly averaged deposition velocities at Whiteface Mountain (WHT), calculated with the dry deposition module, for the landuse map cell.

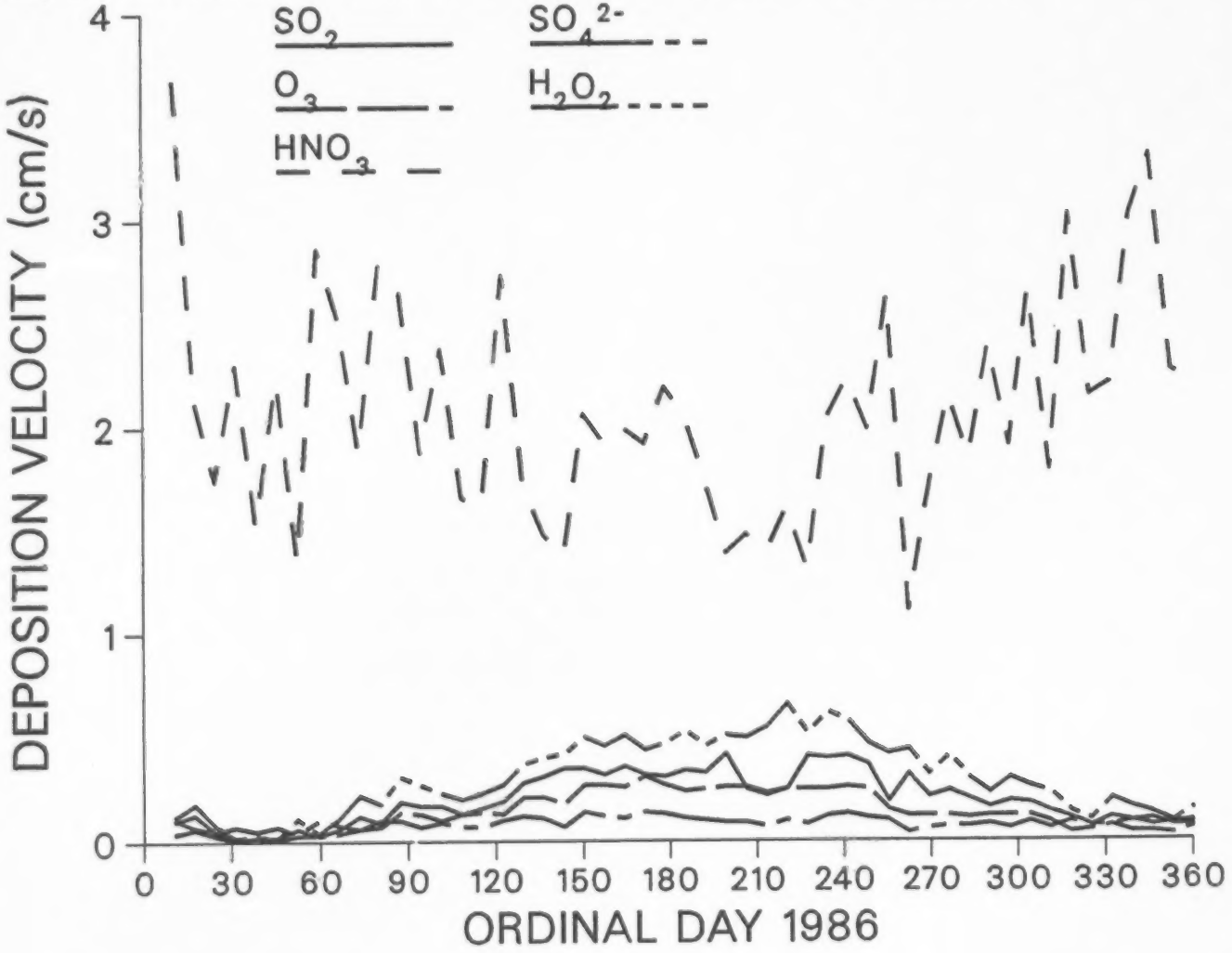

Fig. III.28. Weekly averaged deposition velocities at Whiteface Mountain (WHT), calculated with the dry deposition module, for the RADM grid cell.

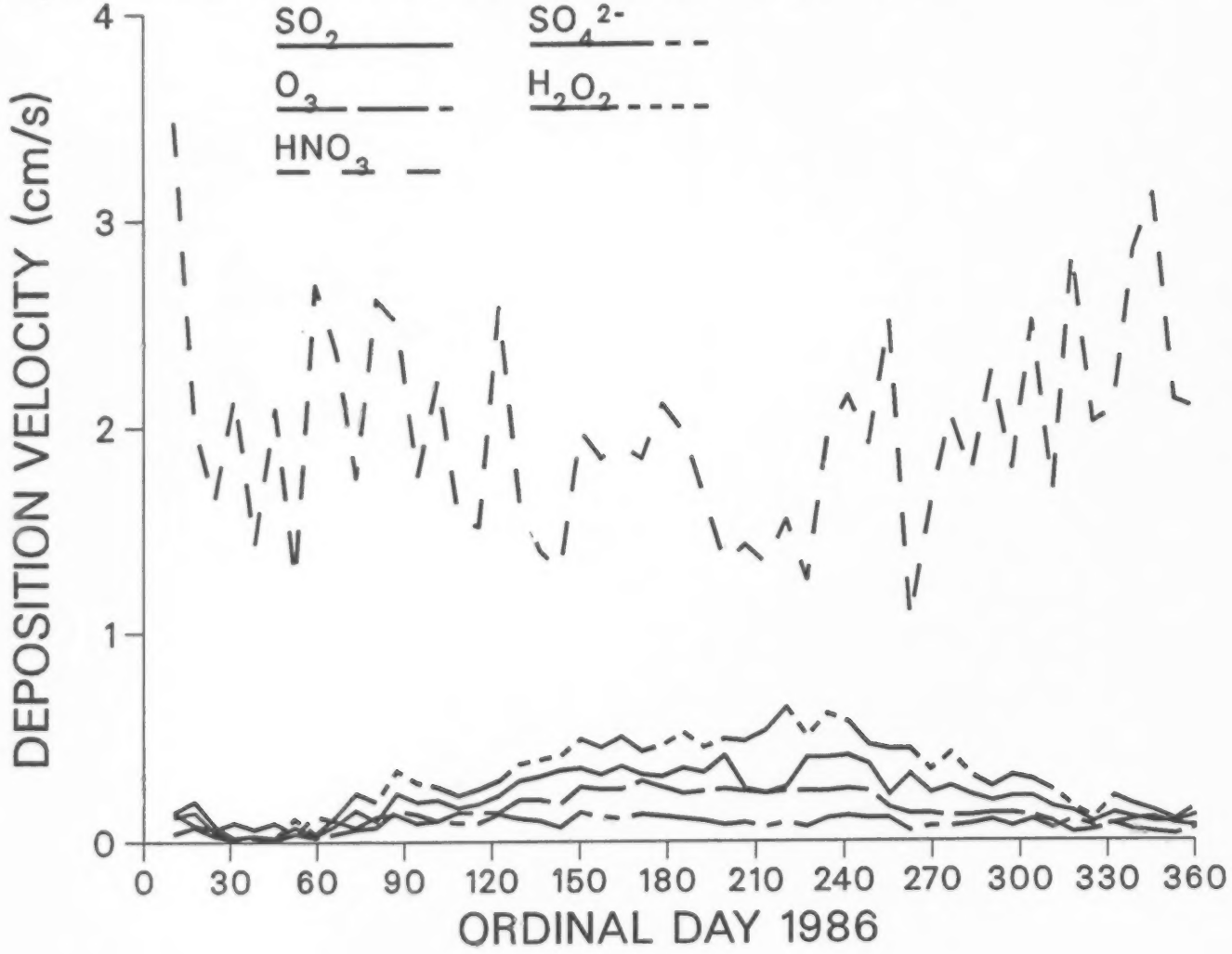

Appendix IV

Plots of vd estimates for additional substances at all seven sites for NO, NO_2, PAN, NH_3, HNO_3, acetaldehyde (ALD, to represent aldehydes other than formaldehyde), HCHO (formaldehyde), methyl hydroperoxide (OP, to represent organic peroxides), peroxyacetic acid (PAA), and formic acid (ORA, to represent organic acids).

Fig. IV.1. Weekly average deposition velocities at Argonne National Laboratory (ARG), calculated for the local site with the dry deposition module.

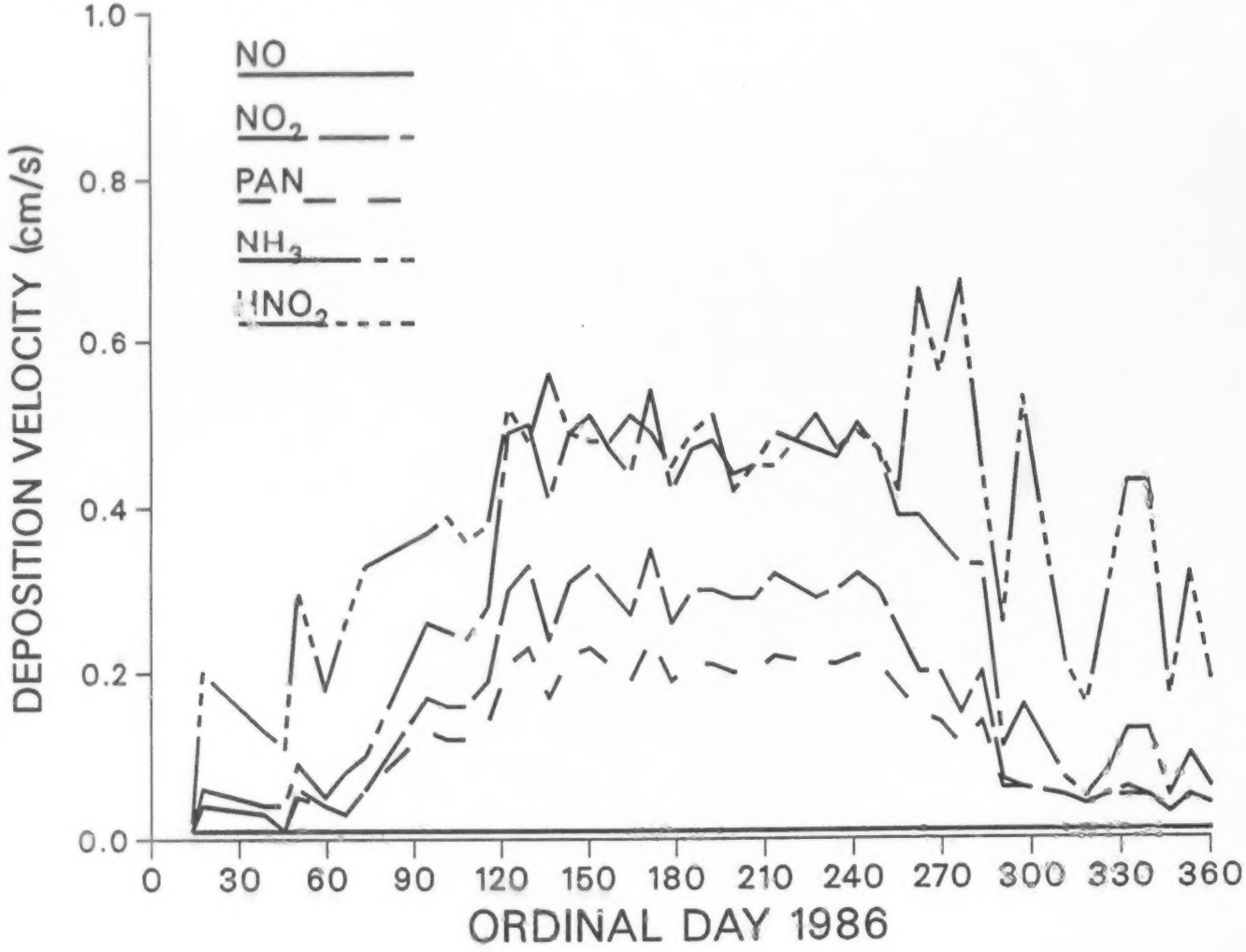

Fig. IV.2. Weekly average deposition velocities at Argonne National Laboratory (ARG), calculated for the local site with the dry deposition module.

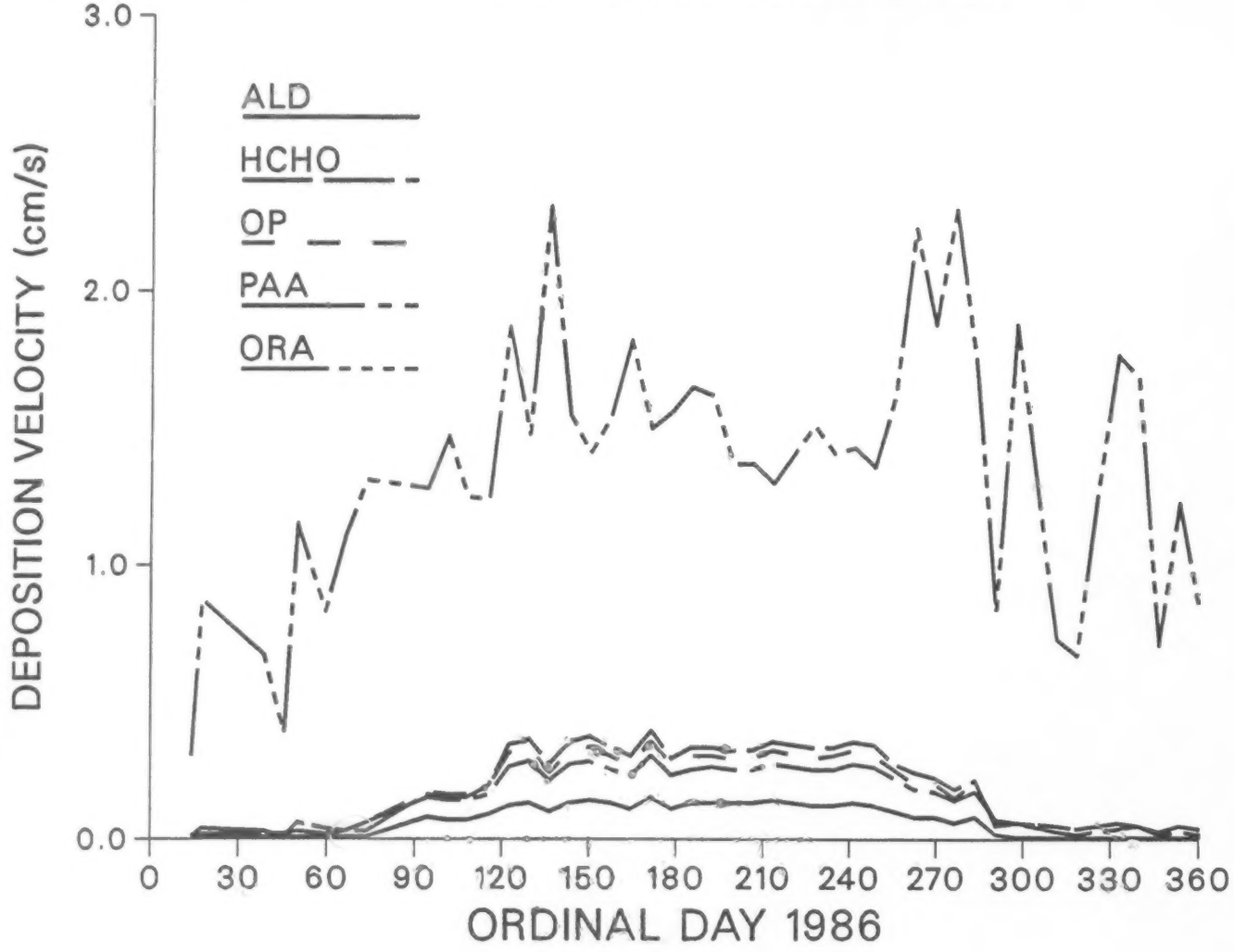

Fig. IV.3. Weekly average deposition velocities at Bondville, IL (BON), calculated for the local site with the dry deposition module.

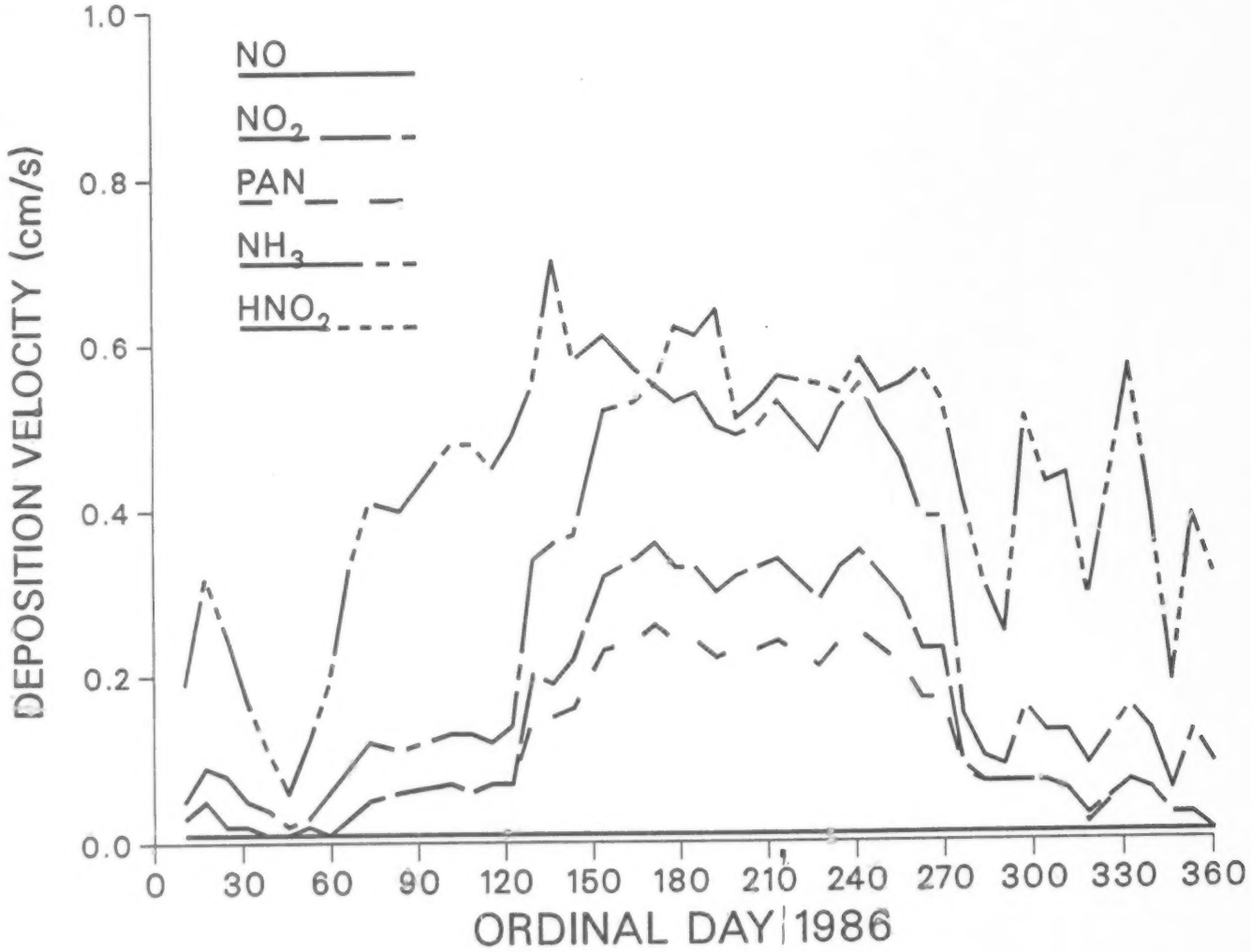

Fig. IV.4. Weekly average deposition velocities at Bondville, IL (BON), calculated for the local site with the dry deposition module.

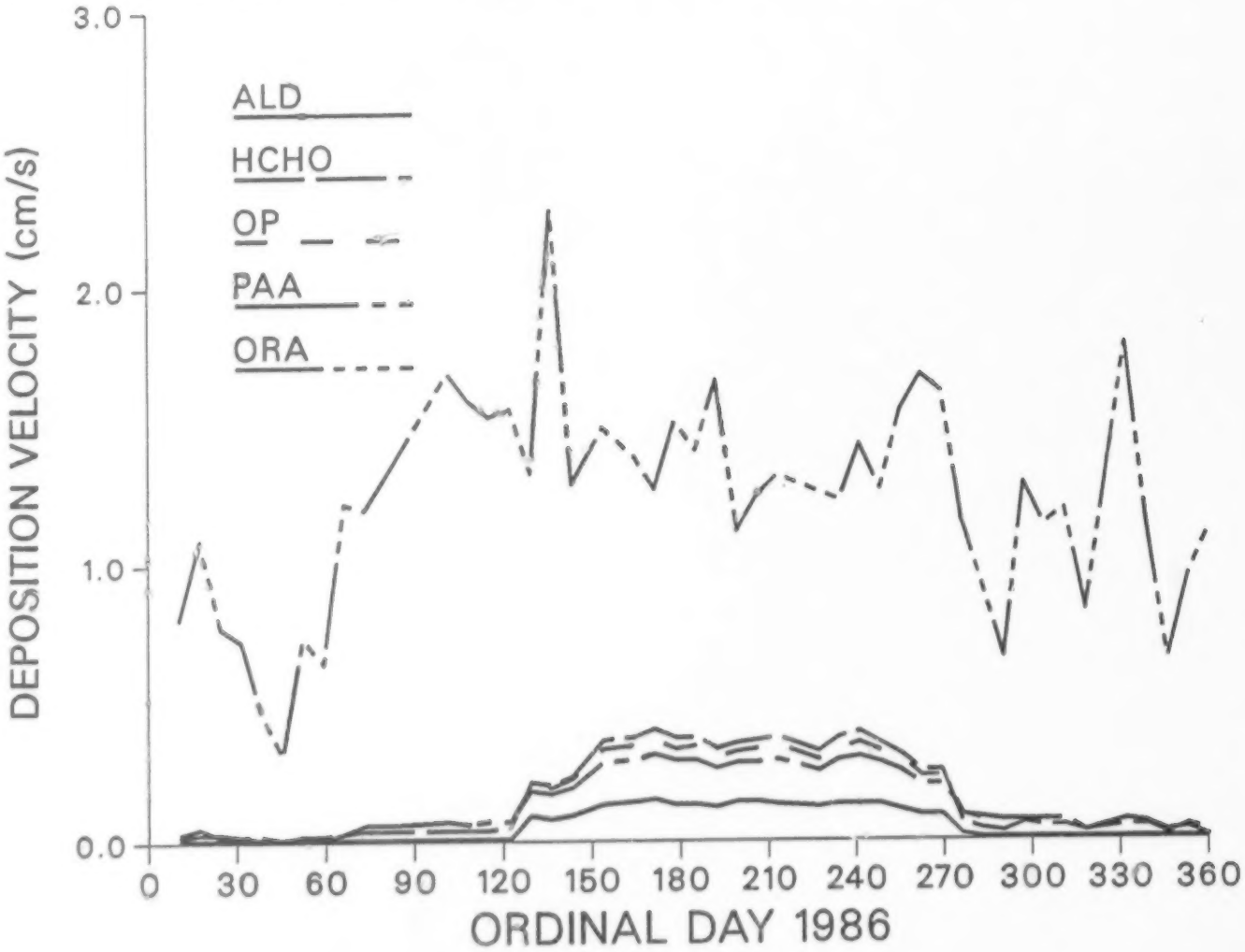

Fig. IV.5. Weekly average deposition velocities at Oak Ridge, TN (OAK), calculated for the local site with the dry deposition module.

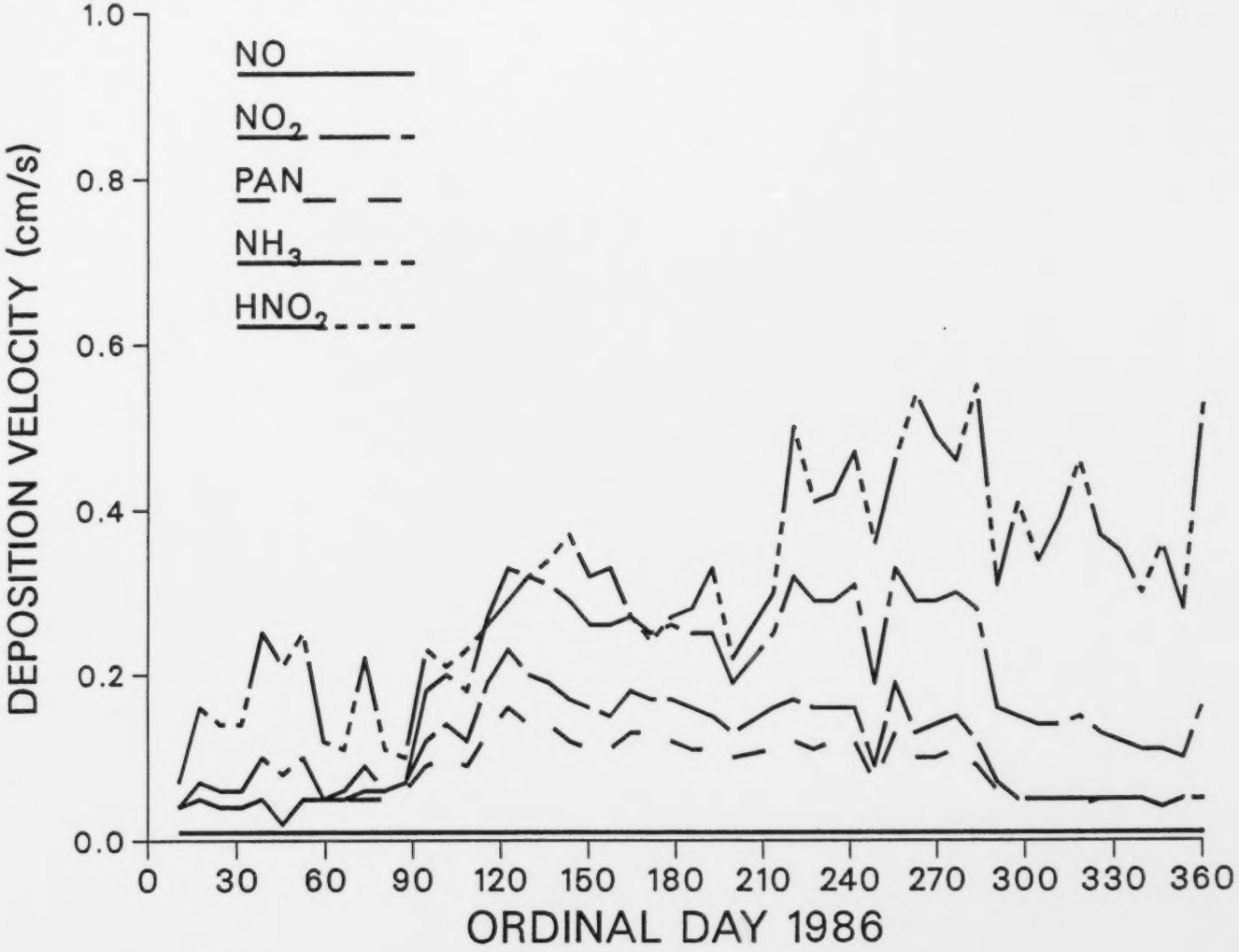

Fig. IV.6. Weekly average deposition velocities at Oak Ridge, TN (OAK), calculated for the local site with the dry deposition module.

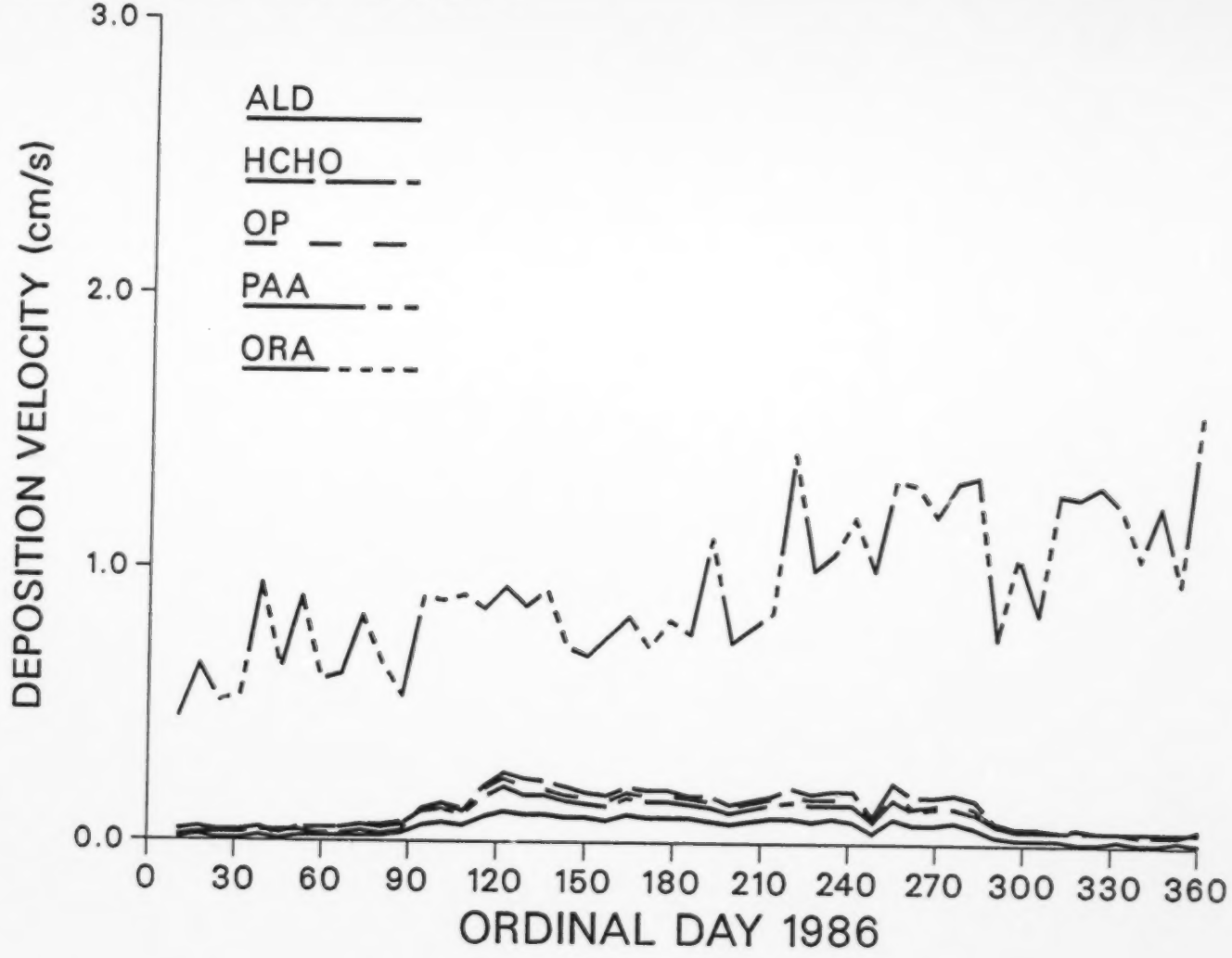

Fig. IV.7. Weekly average deposition velocities at Panola State Park (PAN), calculated for the local site with the dry deposition module.

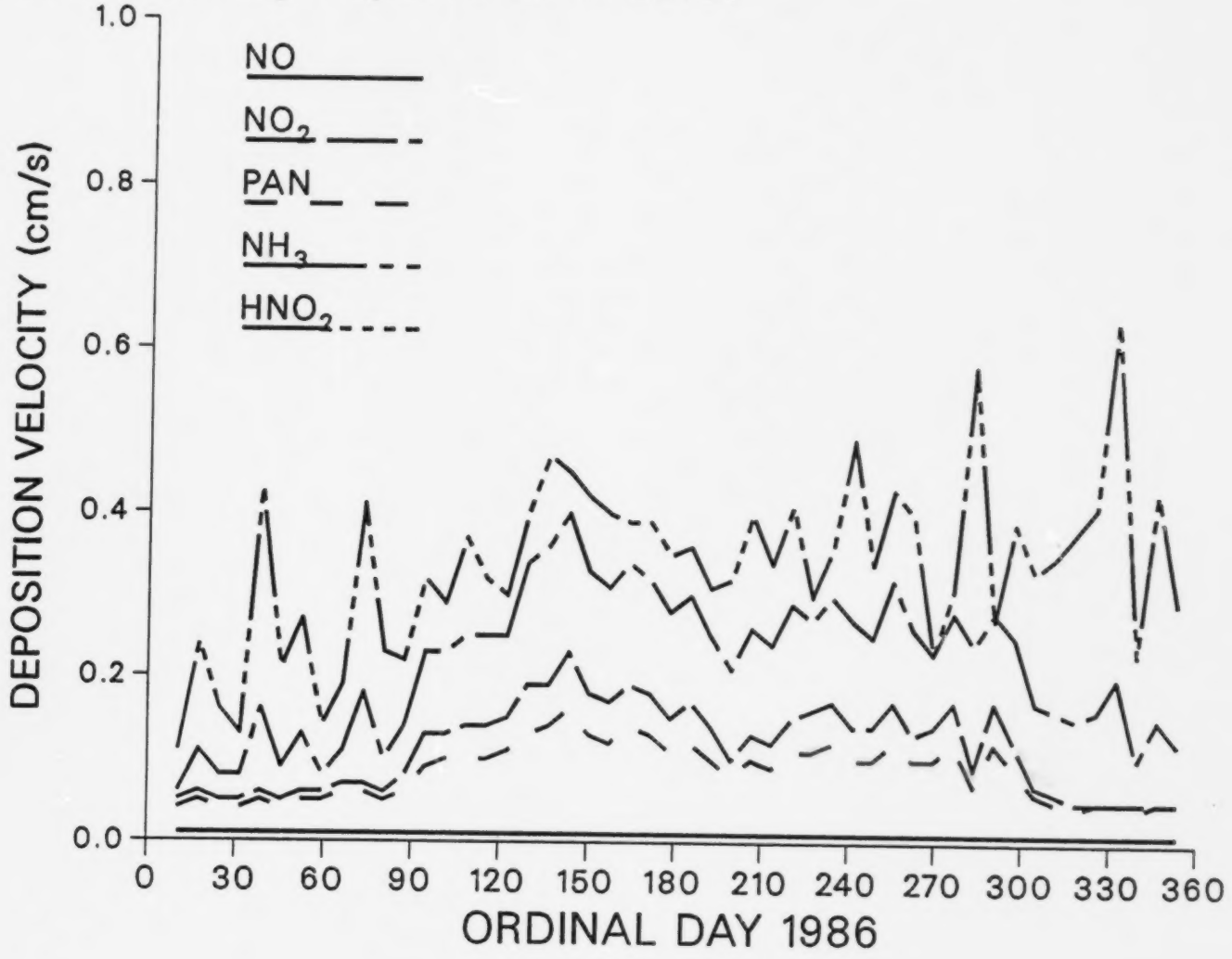

Fig. IV.8. Weekly average deposition velocities at Panola State Park (PAN), calculated for the local site with the dry deposition module.

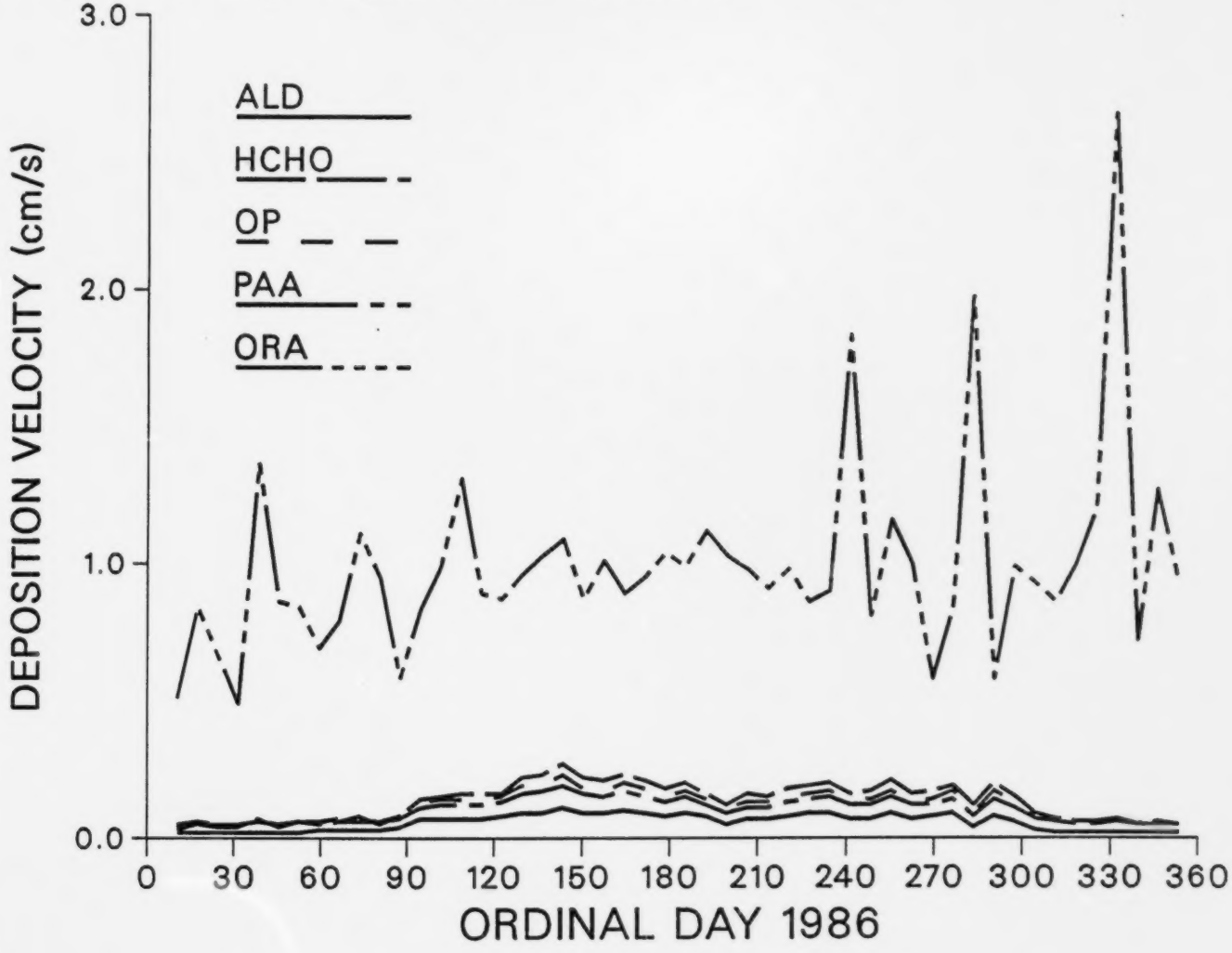

Fig. IV.9. Weekly average deposition velocities at The Pennsylvania State Univ. (PSU), calculated for the local site with the dry deposition module.

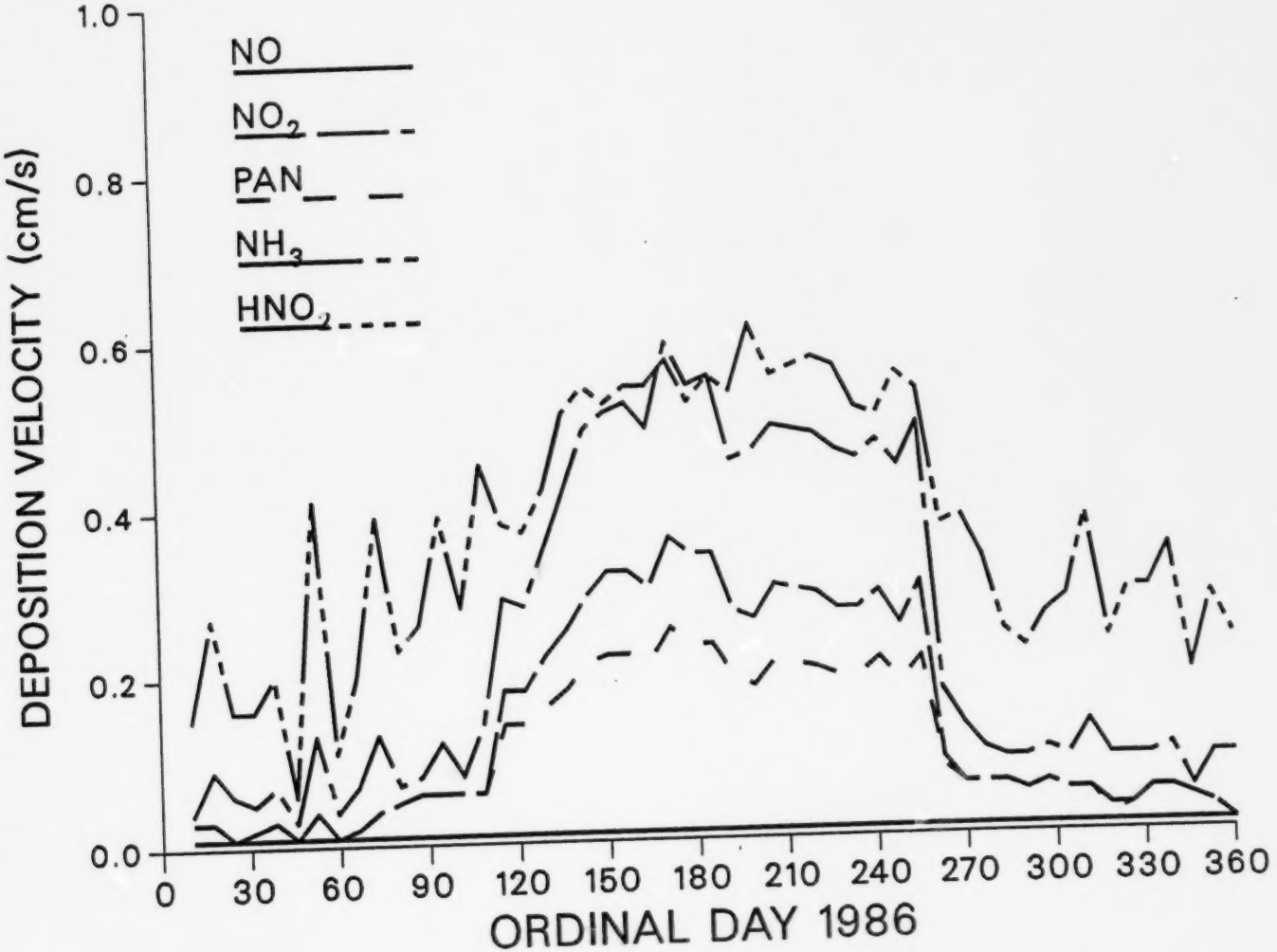

Fig. IV.10. Weekly average deposition velocities at The Pennsylvania State Univ. (PSU), calculated for the local site with the dry deposition module.

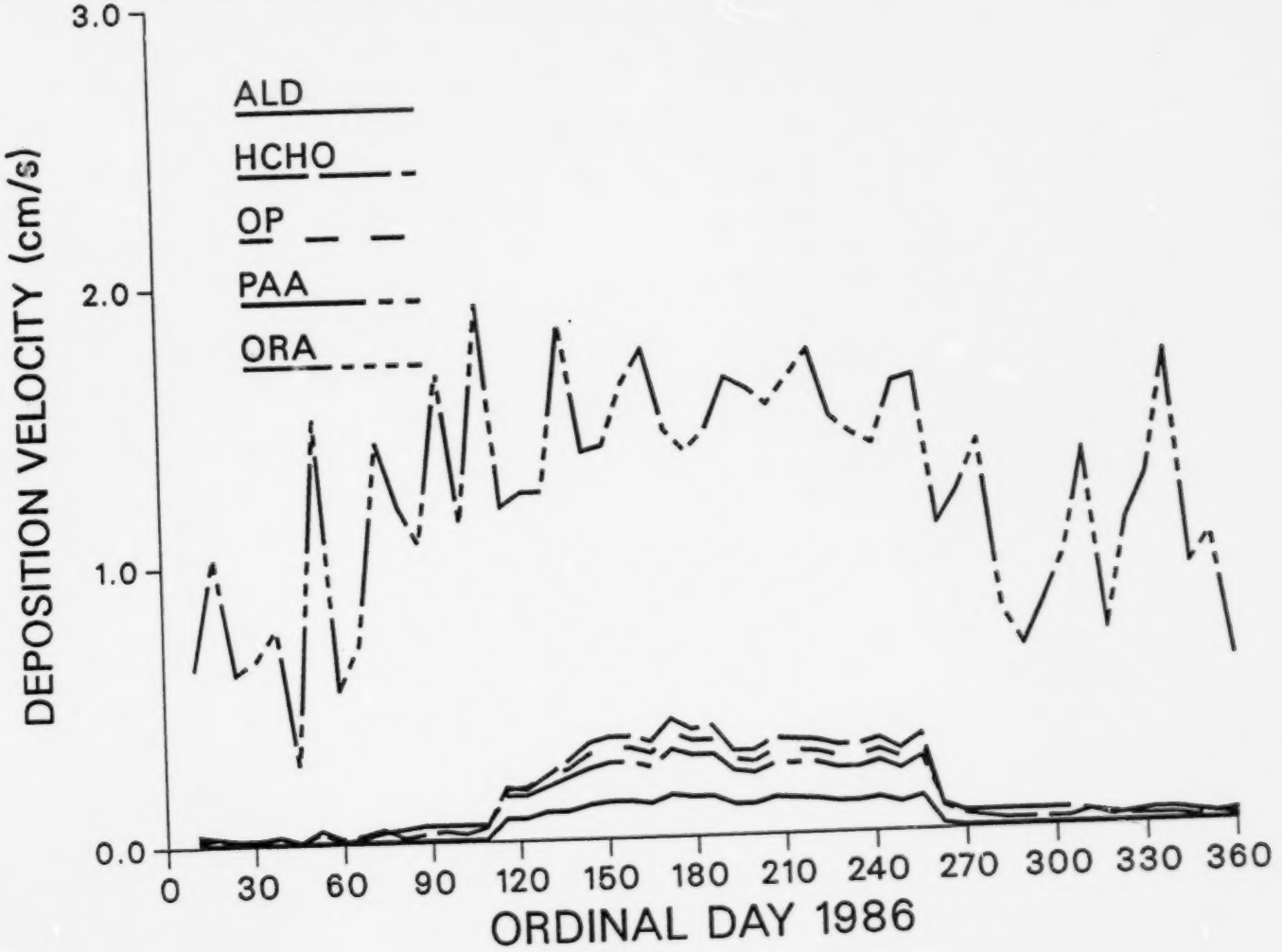

Fig. IV.11. Weekly average deposition velocities at West Point, NY (WST), calculated for the local site with the dry deposition module.

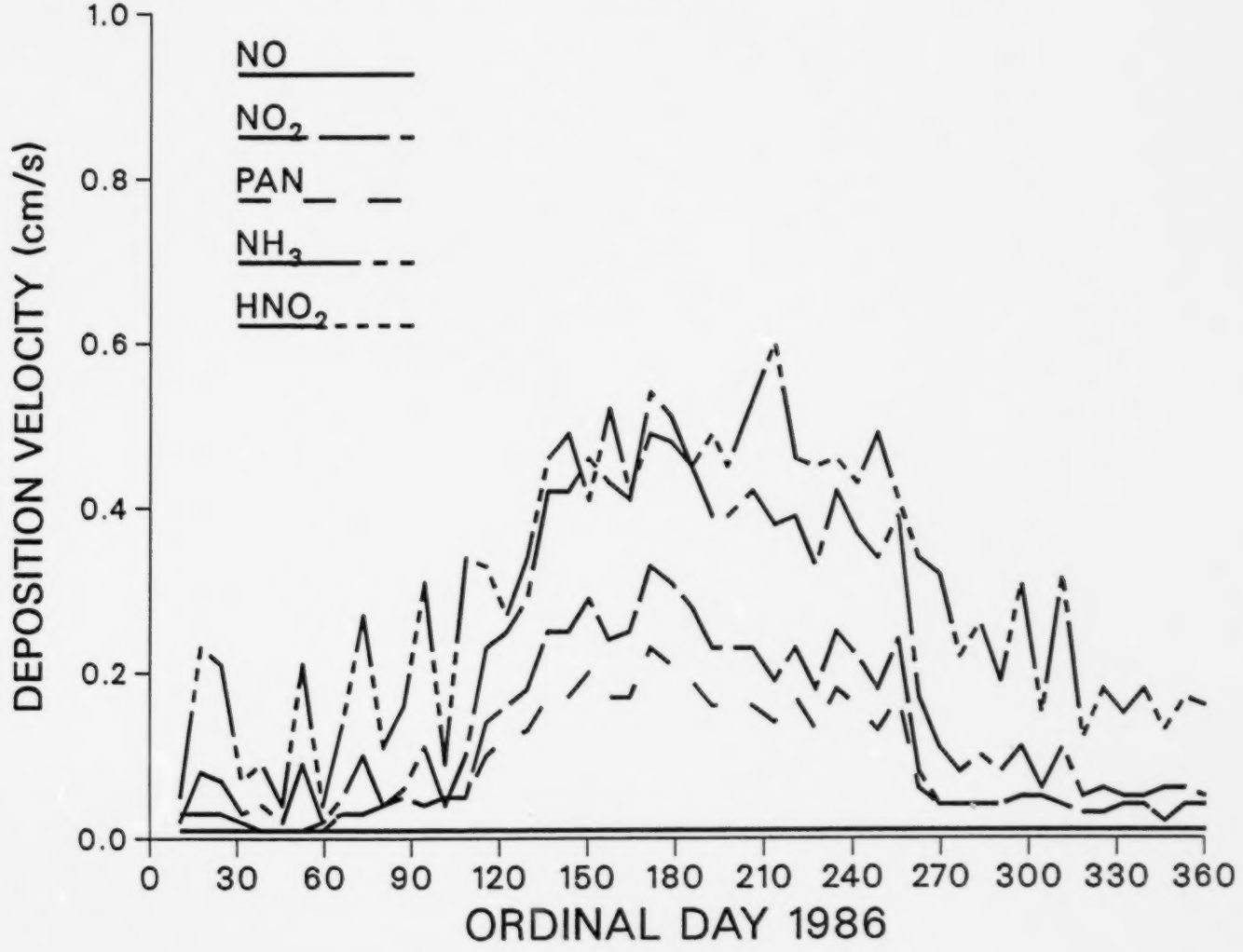

Fig. IV.12. Weekly average deposition velocities at West Point, NY (WST), calculated for the local site with the dry deposition module.

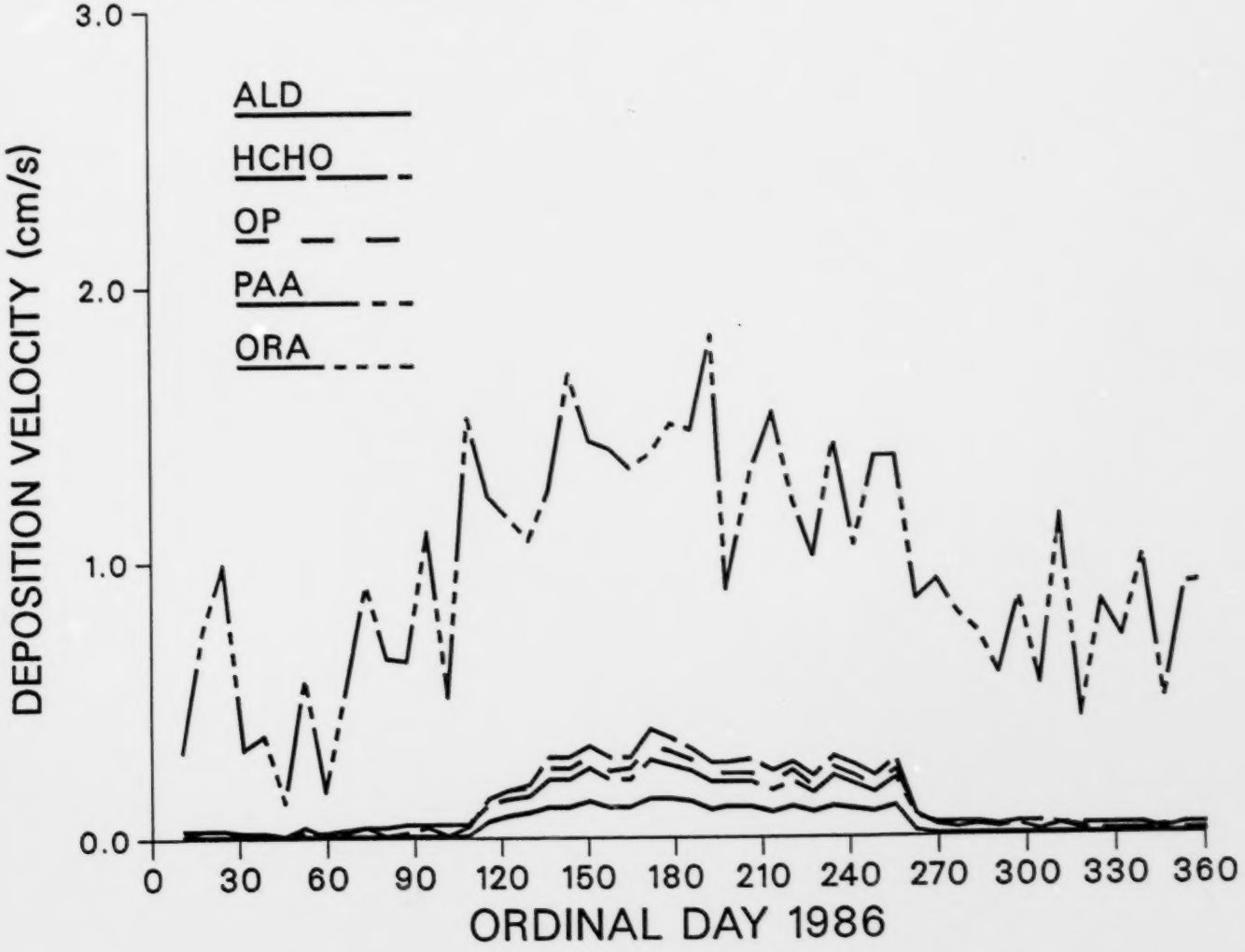

Fig. IV.13. Weekly average deposition velocities at Whiteface Mountain (WHT), calculated for the local site with the dry deposition module.

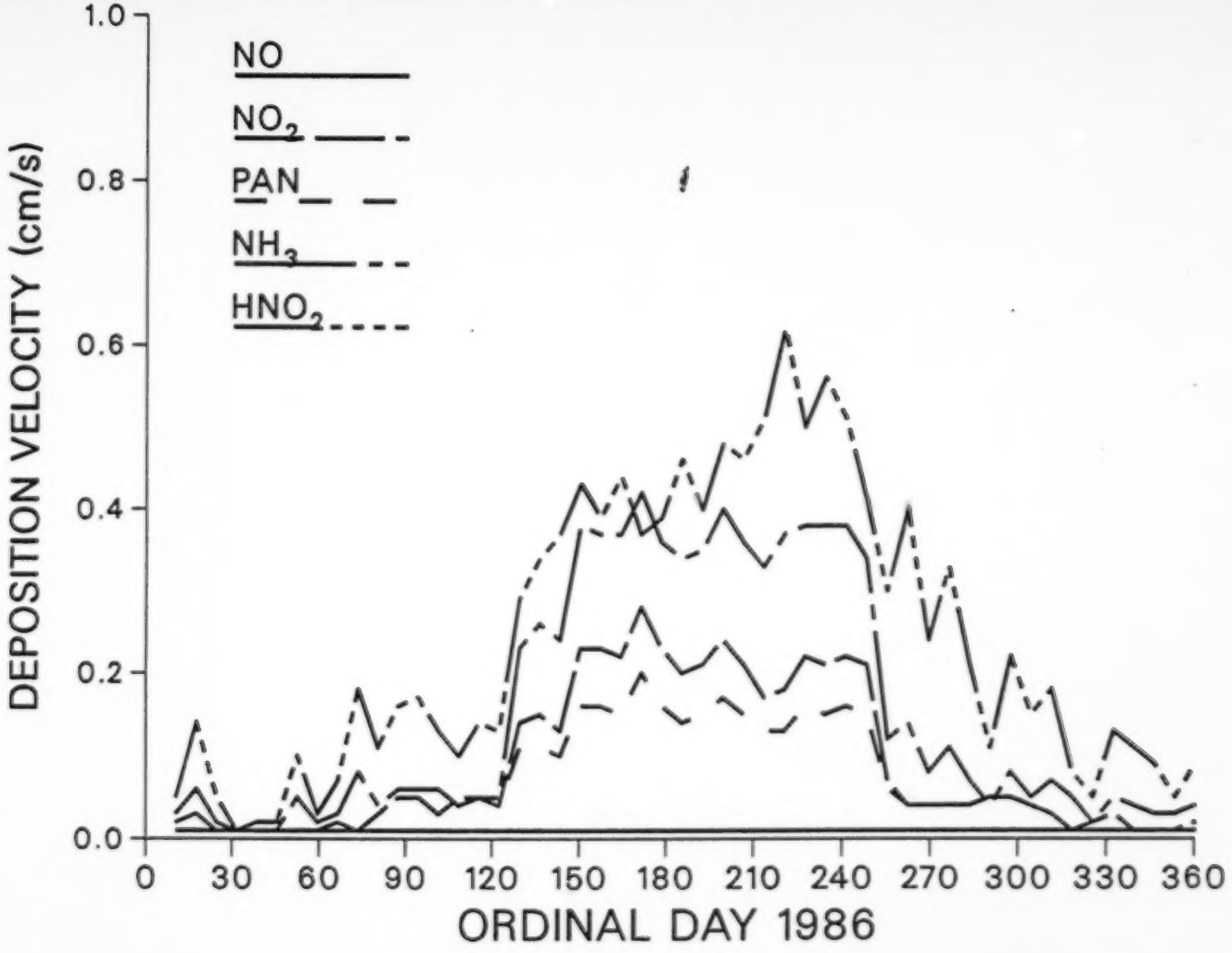

Fig. IV.14. Weekly average deposition velocities at Whiteface Mountain (WHT), calculated for the local site with the dry deposition module.